Field Guide to

Optomechanical Design and Analysis

Katie Schwertz
James H. Burge

SPIE Field Guides
Volume FG26

John E. Greivenkamp, Series Editor

SPIE PRESS
Bellingham, Washington USA

Library of Congress Cataloging-in-Publication Data

Schwertz, Katie M.
Field guide to optomechanical design and analysis / Katie M. Schwertz, Jim H. Burge.
p. cm. – (The field guide series)
Includes bibliographical references and index.
ISBN 978-0-8194-9161-9
1. Optical instruments–Design and construction–Handbooks, manuals, etc. 2. Optomechanics–Handbooks, manuals, etc. I. Burge, James H. II. Title.
TS513.S385 2012
681'.4–dc23
2012013233

Published by

SPIE
P.O. Box 10
Bellingham, Washington 98227-0010 USA
Phone: +1.360.676.3290
Fax: +1.360.647.1445
Email: books@spie.org
Web: http://spie.org

The content of this book reflects the work and thought of the author. Every effort has been made to publish reliable and accurate information herein, but the publisher is not responsible for the validity of the information or for any outcomes resulting from reliance thereon. For the latest updates about this title, please visit the book's page on our website.

Printed in the United States of America.
First printing

Introduction to the Series

Welcome to the *SPIE Field Guides*—a series of publications written directly for the practicing engineer or scientist. Many textbooks and professional reference books cover optical principles and techniques in depth. The aim of the *SPIE Field Guides* is to distill this information, providing readers with a handy desk or briefcase reference that provides basic, essential information about optical principles, techniques, or phenomena, including definitions and descriptions, key equations, illustrations, application examples, design considerations, and additional resources. A significant effort will be made to provide a consistent notation and style between volumes in the series.

Each *SPIE Field Guide* addresses a major field of optical science and technology. The concept of these Field Guides is a format-intensive presentation based on figures and equations supplemented by concise explanations. In most cases, this modular approach places a single topic on a page, and provides full coverage of that topic on that page. Highlights, insights, and rules of thumb are displayed in sidebars to the main text. The appendices at the end of each Field Guide provide additional information such as related material outside the main scope of the volume, key mathematical relationships, and alternative methods. While complete in their coverage, the concise presentation may not be appropriate for those new to the field.

The *SPIE Field Guides* are intended to be living documents. The modular page-based presentation format allows them to be easily updated and expanded. We are interested in your suggestions for new Field Guide topics as well as what material should be added to an individual volume to make these Field Guides more useful to you. Please contact us at **fieldguides@SPIE.org**.

John E. Greivenkamp, *Series Editor*
College of Optical Sciences
The University of Arizona

Field Guide to Optomechanical Design and Analysis

Optomechanics is a field of mechanics that addresses the specific design challenges associated with optical systems. This *Field Guide* describes how to mount optical components, as well as how to analyze a given design. It is intended for practicing optical and mechanical engineers whose work requires knowledge in both optics and mechanics.

Throughout the text, we describe typical mounting approaches for lenses, mirrors, prisms, and windows; standard hardware and the types of adjustments and stages available to the practicing engineer are also included. Common issues involved with mounting optical components are discussed, including stress, glass strength, thermal effects, vibration, and errors due to motion. A useful collection of material properties for glasses, metals, and adhesives, as well as guidelines for tolerancing optics and machined parts can be found throughout the book.

The structure of the book follows Jim Burge's optomechanics course curriculum at the University of Arizona. We offer our thanks to all those who helped with the book's development and who provided content and input. Much of the subject matter and many of the designs are derived from the work of Paul Yoder and Dan Vukobratovich; their feedback is greatly appreciated.

Katie Schwertz
Edmund Optics®

Jim Burge
College of Optical Sciences
University of Arizona

Table of Contents

Table of Contents

Table of Contents

List of Symbols and Acronyms

%TMC	Percent total mass lost
%CVCM	Percent collected volatile condensable material
a	Acceleration
A	Area
CAD	Computer-aided design
COTS	Commercial off-the-shelf
C_p	Specific heat capacity
CTE	Coefficient of thermal expansion
CVD	Chemical vapor deposition
d	Displacement
d	Distance
D	Diameter
D	Thermal diffusivity
D	flexural rigidity
E	Young's modulus
f	Focal length
F	Force, load
f_0	Natural frequency (Hz)
FEA	Finite element analysis
FEM	Finite element method
g	Gravity (9.8 m/s^2)
G	Shear modulus
GD&T	Geometric dimensioning and tolerancing
h	Height, thickness
IR	Infrared
k	Stiffness
K	Bulk modulus
K_c	Fracture toughness
K_s	Stress optic coefficient
l	Length
L	Length
LMC	Least material condition
LOS	Line of sight
m	Magnification
m	Mass
MMC	Maximum material condition
MoS	Margin of safety
n	Index of refraction
NA	Numerical aperture
NIST	National Institute of Standards and Technology

List of Symbols and Acronyms

OPD	Optical path difference
P	Preload
p	Pressure
PEL	Precision elastic limit
ppm	Parts per million (1×10^{-6})
PSD	Power spectral density
psi	Pounds per square inch
P–V	Peak to valley
Q	Heat flux
r	Radius (distance, i.e., $0.5D$)
R	Radius (of curvature)
RSS	Root sum square
RTV	Room-temperature vulcanization
t	Thickness
T	Temperature
UTS	Unified thread standard
UV	Ultraviolet
x, y, z	Distances in the x, y, or z axis
α	Coefficient of thermal expansion
β	Therm-optic coefficient (coefficient of thermal defocus)
γ	Shear strain
δ	Deflection
ΔT	Change in temperature
Δx	Change in lateral distance (x axis)
Δy	Change in lateral distance (y axis)
Δz	Change in axial distance
ϵ	Emissivity
ε	Strain
ζ	Damping factor
θ	Angle
λ	Thermal conductivity
ν	Poisson ratio
ρ	Density
σ	Stress
σ_{ys}	Yield strength
τ	Shear stress
ω	Frequency
ω_0	Natural frequency (rad/s)

Optical Effects of Mechanical Motion

When an optical element in a system is perturbed, the produced image will be affected. An optical element can be perturbed axially (despace), laterally (decenter), or angularly (tip/tilt).

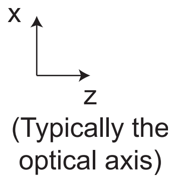

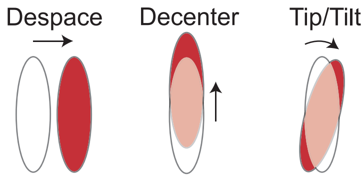

These effects are typically referred to as **line-of-sight (LOS) error**. A dynamic disturbance of the LOS, for example, vibration of a system, is typically called **jitter**. Various sources of jitter in a system can tend to be correlated.

LOS error can be measured from either **object space** or **image space**. If measured from image space, the error shows up as a displacement on the image plane. If measured from object space, the error appears as an angular shift of the object.

The z axis in a coordinate system is typically defined as the **optical axis**, which is the path or direction of light passing through an optical system. It is assumed that this axis passes through the theoretical center of rotationally symmetric elements.

The term *axial* (as in *axial motion*) will therefore refer to the z axis, whereas the term *lateral* refers to the x and y axes.

Lens and Mirror Motion

Lateral motion of a lens will cause both a lateral shift and angular deviation of the light from its nominal path. The magnitude of the shift is a function of the magnification m of the lens:

$$\Delta x_l = \Delta x_i (1 - m)$$

$$\Delta \theta_i \cong \frac{\Delta x_l}{f}$$

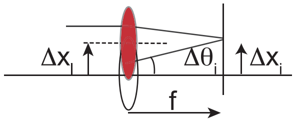

Axial motion of a lens will cause an axial shift of the image focus:

$$\Delta z_l = \Delta z_i \left(1 - m^2\right)$$

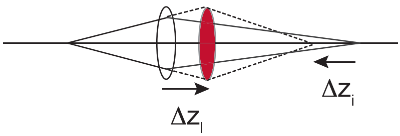

Tilt of a lens will have a negligible effect on image motion; however, aberrations will be introduced into the image.

Regarding **mirror motion**, if a mirror is tilted by a given amount, the light will undergo an angular deviation of twice that amount. If a mirror is displaced axially, the image focus will be shifted by twice the displacement:

$$\Delta \theta_i = 2 \Delta \theta_m$$

$$\Delta z_i = 2 \Delta z_m$$

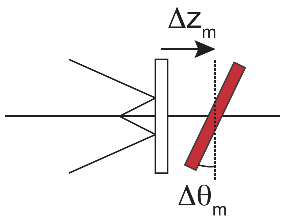

Lateral motion of a flat mirror will have no effect (unless the light falls off the edge of the mirror). **Lateral motion of a mirror** with power will cause the light to undergo an angular deviation, given by

$$\Delta \theta_i \cong \frac{\Delta x_m}{f}$$

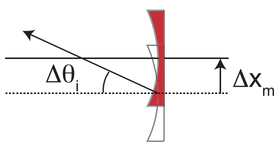

Plane Parallel Plate

Regardless of position or orientation, inserting a **plane parallel plate** in a converging beam will cause a focus shift, given by

$$\Delta z = t\frac{(n-1)}{n}$$

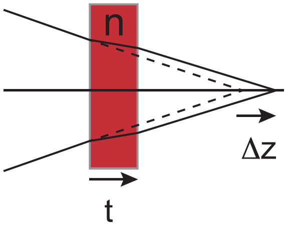

For most glass in the visible spectrum, the focus shift can be estimated by

$$\Delta z \cong \frac{t}{3}$$

Tilt of a plane parallel plate will introduce aberrations and cause a lateral shift in the image, given by

$$\Delta x_i = \frac{t\Delta\theta_p(n-1)}{n}$$

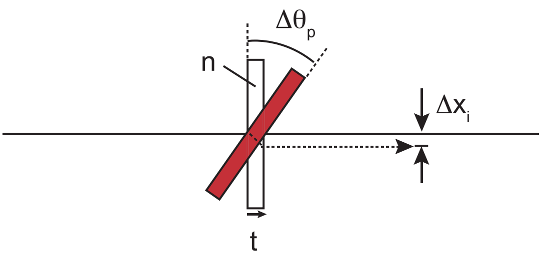

For a 45-deg tilt, the lateral shift can be estimated by

$$\Delta x_i \cong \frac{t}{3}$$

General Image-Motion Equations

The **general image-motion equations** describe the image shift produced by the motion of a single element or group of elements in a system. For tilt or decenter, the amount of image motion can be found by

$$\varepsilon = \frac{D_i \Delta\theta_i}{2NA_{im}} - \frac{NA'_i}{NA_{im}} \Delta y_i$$

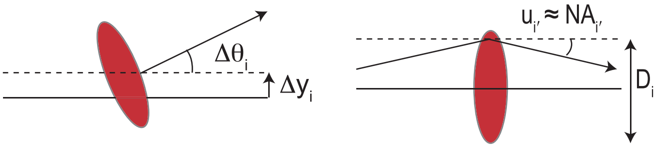

For axial motion of an element or group of elements, the focal shift can be estimated by

$$\Delta z_f = \Delta z_E \left(\frac{NA'^2_i \pm NA^2_i}{NA^2_{im}} \right)$$

or

$$\Delta z_f = \Delta z_E \left(1 \pm m_i^2\right)\left(m_{i+1}^2\right)\left(m_{i+2}^2\right)\cdots\left(m_N^2\right)$$

– for refractive surfaces

+ for reflective surfaces

Δz_f = focal shift from nominal

Δz_E = axial shift of the element(s)

NA_{im} = numerical aperture in the image plane

NA_i = numerical aperture entering element i (estimated by the angle of light entering the element(s) relative to the optical axis)

NA'_i = numerical aperture exiting element i

m_i = magnification of the element(s) in motion

D_i = beam diameter at element i

$\Delta\theta_i$ = change in central ray angle due to perturbation of element i

Image Motion Example

For lens or mirror i with focal length f_i and decenter Δy_i, the resulting **image motion** is

$$\varepsilon \cong \frac{D_i}{2NA_{im}} \frac{\Delta y_i}{f_i}$$

Tilt of mirror j by $\Delta\theta_j$ causes image motion of

$$\varepsilon \cong \frac{D_j}{NA_{im}} \Delta\theta_j$$

Element	Effect of tilt	Effect of axial translation	Effect of lateral translation
Lens	No image motion, adds aberrations	Axial image shift	Lateral image shift, LOS angular deviation
Flat mirror	LOS angular deviation (2× tilt)	Axial image shift (2× translation)	No effect
Powered mirror	LOS angular deviation (2× tilt)	Axial image shift	Lateral image shift, LOS angular deviation
Window	No effect	No effect	No effect

Although some of the perturbations shown here are listed as having no effect, this is for an ideal optic. In reality, imperfections in an element (such as a wedge in a window) mean that a tilt or translation of the component could in fact add to the aberration content of the image or shift the image location. Care should be taken that the motion of an element does not cause the light to fall off the edge of the component or outside of the **clear aperture**.

Rigid Body Rotation

The rotation of a **rigid body** around a single point is equivalent to a rotation around any other point, plus a translation. To calculate the effect of rotating an optical system, the rotation can be decomposed into

- **translation** of the nodal point and
- **rotation** around that point.

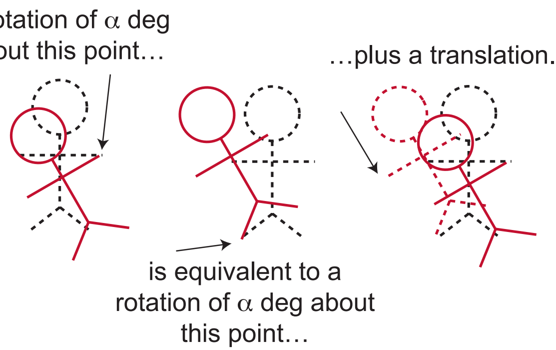

Image motion is caused only by the translation of the nodal point, given an infinite conjugate system.

For example, given a system that rotates a given amount $\Delta\theta$ around point A, the effect can be calculated by

$$\begin{aligned}\Delta\theta \text{ rotation at A} &= \text{rotation at N} + \text{translation from A to N}\\ &= \text{no effect } (0) + (\alpha)(\text{AN})\end{aligned}$$

If an optical system, represented by its principal planes, is rotated around an arbitrary point C, the image motion is given by

$$\Delta x = \Delta\theta\left(\overline{PP'}\right) + \Delta\theta\left(\frac{\overline{CP}}{f}\right)d'$$

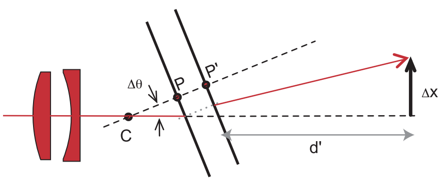

Quantifying Pointing Error

In a given system, many sources of error affect system performance. If each of these causes is independent or approximately independent, the effects combine as a **root sum square (RSS)**. Examples of independent errors include the radii of curvature for each lens, the tilt of one element, or the distortion of an element due to gravity. For each given error x_i, the total error is found by

$$\text{RSS error} = \sqrt{x_1^2 + x_2^2 + x_3^2 + \ldots x_i^2}$$

The total error is dominated by the largest errors, and the smallest contributors are negligible. System performance can be improved most efficiently by *reducing the largest contributors*. The smallest contributors may be increased (by relaxing a requirement) to reduce cost without greatly affecting system performance.

When errors are coupled with each other (e.g., when a group of elements moves together or when multiple elements are positioned relative to a reference surface), the combined effect cannot be found using RSS. Each element contribution should be calculated and summed together, keeping the sign, to find the total system effect.

A useful interpretation of this rule is that by knowing the tolerances x_i to a certain **confidence value**, the RSS then represents the overall confidence level of the analysis. Tolerances are typically defined to a 95% confidence value ($\pm 2\sigma$ for a normal/Gaussian distribution), so the RSS would also represent a net 95% confidence level. NIST provides very detailed online explanations for uncertainty analysis in measurements (see Ref. 1).

Image Orientation

When an image is reflected off of a mirror or travels through a prism, the **orientation** of the image may be altered. A **reverted** image is flipped along a vertical axis, whereas an **inverted** image is flipped along a horizontal axis. An image that experiences a reversion and inversion undergoes a **180-deg rotation**.

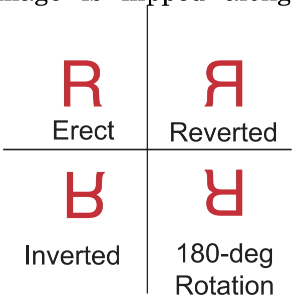

The **parity** of an image describes whether the image is **right-handed** or **left-handed**. If the light experiences an even number of reflections, the image will be right-handed and is said to have "even parity," whereas an odd number of reflections will produce a left-handed image, referred to as "odd parity."

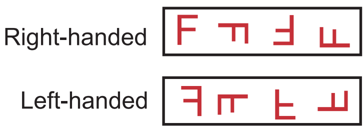

A useful way to visualize image orientation is to use the **pencil bounce trick**. For a reflection in a system, imagine a pencil traveling along the optical axis with a given orientation. "Bounce" the pencil off of the mirror to determine the image orientation for that axis. Repeat this trick with the pencil for each axis to determine the entire image orientation.

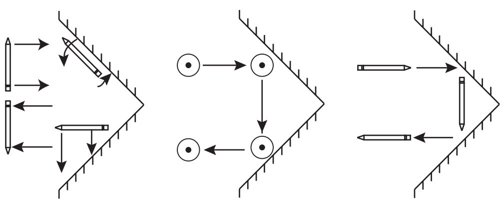

Image Orientation (cont.)

When an object is rotated, the direction of the rotation is named based on the axis of rotation: a rotation in x is called **pitch**, in y is called **yaw**, and in z is called **roll**.

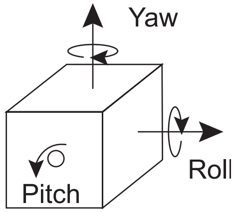

The effect of the image shift from light passing through glass can be accommodated by replacing the glass with an air-space equivalent. If the path length in a glass (with refractive index n) is t, then the **reduced thickness** is t/n.

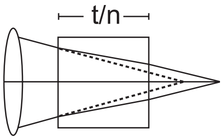

A **tunnel diagram** unfolds the reflections in the optical path through a prism, which permits viewing the path that the light travels. The thickness of a tunnel diagram can be reduced to accommodate the image shift.

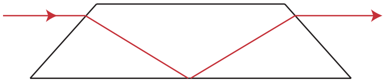

Dove prism

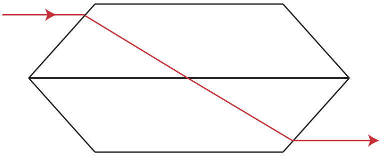

Dove prism tunnel diagram

Mirror Matrices

Matrix formalism can be used to model the reflection of light from plane mirrors. We can represent the x, y, and z components of a light ray with standard vector notation:

Light propagation	Surface normal
$\hat{k}_i = \begin{bmatrix} k_x \\ k_y \\ k_z \end{bmatrix}$	$\hat{n} = \begin{bmatrix} n_x \\ n_y \\ n_z \end{bmatrix}$

For example, light traveling in the z direction would be represented as:

$$\hat{k} = \begin{bmatrix} 0 \\ 0 \\ 1 \end{bmatrix}$$

By multiplying the incoming ray vector with a given **mirror matrix**, the direction of the reflected ray can be determined.

The **law of reflection** states that, under ideal conditions, the angle of incidence of light on a mirror will equal the angle of reflection. This phenomenon can be written in vector notation as

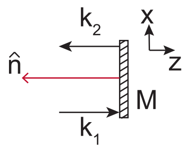

$$\hat{k}_2 = \hat{k}_1 - 2\left(\hat{k}_1 \cdot \hat{n}\right)\hat{n}$$

where $\hat{k}_1$ and $\hat{k}_2$ are the vectors representing the incident and reflected light, respectively. The vector law of reflection can be written in matrix form as

$$k_2 = \mathbf{M} \cdot k_1 \qquad \mathbf{M} = \mathbf{I} - 2\hat{n} \cdot \hat{n}^T = \begin{bmatrix} 1-2n_x^2 & 2n_x n_y & 2n_x n_z \\ 2n_x n_y & 1-2n_y^2 & 2n_y n_z \\ 2n_x n_z & 2n_y n_z & 1-2n_z^2 \end{bmatrix}$$

where **M** is the mirror matrix, and **I** is the identity matrix.

Mirror Matrices (cont.)

Common mirror matrices include the following:

$$\text{Free space: } \mathbf{M} = \begin{bmatrix} 1 & 0 & 0 \\ 0 & 1 & 0 \\ 0 & 0 & 1 \end{bmatrix} \qquad X \text{ Mirror: } \mathbf{M}_x = \begin{bmatrix} -1 & 0 & 0 \\ 0 & 1 & 0 \\ 0 & 0 & 1 \end{bmatrix}$$

$$Y \text{ Mirror: } \mathbf{M}_y = \begin{bmatrix} 1 & 0 & 0 \\ 0 & -1 & 0 \\ 0 & 0 & 1 \end{bmatrix} \qquad Z \text{ Mirror: } \mathbf{M}_z = \begin{bmatrix} 1 & 0 & 0 \\ 0 & 1 & 0 \\ 0 & 0 & -1 \end{bmatrix}$$

As an example, if light is incident at 45 deg on an X mirror (a mirror that has its normal in the x direction),

$$k_2 = \mathbf{M}_x \cdot k_1 = \begin{bmatrix} 0.7 \\ 0.7 \\ 0 \end{bmatrix}$$

$$\hat{n} = \begin{bmatrix} 1 \\ 0 \\ 0 \end{bmatrix} \qquad k_1 = \begin{bmatrix} -0.7 \\ 0.7 \\ 0 \end{bmatrix}$$

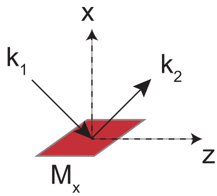

Reflections from multiple mirrors can be represented by reducing the system of reflections into a single 3×3 matrix:

$$\begin{aligned} k_i &= [\mathbf{M}_i \cdots \mathbf{M}_2 \cdot \mathbf{M}_1][k_1] \\ &= \mathbf{M}_{eff} \cdot k_1 \end{aligned}$$

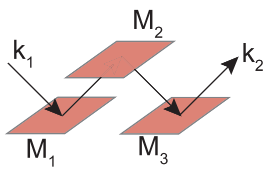

Mirror Rotation Matrices

If a plane mirror is rotated, the following matrix is used for **M**:

$$\mathbf{M}_{rot} = \mathbf{R} \cdot \mathbf{M} \cdot \mathbf{R}^T$$

where the **rotation matrices** are given by:

$$X \text{ Rotation: } \mathbf{R}_x = \begin{bmatrix} 1 & 0 & 0 \\ 0 & \cos\alpha & -\sin\alpha \\ 0 & \sin\alpha & \cos\alpha \end{bmatrix}$$

$$Y \text{ Rotation: } \mathbf{R}_y = \begin{bmatrix} \cos\beta & 0 & \sin\beta \\ 0 & 1 & 0 \\ -\sin\beta & 0 & \cos\beta \end{bmatrix}$$

$$Z \text{ Rotation: } \mathbf{R}_z = \begin{bmatrix} \cos\gamma & -\sin\gamma & 0 \\ \sin\gamma & \cos\gamma & 0 \\ 0 & 0 & 1 \end{bmatrix}$$

Note that a mirror normal to a given axis will be insensitive to rotation in that axis and cause 2θ rotation in each of the other two axes.

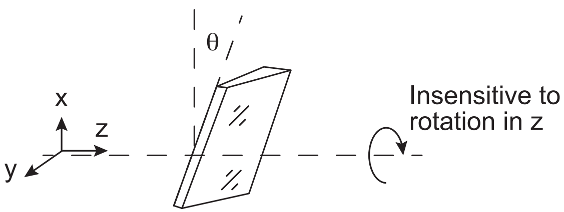

Tilted by θ in y axis
(2θ angular change in y beam direction)

Cone Intersecting a Plane

When a cone of light intersects a tilted plane, for example, when a converging beam is incident on a tilted mirror, a number of **geometric relationships** can be defined (see figure below):

$$W = D + 2L \cdot \tan\alpha \qquad A = E + F$$

$$E = \frac{W \cdot \cos\alpha}{2\sin(\theta - \alpha)} \qquad G = (A/2) - F$$

$$F = \frac{W \cdot \cos\alpha}{2\sin(\theta + \alpha)} \qquad B = \frac{AW}{\sqrt{(A^2 - 4G^2)}}$$

If the beam is collimated, then both $\alpha = 0$ and $G = 0$, and the equations above reduce to:

$$W = D = B \qquad E = F = \frac{W}{2\sin\theta} \qquad A = \frac{W}{\sin\theta}$$

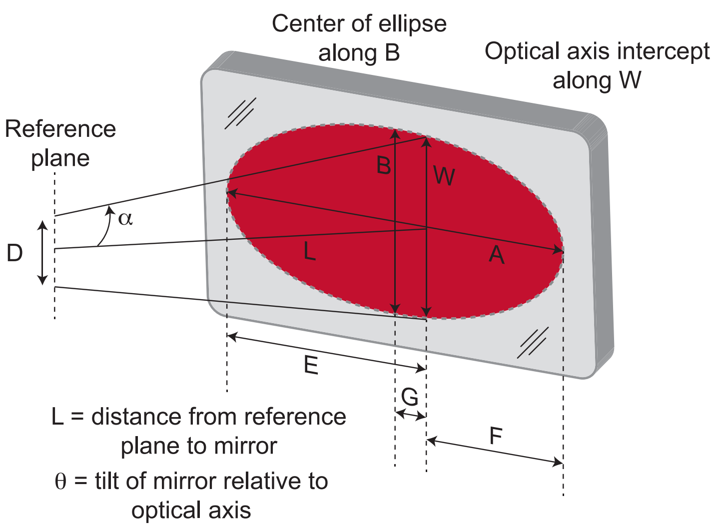

Stress and Strain

In mechanics, a body can be subjected to many forces. The most common way of defining these forces is by classifying them as a **stress** or a **strain**. Stress σ occurs when a body is subjected to a force or load, which is quantified by dividing the applied force F by the cross-sectional area A on which the force is acting. The units of stress are **psi** (pounds per square inch) or **Pascals** (N/m^2).

Pa = N/mm^2
1 psi = 6895 Pa
1 MPa = 145 psi

$$\sigma = \frac{F}{A}$$

This equation assumes that the force is applied normal to the cross-sectional area; when the force is applied tangential to a surface V, it is called shear stress τ:

$$\tau = \frac{V}{A}$$

Strain ε occurs when a body is subjected to an axial force: it is the ratio of the change in length of the body to the original length.

$$\varepsilon = \frac{\Delta L}{L}$$

Shear strain γ, which is a function of the shear modulus of the material G, occurs when the body is strained in an angular way. Strain is unitless, whereas shear strain is expressed in radians. Stress and strain can be the result of a **compressive** or **tensile** force.

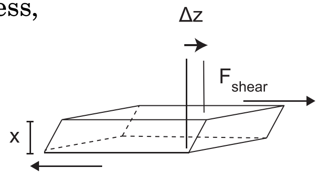

$$\gamma = \frac{\Delta z}{x} \qquad \gamma = \frac{\tau}{G}$$

$$\tau = \frac{dF_{shear}}{dA}$$

$$\varepsilon = \frac{\sigma}{E} \qquad \sigma = \frac{dF_{normal}}{dA}$$

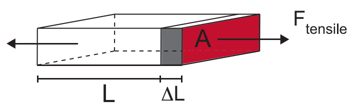

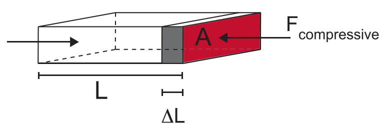

Stress and Strain (cont.)

If a compressive force is placed along one axis of a material, it will bulge or expand in another axis (this is especially true for rubber). This effect is called the **Poisson effect** or **bulge effect**. From this effect, a variable may be defined that describes the change in an object's dimension, relative to the other dimensions, due to a force; this is known as the **Poisson ratio** [$\nu = -(\epsilon_x/\epsilon_y)$], and for most materials it is in the range of 0.25 to 0.35. Rubber is close to the limiting value of 0.5, with volume being conserved.

Another important material property is **Young's modulus** E (also called the modulus of elasticity), which describes the stiffness of a material; it is defined as the ratio of stress to strain. Another useful material property is the **bulk modulus** K, which defines the compressibility of a material under uniform pressure. It is defined as [$(\Delta V)/V = P/K$] or, for isotropic materials, [$K = E/3(1-2\nu)$]. The following relationships are true for a homogeneous, linear, isotropic material:

	(E,G)	(K,G)	(G,ν)
$K =$	$\frac{EG}{3(3G-E)}$	—	$\frac{2G(1+\nu)}{3(1-2\nu)}$
$E =$	—	$\frac{9KG}{3K+G}$	$2G(1+\nu)$
$G =$	—	—	—
$\nu =$	$\frac{E}{2G}-1$	$\frac{3K-2G}{2(3K+G)}$	—
	(E,ν)	(K,ν)	(K,E)
$K =$	$\frac{E}{3(1-2\nu)}$	—	—
$E =$	—	$3K(1-2\nu)$	—
$G =$	$\frac{E}{2(1+\nu)}$	$\frac{3K(1-2\nu)}{2(1+\nu)}$	$\frac{3KE}{9K-E}$
$\nu =$	—	—	$\frac{3K-E}{6K}$

Strain-vs-Stress Curve

A typical **stress-versus-strain curve** for metal is shown below:

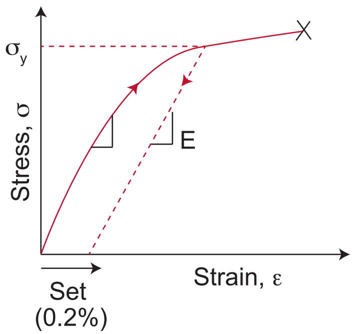

When a material is near its breaking point, it no longer acts in a linear fashion. The stress at which the curve is no longer linear is called the **proportional limit**. As the curve loses linearity, there is a point at which the forces on the body can be released before the breaking point is reached; if this happens, then the body will return to equilibrium. However, at some point the stress and strain will be too great on the material, and it will be permanently deformed. The minimum point at which this occurs is called the **yield strength** σ_y.

When permanent deformation occurs, if the forces are released from the object, the curve will return to zero but with a displacement in the x axis. This displacement is known as the **set**. The **precision elastic limit** (σ_{PEL}) defines when the set is equal to 1 **ppm** (parts per million) (parts per million, i.e., 1 part in 10^{-6}).

The maximum stress a material can withstand before failure is called the **ultimate strength** (X in the figure above) of the material. The stress-vs-strain curve for a glass is slightly different: the relationship is linear up to the point that the glass breaks.

Safety Factor

A **safety factor** describes the ability of a system to withstand a certain load or stress compared to what it will actually experience.

Safety factor = allowed stress / applied stress

For optics and optical systems, *a safety factor of* 2–4 *is typically applied*. Decisions about the safety factors should consider the importance of the application, the familiarity of the materials and conditions, and whether or not personal safety is involved.

The **margin of safety** (MoS) is a measure of the extra capacity or ability of a design. Typically, the MoS is set as a requirement for an application by either a national standard or a regulatory agency/code:

Margin of safety = safety factor – 1

Any positive number implies added safety or capacity over the design load, whereas a MoS of 0 (safety factor of 1) implies that failure is imminent.

Material property	Symbol	Units	Favorable condition
Coefficient of thermal expansion (CTE)	α	10^{-6} m/m/°C	Low
Young's modulus	E	GPa	High
Density	ρ	g/cm^3	Low
Poisson ratio	ν	—	—
Thermal conductivity	λ	W/m-K	High
Thermal diffusivity	D	m^2/s	High
Specific heat capacity	C_p	J/kg-K	Low
Specific stiffness	E/ρ	N-m/kg	High

Glass Strength

Glass is a brittle material, and if it fails, it will typically fail by fracture. Small surface flaws are present in any glass, and when placed under stress, these flaws can propagate and cause catastrophic failure.

- As a conservative rule of thumb, glass can withstand **tensile stresses** of 1,000 psi (6.9 MPa) and **compressive stresses** of 50,000 psi (345 MPa) before problems or failures occur.
- For tensile stress, these limits can be increased to 2,000 psi for polished surfaces or 4,000 psi for instantaneous loads.

Unfortunately, there is no characteristic strength value for a given glass. The tensile and compressive strength of any given optic depends on a large variety of factors, including the area of the surface under stress, surface finish, size of internal flaws, glass composition, surrounding environment, and the amount and duration of the load. In general, glass is weaker with increasing moisture in the air and is able to withstand rapid, short loads better than slow lengthy loads.

Glass failure is always due to the propagation of flaws, but there are a number of ways to model this effect. One method involves looking at the statistical effect of the surface finish on glass failure. The distribution of surface flaws is examined, and failure prediction is based on test data. Another approach assumes that the size of the flaw is known and predicts failure based on fracture mechanics.

Glass corners are fragile—always use a bevel unless a sharp corner is needed (as in a roof for a prism), in which case, protect the corner.

Glass Strength (cont.)

Weibull statistics are commonly used to predict the probability of failure and strength of a glass. This approach assumes that flaws and loads remain constant over time. The mathematical distribution is given by

$$P_f = 1 - e^{-\left(\frac{\sigma}{\sigma_0}\right)^m}$$

P_f = probability of failure

σ = applied tensile stress at the surface

σ_0 = characteristic strength (stress at which 63.2% of samples fail)

m = Weibull modulus (indicator of the scatter of the distribution of the data)

A list of Weibull parameters are shown below for some common glasses (see Ref. 2). These values are a strong function of surface finish. The probability of failure is also displayed for an applied stress of 6.9 MPa (1,000 psi).

Material	Fracture toughness (MPa–$\sqrt{m}$)	m	σ_0 (MPa)	P_f	Surface finish
N-BK7	0.85	30.4	70.6	0	SiC 600
N-BK7	0.85	13.3	50.3	3.36×10^{-12}	D4
N-BaK1	—	8.2	58.9	2.31×10^{-3}	SiC 600
F2	0.55	25	57.1	0	SiC 600
SF6	0.7	5.4	49.2	2.47×10^{-5}	SiC 600
Zerodur®	0.9	5.3	293.8	2.5×10^{-9}	Optical polish
Zerodur®	0.9	16	108	0	SiC 600

Stress Birefringence

For a given stress, a material will fail if a flaw exceeds the critical length a_c:

$$a_c = \left(\frac{K_c}{2\sigma_0}\right)^2$$

a_c = critical depth of flaw
K_c = fracture toughness of glass (material property)
σ_0 = applied tensile stress

The maximum flaw depth can be estimated to be three times the diameter of the average grinding particle used for the final grinding operation.

Stress birefringence is the effect produced when an optic has a different index of refraction for light polarized parallel or perpendicular to the stress. It is expressed in terms of optical path difference (OPD) per unit path length of the light (nm/cm).

Residual stress is always present in glass due to the annealing and/or fabrication process. However, additional stress birefringence can result from stress being placed on the glass. The residual stress present in glass can be quantified by referencing a grade.

Grade	Stress birefringence (nm/cm)
1	≤ 4 (precision annealing)
2	5–9 (fine annealing)
3	10–19 (commercial annealing)
4	≥ 20 (coarse annealing)

Permissible OPD per cm glass path	Typical applications
< 2 nm/cm	Polarization instruments Interference instruments
5 nm/cm	Precision optics Astronomical instruments
10 nm/cm	Photographic optics Microscope optics
20 nm/cm	Magnifying glasses Viewfinder optics
Without requirement	Illumination optics

Stress Birefringence (cont.)

The wavefront retardance between polarization states ΔW_p that occurs in a glass under an applied stress (expressed in waves) can be found by $\Delta W_p = (K_s \sigma t)/\lambda$, where σ is the applied tensile or compressive stress and t is the thickness (path length of light).

The **stress optic coefficient** K_s is a material property expressed in mm^2/N and is typically provided on the data sheet for a given glass; it describes the relationship between the applied stress on a material and the resulting change in **optical path difference**.

As a general estimate, 1 nm/cm of birefringence is incurred for every 5 psi of stress (assuming that $K_s = 3 \times 10^{-12}$/Pa).

Material	Stress optic coefficient (10^{-12}/Pa) at 589.3 nm and 21°C
N-BK7	2.77
F2	2.81
SF6	0.65
N-K5	3.03
N-SK11	2.45
Borofloat borosilicate	4.00
CaF_2	–1.53 @ 546 nm $(q_1 - q_2)$
Fused silica	3.40
Zerodur®	3.00
ZnSe	–1.60

Kinematic Constraint

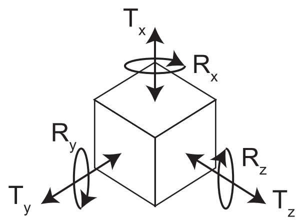

A rigid body has six **degrees of freedom**: translation in X, Y, Z, and rotation in X, Y, Z. Some bodies are insensitive to a given degree of freedom because of their geometry; a sphere, for example, is insensitive to rotation in all axes, so it only has three translational degrees of freedom. When the number of degrees of freedom of an object is reduced by mechanically connecting it to another surface, a **constraint** has been placed on the object. **Rigid constraints** are stiff and do not move; they provide the reaction force necessary to maintain the position of a component. A **preload force** is an applied, constant force that ensures a contact is in compression, but it is *not* a constraint alone.

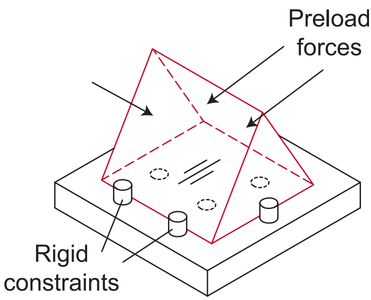

The principle of **kinematic design** is to constrain all of the degrees of freedom of a rigid body without **overconstraint**, a state in which more than one constraint is placed on a particular degree of freedom. Overconstraint typically reduces performance in a system (due to binding and distortions) and can increase cost due to requiring tight tolerances. Conversely, an **underconstrained** system allows unwanted motion and "play" in the parts. A properly constrained kinematic design can provide high stability as well as the ability to separate components and accurately rejoin them.

Example Constraints and Degrees of Freedom

Optical elements in a system must be mounted in a repeatable manner and without distorting the element. A kinematic mount uses ball bearings to provide the necessary motion constraints for a mounted element and the ability to insert and remove the elements as needed. Since point contacts are well defined, submicron repeatability is possible depending on the surface finish, load, and friction.

The ball bearings can be held kinematically in a variety of ways, depending on what **degrees of freedom** need to be constrained:

- **Ball in seat** (three planes, three balls): Constrains all three translational degrees of freedom.

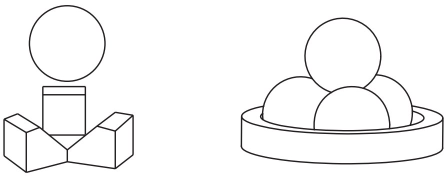

- **Ball in V-groove**: Constrains two translational degrees of freedom. The optimum contact angle of the groove is 60 deg.

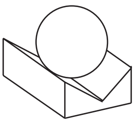

- **Ball on two rods**: Constrains two translational degrees of freedom.

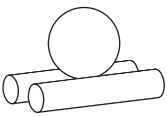

- **Ball on flat surface**: Constrains one translational degree of freedom.

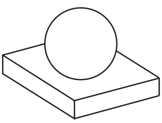

Semi-Kinematic Design

Semi-kinematic design uses the same geometry and ideas as kinematic design but allows slight overconstraint to occur. Point contacts are replaced with small-area contacts to reduce stresses that occur in a purely kinematic design. Additional support points may be added to a purely kinematic design to create a semi-kinematic design, in which case a group of supports may act as a single kinematic constraint.

A practical implementation of this concept is a ball in a cone. This design constrains all three translational degrees of freedom, but it is semi-kinematic because the interface is a line contact rather than a point contact.

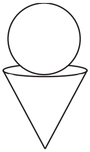

Two common kinematic mount systems are illustrated below: a flat, groove, and seat (top), and three grooves (bottom). A flat, groove, and cone configuration is a common semi-kinematic design used for mounts.

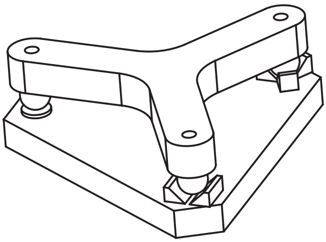

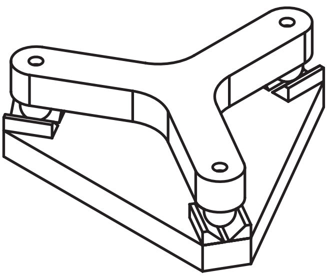

Issues with Point Contacts

Kinematic design assumes infinitely rigid bodies and **point contacts** between parts. There is low **stiffness** at a point contact because a small amount of force can cause displacement of the mount. A preload force in the direction normal to the interface is required for stability. The stiffness k, displacement u, and contact radius a of a ball contacting a flat surface due to a force F can be found using the equations below:

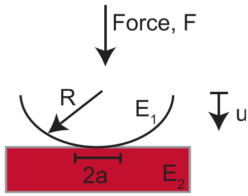

$$u = 0.8\left(\frac{F^2 E_e^2}{R}\right)^{1/3}$$

$$a = 0.9(FRE_e)^{1/3}$$

$$k = \frac{dF}{du} \cong 1.875\left(\frac{RF}{E_e^2}\right)^{1/3}$$

$$E_e = \frac{1-\nu_1^2}{E_1} + \frac{1-\nu_2^2}{E_2}$$

High **stress** can occur at a point contact due to the preload force (normal to the surface) as well as friction (tangential to the surface), which may cause damage to the materials. Lubrication can decrease the stress due to friction. The maximum compressive stress occurs at the center of the point contact and is given by

$$(\sigma_c)_{max} = 1.5\frac{F}{\pi a^2}$$

Issues with Point Contacts (cont.)

A **cylinder** with radius R, applying force F over length L, creates a line contact rather than a point contact. The contact width b and maximum compressive stress can be found by

$$b = 2.3\left(\frac{F}{L}RE_e\right)^{1/2} \qquad (\sigma_c)_{max} = 0.6\left(\frac{F/L}{RE_e}\right)^{1/2}$$

For both spheres and cylinders, the maximum shear stress is approximately one-third of the maximum compressive stress or yield stress:

$$\tau_{max} \cong \frac{(\sigma_c)_{max}}{3}$$

For two convex spheres or cylinders with radii R_1 and R_2, use the equivalent radius:

$$\frac{1}{R} = \frac{1}{R_1} + \frac{1}{R_2}$$

Repeatability is also a concern with point contacts and is a function of geometry. The nonrepeatability per ball or plane interface is given by the following:

$$\rho \approx \mu\left(\frac{2}{3R}\right)^{1/3}\left(\frac{F}{E}\right)^{2/3}$$

μ = friction coefficient
R = ball radius
E = Young's modulus

Friction coefficients vary greatly with system conditions (presence of lubrication, type of lubrication, etc.). Steel on steel has $\mu \approx 0.8$ when it is dry/clean and $\mu \approx 0.16$ when lubricated. Aluminum on aluminum has $\mu \approx 1.25$ when dry/clean and $\mu \approx 0.3$ when lubricated.

Precision Motion

When multiple **precise motions** need to made in a system, **stages** are typically the solution. Stages can be classified as linear, rotational, tilt, or multi-axis. Any type of stage will have a few elements in common:

- **System of constraints**: Allows motion in the desired degree of freedom but constrains other degrees.
- **Actuator**: Drives the stage motion, either electrically or manually.
- **Encoder**: Measures stage motion; the actuator may sometimes serve as the encoder.
- **Lock** (optional): Maintains the stage position.

When choosing a stage for a specific application, some general factors that should be taken into account include:

- repeatability
- resolution
- cost
- errors in motion
- load capacity
- travel range
- encoding accuracy
- stiffness
- stability
- velocity of motion
- overtravel protection
- environmental sensitivity
- locking mechanisms

For a study on the cost and performance tradeoffs for manual linear stages, see page 122 in the appendix.

Specifications for stages are found using various methods. The actual achievable resolution, repeatability, etc., may be very different depending on the user's specific application and operating conditions. Be cautious of claims that seem too good to be true.

Stage Terminology

For **stage** motion, **precision**, also called **repeatability**, refers to how often a stage returns to the same position after repeated attempts. **Accuracy**, also called position error, refers to how closely the stage moves to a desired location. In general, precision can be achieved without accuracy, but the reverse is not true.

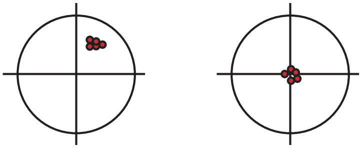

Resolution is the size of the smallest *detectable* incremental motion a stage can make. The more friction that occurs in the bearings, the lower the resolution produced. It is typically defined by the limit of the encoder precision. The **sensitivity** of a stage is the minimum input capable of producing an output. It is often (incorrectly) used to indicate resolution.

Travel range is defined as the length of travel that a stage can provide, typically established by hard stops that mechanically limit motion at each end. Overtravel protection is a feature sometimes used on stages that are controlled electronically, thus avoiding any accidental component collisions.

Angular deviation defines the maximum amount of angular motion that occurs from true linear over the entire travel range of a stage. It is defined in terms of pitch (angular deviation in x), yaw (angular deviation in y), and roll (angular deviation in z).

The **load capacity** of a stage defines the amount of static load that can be held by a stage without adversely affecting the stage motion and resolution. Typically, the load capacity is defined for loads in both the vertical and horizontal direction. To achieve the maximum load capacity tolerated, the load is centered and normal to the stage surface. Overloading a stage can cause damage to the bearings.

Linear Stages

Linear stages provide travel in X, Y, Z, or any combination thereof.

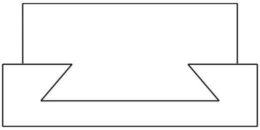

Dovetail stages are the simplest type, consisting of two flat surfaces sliding against each other. This geometry provides high stability, long travel, and large load capacities. Due to the amount of friction, very precise control is difficult.

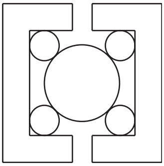

Ball-bearing stages are the most common type, consisting of a single or double row of ball bearings guided by V-grooves or hardened rods. These stages have very low friction and moderate load capacity (depending on the exact ball-bearing geometry used). The **gothic-arch**-style ball bearing has increased contact area over a conventional ball bearing.

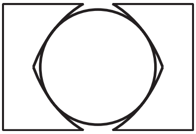

Crossed-roller bearings have the same advantages as ball-bearing stages but with higher stiffness and load capacities. These stages replace ball bearings with orthogonally alternating cylindrical rollers, providing a line contact instead of a point contact.

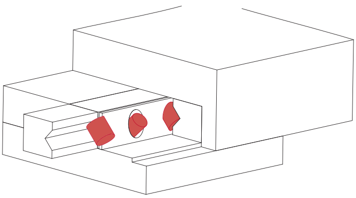

Flexure stages stages provide very high precision motions but typically have a small travel range. These stages use the deformation of a high-yield-strength material to provide motion.

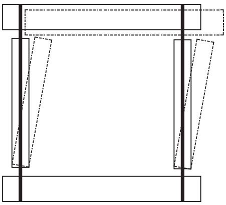

Rotation and Tilt Stages

Rotation stages provide radial motion for a component. The major sources of error for a rotational stage are:

- **concentricity** (**eccentricity**)
- **wobble**
- **axial runout**

Concentricity or **eccentricity** is the deviation of the center of rotation of the stage as it rotates (i.e., the stage is not perfectly centered). **Wobble** is the amount of angular deviation of the axis of rotation that occurs during one revolution. **Axial runout** is the amount of axial motion that occurs during one revolution. A dial indicator can be used to measure each of these errors as the stage is rotated.

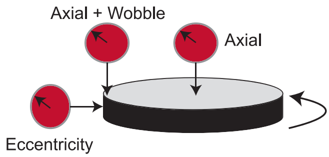

Tilt stages provide angular adjustment in X, Y, Z, or any combination thereof. They are often referred to as tip/tilt stages.

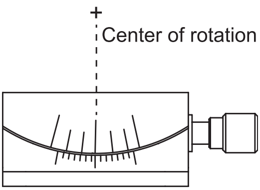

A **goniometer** is a unique tilt stage that has its center of rotation above the stage. The advantage of goniometers is that the motion is purely rotational, whereas traditional **tip/tilt stages** incur a small translation when adjusted.

A **ball-and-socket** stage provides 360-deg tilt in the horizontal and up to ±90-deg tilt from vertical, depending on the specific model. This type of stage provides coarse positioning and a simple lock/unlock lever to manipulate the stage position—useful for positioning detectors and targets.

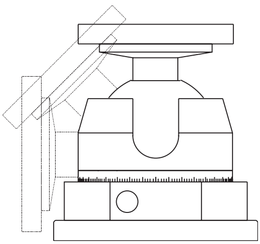

Errors in Stage Motion

Many stages combine translational, angular, and rotational motion. A complicated stage that provides motion in all six degrees of freedom is a **Stewart platform**, a **positioner** with a stage mounted on linkages, or legs, that are free to pivot and rotate at the ends. By adjusting the length of the legs, each freedom of motion may be adjusted individually. This type of stage typically requires software control due to its complexity. One common Stewart platform is a hexapod positioner, which has a stage mounted on six legs.

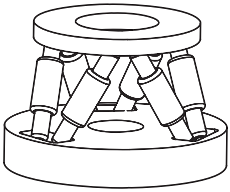

The main error associated with linear stages is **Abbe error** ($\theta \times h$, where h is the Abbe offset), a displacement error between the encoder and the point being measured, which often occurs when a component is mounted on a post. It is caused by an angular error in the bearings, thus tilting the component. Abbe error can be reduced by lowering the height of the component or by using a higher-quality stage to reduce wobble.

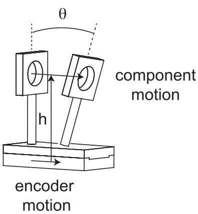

If a stage is traveling in one direction and then moved in the reverse direction, the stage will not reverse immediately. This issue is referred to as **backlash** and is a mechanical error; the motion error corresponding to the nonlinearities that arise from backlash is called **hysteresis**. Backlash is easily noticed with lower-quality stages that have "play" or "slop" in the manual driver. It can be reduced by applying a preload force so that the driver and the stage remain in contact at all times. An error that occurs in multi-axis stages is **cross-coupling**, i.e., the desired motion is in only one axis, but due to the non-ideal nature of a stage, a small motion will occur in another axis.

Standard Hardware

When assembling a system, many standard pieces of hardware can be employed. **Screws** can be used as fasteners and adjusters; they provide a larger range of motion than shims and can be used for one-time adjustments if potting epoxy or a jam nut is used. The resolution of the adjustment is limited by the thread pitch and friction in the joint.

Under the **Unified Thread Standard (UTS)** used in the United States, screws are defined by (diameter in inches) – (threads per inch) × (length in inches), e.g., $^1/_4 - 20 \times 1$. Metric screws are defined by (diameter in mm) × (mm per thread) × (length in mm), e.g., M8 × 1 × 25.

The screw size is noted as an integer number (e.g., a #6 screw) for diameters smaller than $^1/_4$ inch; the formula to calculate the major diameter of a numbered screw (≥#0) is (major diameter) = (screw #) × $0.013'' + 0.060''$.

Many other thread standards are available based on region and application. According to the UTS, screws are typically defined as having "coarse" or "fine" threads that fall into certain thread classes. The coarse-thread series, **UNC**, is the most commonly used series for bulk production. The fine-thread series, **UNF**, is used for precision applications.

Thread classes range from 1–3, followed by either an A (referring to external threads) or B (referring to internal threads).

- Classes **1A** and **1B** are used for quick and easy assemblies where large amounts of clearance are acceptable.
- Classes **2A** and **2B** are the most common classes of thread.
- Classes **3A** and **3B** have very tight tolerances and allow no clearance in assembly.

Example Screws

Common screw-drive types:

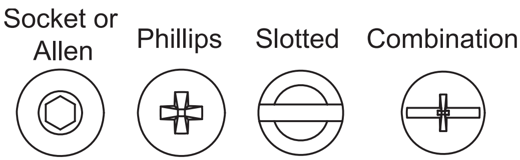

Common screw-head styles:

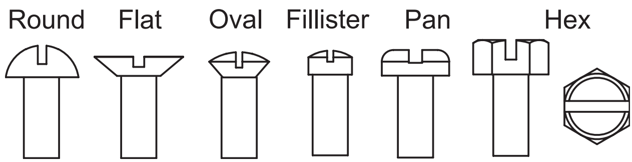

Common socket-head screws:

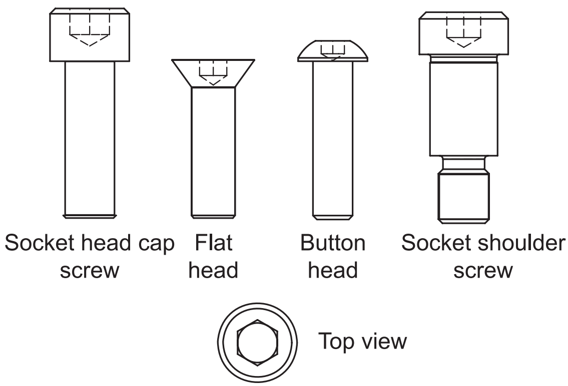

Tapping is the process by which threads are cut into the inside surface of a hole. The proper-size tap must be chosen for a fastener of a given diameter and thread pitch. To obtain a tap drill size, use the following formula and drop all but the first decimal:

$$\text{Root diameter} \approx \text{screw diameter} - \text{thread spacing}$$

Fastener Strength

The first three threads of a screw take about three-quarters of the entire load. The remaining quarter load is taken by around the sixth thread. Since this is the case, having an engagement length for the screw that is longer than 1.5× the nominal diameter provides almost no added strength. The actual load distribution in the threads varies depending on a variety of factors, including the materials used, the setup, and the size of the load. Some special fasteners (e.g., Spiralock®) are designed to provide a more evenly distributed load across the first 5–6 threads for applications where the load distribution is a concern.

Under the English system, the strength level of a fastener is given by its **grade**. For the metric system, the strength level is given by its **property class**. Note that similar numbers for grade and property class do not mean similar strengths. The strength of the threads is greater than the **strength of the fastener** as long as the threads are engaged over one diameter.

English			
Grade	**Head marking**	**For inch diameters**	**Tensile strength (psi)**
2	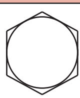	1/4 to 3/4	74,000
		7/8 to 1 1/2	60,000
5	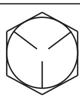	1/4 to 1	120,000
		Over 1 to 1 1/2	105,000
8	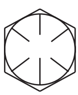	1/4 to 1 1/2	150,000

Fastener Strength (cont.)

Metric			
Property class	**Head marking**	**For metric diameters**	**Tensile strength (psi)**
5.6	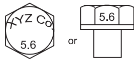	M12–M24	72,500
8.8	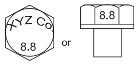	M17–M36	120,350
10.9	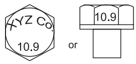	M6–M36	150,800

Socket head cap screw markings:

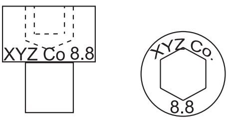

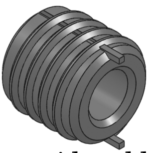

When using fasteners in soft materials, including aluminum, **threaded inserts** should be used for added robustness. These are small coils of strong metal material that can be inserted into a tapped hole. They can provide added strength, robustness, corrosion resistance, and act as a repair for stripped threads. There are a large variety of styles and types of threaded inserts as well as varying materials and lengths. Care should be taken as to what metals are being used for the threaded inserts and the fastener that will come into contact with them. There is a higher likelihood that **galling** will occur if the same material is used for both components.

Galling is a form of surface damage that occurs when solids are rubbed together. Material is transferred from one surface to another, creating abrasive surfaces and increasing adhesion. Galling causes concern because it cannot be remedied once it has occurred and will usually cause some loss of functionality in the affected part. Anti-galling threaded inserts are available as well as special inserts for vacuum applications (e.g., Nitronic®).

Tightening Torque

Tightening torque values are calculated from the following formula:

$$T = KDP$$

where T is the tightening torque, K is the torque-friction coefficient, D is the nominal bolt diameter, and P is the bolt clamp load developed by tightening.

The **clamp load** is also called **preload** or initial load. It is calculated by assuming that the usable bolt strength is 75% of the bolt proof load multiplied by the tensile stress area of the threaded section of each bolt size. Higher or lower values can be used depending on the application requirements and judgment of the designer.

Washers can serve many functions, such as protecting a surface from the screw head, providing an even load distribution from the screw head, providing a seal, or acting as a shim or spring.

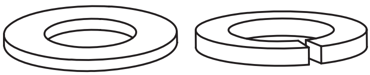

There is a wide variety of washers available for various functions and geometries required by a system. Some provide locking abilities, pressure sealing, bonding, or vibration-damping. Others are slotted, clipped, countersunk, square, or flanged. See the Torque Charts in the appendix for suggested tightening torque values to produce corresponding bolt clamping loads.

Adjusters

Small mechanical adjustments are often needed in the assembly and use of optical systems. **Adjusters** should be chosen to provide adequate resolution in the desired degree of freedom while all other degrees of freedom remain fully constrained. It is important to consider:

- the total range of the adjustment needed
- how often the adjustment must be made
- the required stability for all degrees of freedom
- the required stiffness

Oftentimes, both a coarse and fine adjustment are required.

Common **manual drivers** for stages include thumbscrews and micrometers. **Micrometers** provide a way to measure the amount of motion per revolution of the driver, whereas **thumbscrews** simply provide a way to move the stage.

Push-pull screws are an adjustment mechanism in which two screws are used to move a plate relative to a fixed baseplate. This device controls only one degree of freedom, but it provides a large range of motion combined with fine resolution. The system can be made self-locking using jam nuts or epoxy; however, this arrangement can cause distortion and stress in the mechanical parts. Push-pull screws are not as stable as shims and are limited by thread pitch and friction. Off-the-shelf solutions that provide this type of motion area are available as well, such as Micposi.

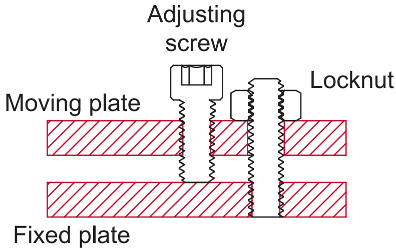

Differential Screws and Shims

A **differential screw** is an adjustment mechanism that uses two screws with different thread pitches. The resultant motion of the adjuster is proportional to the difference in the two pitches, allowing for finer resolution than a screw with a single-thread pitch.

Thread pitch refers to the crest-to-crest spacing between threads. If a screw is specified as having 20 threads/in, then the distance between each thread (the thread pitch) is 0.05″.

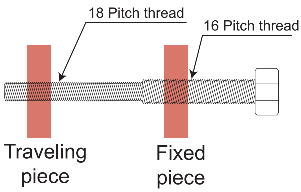

If the thread pitches TP_1 and TP_2 are such that $TP_2 > TP_1$, then the resultant thread pitch (TP_{eff}) of the differential screw is:

$$\mathrm{TP}_{eff} = \mathrm{TP}_2 - \mathrm{TP}_1$$

As an example, using 1/4–20 ($\mathrm{TP}_2 = 0.05''$) and 1/4–28 ($\mathrm{TP}_1 = 0.036''$) threads, each rotation moves the screw 0.05″, but the nut (traveling piece) only moves 0.014″. The effective pitch of 0.014″ is equivalent to 70 threads/in.

Shims are thin pieces of material used for one-time spacing adjustments and are a very stable solution. A variety of shim types exist for various functions. Note that before deciding to use shims, a good way to determine the required spacer thickness is needed. There are also a variety of **washer** types that can provide small adjustments or act as shims.

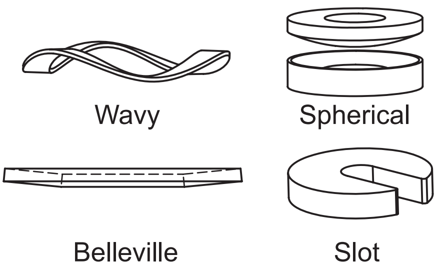

Liquid Pinning

Liquid pinning is a useful way to fix a component after adjustment, whereby adhesive is applied in a thin layer around a fixed pin in a hole. This procedure provides room to adjust a component around the pin as well as a locking mechanism; liquid pinning is a common method used for fixing a lens cell after centration adjustments. The radial stiffness k_r of a liquid pin is given by

$$k_r = \frac{\pi}{2}\frac{d_p L_p}{r_a}\left(\frac{E_a}{1-\nu_a^2}+G_a\right)$$

d_p = pin diameter

L_p = length (height) of adhesive bond in contact with pin

r_a = average radial thickness of adhesive around the pin

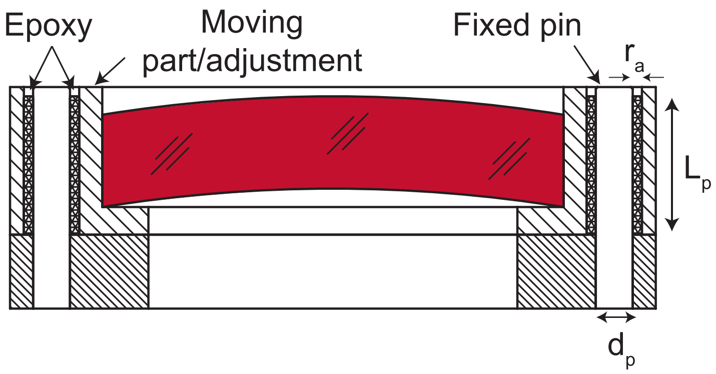

An alternate format for liquid pinning involves placing a bushing around each pin. The adhesive is then applied to the hole and bushing rather than directly to the pin, allowing the component to still be removed.

Electronic Drivers

Common **electronic drivers** include steppers, DC servo or brush motors, and piezoelectric actuators. **Stepper motors** provide a specific number of discrete steps in response to electrical current. **Microsteppers** are also available that provide small increments of motion within a full step. Stepper motors will remain in the same position even when power is removed, whereas a microstepper will move to the nearest full step if power is removed.

Servos provide high speed, resolution, and accuracy, but low stability with time. They require constant power or an external brake to maintain their position if power is removed.

Piezoelectric actuators use crystals that expand contract when voltage is applied to them. They can provide very high-resolution motion over a limited travel range. Piezos suffer from nonlinearities and hysteresis effects, and require constant power to maintain position.

An **open-loop-control** device provides automated motion control, but it does not measure that motion or receive feedback about how accurately the motion was made. These devices can provide very small motions and are relatively inexpensive. Many piezoelectric devices and stepper motors use open-loop control.

In a **closed-loop-control** system, the motion of the stage is measured and compared to the desired input to determine the amount of error. This feedback can be provided using a variety of techniques, all with various levels of accuracy. Position, velocity, and/or torque feedback are typically required, depending on the specific application. The system then corrects the error, providing more accuracy than is available with open-loop-control systems. Servo motors are often closed-loop systems.

Flexures

Flexures provide a means of precise adjustment using the elastic deflection of materials due to an applied force; they can provide very rigid constraints in certain directions while still maintaining compliance in others. Flexures have low hysteresis, low friction, and are suitable for small rotations (<~5 deg) and translations (<~2 mm). They can also provide mechanical and thermal isolation of an optical element from its housing. Flexures typically cannot tolerate large loads, and there must be low residual stress in the flexure from fabrication.

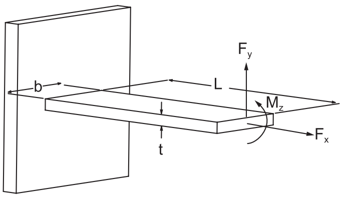

Large tensile loads may be tolerated in one direction, based on the geometry of the flexure. The most simple and common type of flexure is the **single-strip** or **leaf**, useful for small rotations.

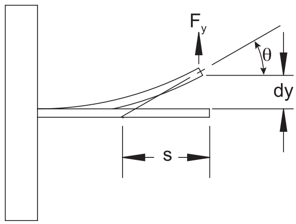

We define the blade length L, Young's modulus E, thickness t, and width b; the moment of inertia $I = (1/12)bt^3$.

The material choice for a flexure will depend on a variety of factors, including the material's compliance, fracture toughness, thermal properties, corrosion resistance, and stability over time. The greatest compliance, given the same length flexure, is achieved by the material with the greatest **reduced tensile modulus**, defined as the ratio of the yield strength σ_{ys} of the material to Young's modulus E. The higher the reduced tensile modulus is, the more desirable the material for use as a flexure.

Flexure material	E (GPa)	σ_{ys}/E (10^{-3})
Stainless steel 17-4	193	4.39
Titanium 6AL-4V	108	7.27
Invar 36	148	4.75
Beryllium copper	115	7.14
Aluminum 6061-T6	68	3.85

Stiffness Relations for Single-Strip Flexures

For simple loading, the **stiffness relations** are

$$\kappa_{\theta_z} = \frac{M_z}{\theta_z} = \frac{EI}{L} \qquad k_y = \frac{F_y}{dy} = \frac{3EI}{L^3} \qquad k_x = \frac{F_x}{dx} = \frac{Ebt}{L}$$

$$\frac{F_y}{\theta_z} = \frac{2EI}{L^2} \qquad \frac{M_z}{dy} = \frac{3EI}{L^3}$$

where κ is used for the bending stiffness. The maximum stress in the flexure is

$$\frac{6M}{bt^2} \quad \text{or} \quad \frac{6FL}{bt^2}$$

The stiffness relations change in the presence of a tensile (T) or compressive (C) force F_x, which is positive for T and negative for C:

$$\kappa_{\theta_z} = \frac{M_z}{\theta_z} = \begin{cases} \dfrac{EI}{L}\omega \coth\omega \text{ (T)} \\ \dfrac{EI}{L}\omega \cot\omega \text{ (C)} \end{cases} \cong \frac{EI}{L}\left(1 + \frac{F_x L^2}{3EI}\right)$$

$$k_y = \frac{F_y}{dy} = \begin{cases} \dfrac{F_x \omega}{L[\omega - \tanh(\omega)]} \text{ (T)} \\ \dfrac{F_x \omega}{L[\tan(\omega) - \omega]} \text{ (C)} \end{cases} \cong \frac{3EI}{L^3}\left(1 + \frac{2}{5}\frac{F_x L^2}{EI}\right)$$

$\omega = \sqrt{\dfrac{F_x L^2}{EI}}$ Critical buckling limit is $\omega = \pi/2$.

As a rule of thumb, limit the compressive force to 20% of critical.

For small deflections, consider the end motion as a rotation around a virtual pivot at distance s from the end:

$$s = \frac{dy}{\tan\theta_z} \approx \frac{2}{3}L$$

Parallel Leaf Strip Flexures

Two **parallel leaf strips** can be used for small translational motions in a **rectilinear** or **parallel spring guide**. The stiffness relations for simple loading are

$$\kappa_{\theta_z} = \frac{M_z}{\theta_z} = \frac{Ebtd^2}{2L} \qquad k_y = \frac{F_y}{dy} = \frac{24EI}{L^3} = 2Eb\left(\frac{t}{L}\right)^3$$

$$k_x = \frac{F_x}{dx} = \frac{2Ebt}{L}$$

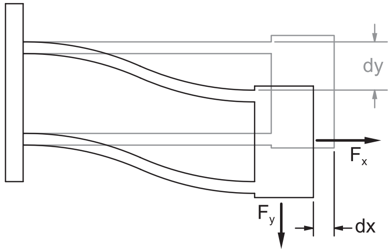

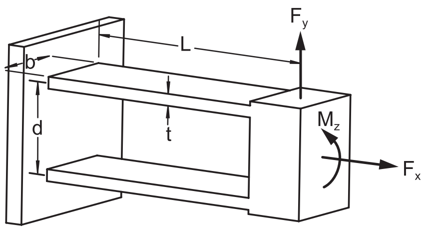

The motion due to the bending of the blades is not purely parallel; the resulting axial motion is

$$dx = -\frac{2}{3}\frac{dy^2}{L}$$

The part will rotate if the flexures have different length ΔL or if the flexures are not parallel, with separation varying by Δd over the length:

$$\text{Flexures differ in length: } \theta = \frac{\Delta L}{2L}\frac{dy^2}{d}$$

$$\text{Flexures not parallel: } \theta = \frac{\Delta d}{L}\frac{dy}{d}$$

Stiffness Relations for Parallel Leaf Strip Flexures

The **stiffness relations** change in the presence of a tensile (T) or compressive (C) force F_x, which is positive for T and negative for C:

$$k_y = \frac{F_y}{\delta y} = \begin{cases} \dfrac{F_x}{L}\dfrac{1}{\left(1-\dfrac{\tanh\gamma}{\gamma}\right)} & \text{(T)} \\ \dfrac{F_x}{L}\dfrac{1}{\left(\dfrac{\tan\gamma}{\gamma}-1\right)} & \text{(C)} \end{cases} \cong \frac{2Ebt^3}{L^3}\left(1+\frac{3}{5}\frac{F_xL^2}{Ebt^3}\right),$$

$$\gamma = \sqrt{\frac{F_xL^2}{8EI}}$$

Cross-strip pivots allow rotation with two or more flat strips that attach between a fixed base and a moving platform. These are commercially available and are useful for applications that require larger angular deflections.

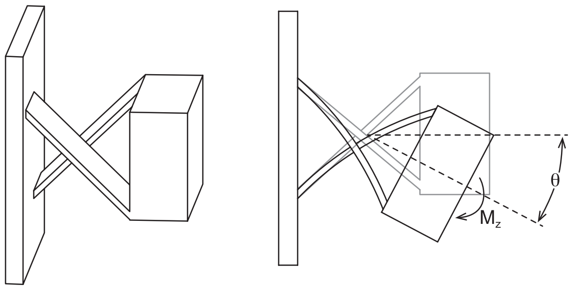

For small deflections, the axis of rotation is located at the intersection of the blades. The stiffness of the two-blade system under simple loading is given by

$$\kappa_{\theta_z} = \frac{M_z}{\theta} = \frac{2EI}{L}$$

The stiffness is increased proportionally with additional blades; a three-blade design is common.

Notch Hinge Flexures

The **notch hinge** is also a common geometry for flexures. These provide added stiffness over a leaf hinge and have a better-defined center of rotation. Examples include the **leaf**, **circular/elliptical**, and **toroidal hinge**.

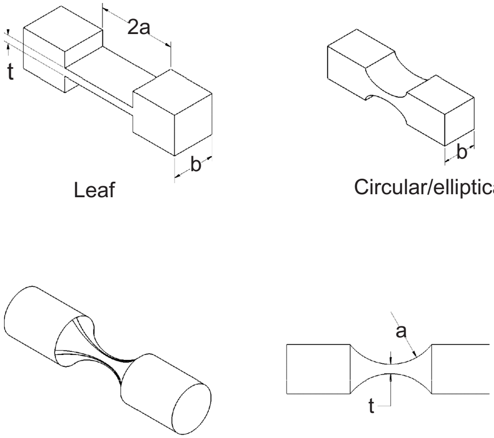

Leaf

Circular/elliptical

Toroidal

The bending stiffness $\kappa_\theta = (M_z/\theta_z)$, axial stiffness $k_x = (F_x/\delta_x)$, and maximum bending stress σ_y are given below, assuming $t \ll a$.

	Leaf	**Circular**	**Toroidal**
κ_θ	$\dfrac{Ebt^3}{24a}$	$\dfrac{2Ebt^{5/2}}{9\pi a^{1/2}}$	$\dfrac{Et^{7/2}}{20a^{1/2}}$
k_x	$\dfrac{Ebt}{2a}$	$\dfrac{Eb^3}{12\pi a^2}\left(\sqrt{\dfrac{a}{t}}-\dfrac{1}{4}\right)^{-1}$	$\dfrac{Et^{3/2}}{2a^{1/2}}$
σ_y	$\dfrac{6M}{bt^2}$	$\dfrac{6M}{bt^2}$	$\dfrac{30M}{t^3}$

Hinge flexures are frequently used to control the line of action for a support member. If properly designed, the line of action of the force will go through the center of the hinges.

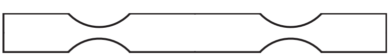

Adhesives

Adhesives are useful for mounting and bonding optical and mechanical components; compared to glass and metal, they typically have high Poisson ratios, low stiffness, and much higher CTE values. Using an adhesive is a relatively quick, simple, and inexpensive mounting solution commonly used in optomechanics.

- **Adhesion** is the bonding of two dissimilar materials to each other (in this case, an adhesive to a substrate). The **adhesive strength** is limited by the preparation of the surface and is improved with the use of a primer.
- **Cohesion** is the force of attraction between similar molecules that determines the internal strength of a material. The **cohesive strength** is the fundamental limit of the strength of the adhesive material.

With static loading, most adhesives will creep, which mitigates slowly varying stresses in the bond (e.g., those due to temperature changes).

Optical adhesives are used to cement optical components together (e.g., doublets and achromats). The optical qualities of the adhesive are important: the adhesive must be transparent in the appropriate wavelength. **Structural adhesives** are used for the mechanical parts of a system; it is important that they have high strength and high stiffness. **Elastomers** are rubbery adhesives used for sealing, providing compliance, and providing athermalization between metals and/or glasses.

Cyanoacrylates (i.e., superglue) are used for thread locking and have high strength, good adhesion to metal, and rapid cure times; however, they have a high potential to ruin optical coatings due to their high outgassing—they are not recommended for use in the vicinity of coated optics.

Adhesive Properties

Issues to keep in mind when using adhesives:

- Surface preparation and cleanliness are critical.
- Curing can be accelerated with a higher temperature, which usually increases bond stress.
- Adhesives have limited shelf lives.
- Two-part adhesives are sensitive to mixing ratios.
- If the bond is critical, it is important to test to failure.
- Recommended safety factor is >3.

Important **adhesive properties** to consider when choosing an adhesive include strength, stability, stiffness, thermal issues, outgassing, cure time, viscosity, shrinkage during curing, and ease of assembly and disassembly.

Outgassing is the process by which adhesives release materials in gaseous form. These released molecules can then condense and contaminate optical surfaces and coatings. This process is most severe in a vacuum or at elevated temperatures, but adhesives can also outgas at room temperature. Outgassing is quantified by **percent total mass lost (%TML)** and **percent collected volatile condensable material (%CVCM)**. NASA provides requirements for these values of <1% TML and <0.1% CVCM for space applications, which should be followed for optical applications. NASA also maintains a very useful database of the outgassing properties of adhesives and other material (see Ref. 3).

In many designs, the **stiffness** k of the adhesive is an important design parameter. Stiffness is defined as the amount of force required to create a unit deflection depending on the geometry and modulus of the material used. Using the correct modulus value is important for proper analysis of adhesive behavior. Typically, stiffness is defined by

$$k = \frac{EA}{t}$$

Compliance c is the inverse of stiffness ($c = 1/k$) and is used to describe how much "give" a material has.

Adhesive Thickness and Shape Factor

When the thickness of the adhesive is very small compared to the area of the bond, the bulk modulus K is used in place of Young's modulus. For shear stiffness, the shear modulus G is used in place of Young's modulus.

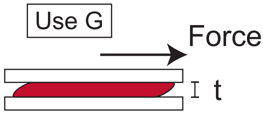

$$k = \frac{KA}{t} \qquad k_{shear} = \frac{GA}{t}$$

There is a transition area between using Young's modulus versus the bulk modulus. When using a bond that is neither explicitly "thick" nor "thin" compared to the area of the bond, a general axial stiffness can be determined by using the effective modulus E_c:

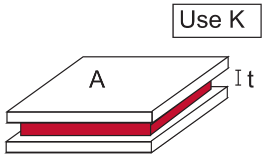

$$E_c = E\left(1 + 2\varphi S^2\right)$$

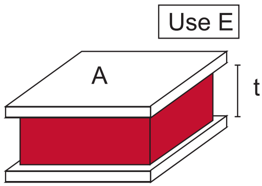

where φ is the material compression coefficient (~0.6 for RTV), and S is the shape factor.

The **shape factor** applies the effect of the geometry to the compression modulus and is defined as the ratio of the load area to the bulge area:

$$S = \frac{A_L}{A_B}$$

where A_L is the load area, and A_B is the bulge area. As an example, for a rectangular bond, the shape factor is:

$$S_{rect} = \frac{(length)(width)}{2t(length + width)}$$

Thermal Stress

The thermal expansion of an adhesive is typically much higher than the substrates it is bonding. The effect due to the large expansion of the adhesive is mitigated by its high compliance, so the substrate expansion dominates. This is not true for very low temperatures where the modulus of the adhesive will increase by orders of magnitude. The maximum shear stress τ_{max} experienced by the adhesive will occur at the farthest point from center and is quantified by

$$\tau_{max} = \frac{\Delta T G(\alpha_1 - \alpha_2)}{Bt}$$
$$\times \left\{ \frac{1}{1+\nu_1} \left[\frac{1-\nu_1}{Br} - \frac{I_0(Br)}{I_1(Br)} \right] + \frac{1}{1+\nu_2} \left[\frac{1-\nu_2}{Br} - \frac{I_0(Br)}{I_1(Br)} \right] \right\}$$
$$B = \left[\frac{G}{t} \left(\frac{1}{E_1 h_1} + \frac{1}{E_2 h_2} \right) \right]^{\frac{1}{2}}$$

where G is the shear modulus of the adhesive, α_1 and α_2 are the coefficients of thermal expansion of the bonded materials, t is the bond thickness, E_1 and E_2 are the Young's modulus values of the bonded materials, h_1 and h_2 are the height/thicknesses of the bonded materials, and r is the maximum bond dimension from the center to the edge (radius).

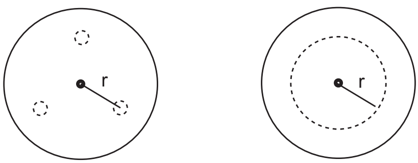

This equation assumes flat, circular plates where the bond covers the entire area between the two substrates. The bending of the substrates is included in the equation. For small bonds (with a maximum dimension less than a few mm), this can be estimated by:

$$\tau_{max} = \frac{Gr}{t}(\alpha_1 - \alpha_2)\Delta T$$

Choice of Bond Size and Thickness

When **bonding materials**, one large bond or multiple small bonds may be used. Using multiple small bonds reduces induced distortions and minimizes thermal effects, but will provide less stiffness and increase stress in the adhesive. The minimum area of the bond can be found by

$$A_{min} = (m a_g f_s)/J$$

where m is the mass of the optic, a_g is the worst-case expected acceleration factor (in g's), f_s is the safety factor (2–5 is recommended), and J is the shear strength of adhesive. This equation may also be used to determine the maximum acceleration a bond of a given size can withstand. The bond should have even thickness over the entire area to prevent imparting a moment and causing distortion of the bonded elements. To maintain correct spacing for an adhesive thickness, spacers, wires, or shims of the desired thickness can be placed evenly on the bonding surface. Another approach involves mixing small glass beads having diameters equal to the desired thickness into the adhesive before bonding.

For **cemented doublets**, the thickness of the adhesive is typically around 8–12 μm, depending on a variety of factors, including the $f/\#$ of the optics, adhesive properties, and the specific application. A typical procedure for cementing optical elements has the following steps:

1. Thoroughly clean the surfaces to be bonded and check for dust (using interference fringes).
2. Raise the upper element enough to place the determined amount of adhesive onto the exposed lower element.
3. Set the upper element on the adhesive and slowly move in all lateral directions.
4. Ensure precise alignment using a jig (often three-point equispaced contacts on each element).
5. Verify the thickness of the bond around the entire area to ensure uniformity. This can be done by measuring the edge thickness around the rim after cementing.

Lens Mounts: Off the Shelf

The accuracy in mounting a lens is limited by the tolerancing of a number of lens parameters. These include but are not limited to:

- outer diameter
- center thickness
- sag
- optical and mechanical axis
- wedge
- edge flat

A variety of **commercial off-the-shelf (COTS)** lens mounts are available for optical systems. Off-the-shelf mounts have the advantage of shorter lead times and lower cost than a custom design. Changing the lens held by a COTS mount is quick and simple, and most mounts can be used for a variety of lenses.

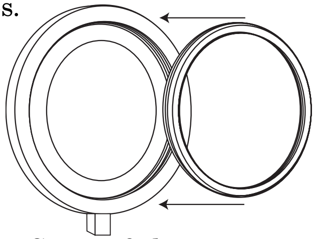

When choosing a mount, note that shorter-focal-length lenses will be more susceptible to centration errors.

A **cell and threaded retaining ring** is a common way to mount lenses with high stability. Some of these mounts include two-axis adjusters for centration control. However, there is no tilt adjustment, and because the retaining ring is a specific size, only lenses with that particular diameter can be held by the mount.

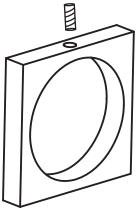

A **cell and set screw** is a simple, low-cost, and low-precision edge mounting device. This mount has low stability, and it poorly controls centration and tilt. The set screw should contact the lens edge at its center to avoid imparting a moment in the glass. Nylon-tipped set screws are typically used with this configuration to avoid stressing the optic.

Lens Mounts: Off the Shelf (cont.)

A **snap ring** (or **retaining ring**) provides another simple, low-cost, low-precision mounting method.

In this mount, a ring is "snapped" into a groove made in the cell holding the lens. Either clearance must be allowed or else the cell should be heated and the ring cooled for easy assembly.

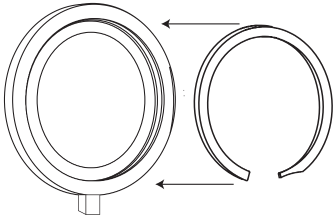

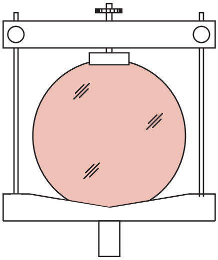

The **V-groove clamp mounts** are low-cost and low-precision pieces but are able to accommodate a large range of lens diameters. The lens sits in a V-base, and a clamp holds the lens down from the top. No tilt adjustments are available, and the centration must come from adjustments to the height of the support post.

An **adjustable-diameter mount** has three lateral supports equally spaced around the diameter of the lens. Each support can be adjusted individually, allowing for different diameters to be mounted with the ability to center the lens. Good centration is difficult with this mount, and no tilt adjustments are available.

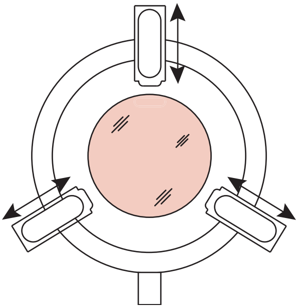

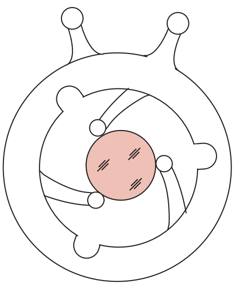

The **three-pronged lens mount** will self-center lenses with a spring-loaded clamp of three prongs. Because of the automatic centration capabilities, this mount is slightly more expensive than other off-the-shelf mounts. Tilt errors are also typically present.

Lens Mounting: Custom

In general, the two main approaches to custom mounting an optical component are **clamping** and **bonding**.

Pros and cons of bonding:

- One-time assembly, difficult to take apart
- Stiff in normal direction, compliant in shear
- Allows for adjustment before curing
- Possibility of outgassing that can affect coatings
- Large CTEs can cause stresses over temperature
- Provides some compliance, reduces stress from shock loading
- Requires careful surface preparation and may require special jigs and procedures

Pros and cons of clamping:

- Allows for disassembly
- Can easily separate constraint and preload force
- Can cause large stresses and affect survival
- Can cause distortions
- Can be designed for thermal expansion

Placing a lens in a **cell** and securing it in place with a **threaded retaining ring** is a common clamping method for holding lenses with good stability.

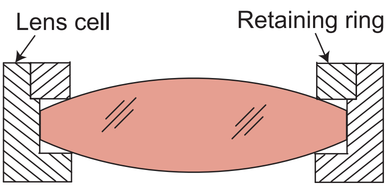

As little force as possible should be imparted on the lens. The retaining ring and cell should contact the lens at the same diameter to avoid imparting a moment on the lens. Class-1 (or possibly 2) threads should be used on the retaining ring to maintain a loose thread fit. An O-ring can be placed in the retainer to reduce stress on the lens.

Calculating Torque and Clearance

By holding the lens in place with an axial preload, like that imparted by a retaining ring, the mount can help the system survive certain acceleration levels. The preload needed for a given acceleration can be estimated as $P = ma_g$, where a_g is the acceleration factor (times gravity).

The **preload torque** for the retaining ring is given by

$$P = Q/[D_T(0.577\mu_M + 0.5\mu_G)]$$

where μ_M and μ_G are the coefficients of sliding for metal-to-metal and glass-to-metal, respectively, Q is the applied torque, and D_T is the thread pitch diameter.

Black anodized aluminum has μ_M of about 0.19, whereas anodized aluminum against polished glass gives a μ_G value of about 0.15. Friction-coefficient values can vary greatly depending on the specific system conditions. For common metal and glass types, this equation is approximately $P = (5Q)/(D_T)$.

Typically, the glass has a lower coefficient of thermal expansion than the metal mount, so **clearance** should be included between the cell wall to account for thermal changes. An estimate of the amount of required clearance is as follows:

$$\text{clearance} = (1/2)(\Delta T)(D)(\alpha_c - \alpha_g)$$

where D is the lens diameter, and α_c and α_g are the cell and glass CTE, respectively.

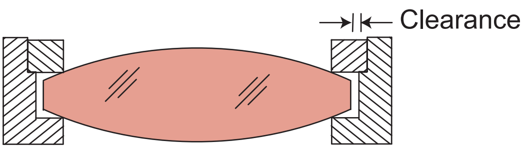

A negative clearance indicates an interference, which produces stress in both the lens and the cell (see the page on Determining Thermally Induced Stress for an example). For large temperature increases, the preload is reduced due to the expansion of the metal away from the glass, possibly allowing the optic to shift.

Potting a Lens with Adhesive

Using an **elastomeric adhesive** for **potting a lens** in its holder is a simple mounting technique that allows for looser edge tolerances on lenses and mounts; elastomer is inserted between the lens edge and the retainer to hold the optic in place. UV-curing compounds are especially quick for assembly. The elastomer is typically injected with a syringe into injection holes in the mount. The lens should be centered before injection and kept centered with a jig during curing.

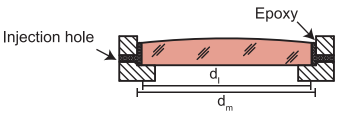

Care should be taken in choosing the adhesive to avoid those that outgas and haze surfaces. Elastomeric mounting makes it difficult to disassemble a system at a later point in time if adjustments need to be made. If the elastomer layer is thick enough, the lens will essentially be athermalized in the radial direction (the epoxy will deform to compensate for changes in material length). To calculate the bond thickness for an athermalized bonded mount, the **Bayar equation** can be used, which is a simple equation that considers only the radial thermal expansion.

$$h = \frac{d_l(\alpha_m - \alpha_l)}{2(\alpha_a - \beta_m)}$$

It assumes that $\alpha_a > \alpha_m > \alpha_l$ (where the subscripts represent the adhesive, mount, and lens, respectively) and that there is no axial or tangential strain in the adhesive. This equation is generally not the most accurate for a continuous bond around the circumference of an optic. It can serve as an approximation, however, for the upper limit of the bond thickness in a system with multiple bond segments around the circumference. The **van Bezooijen** or **Muench equation** provides improved accuracy by allowing the adhesive to expand in the tangential and axial directions. The lower limit for an athermal bond is continuous around the optic circumference:

$$h = \frac{d_l}{2} \frac{(\alpha_m - \alpha_l)}{\alpha_a - \alpha_m + \frac{2\nu}{1-\nu}\left(\alpha_a - \frac{\alpha_l - \alpha_m}{2}\right)}$$

Clamped Flange Mount

Another method of holding lenses (as well as mirrors and windows) involves a **flange retainer** that is clamped against the optical component. This setup is especially useful for lenses with apertures large enough that a retaining ring would prove difficult to manufacture. The preload of a flange is more easily calculated and calibrated than a retaining ring. By threading the outside of the cell, a threaded cap can be used in place of screws for the clamping force to be continuous around the mount rather than in discrete places.

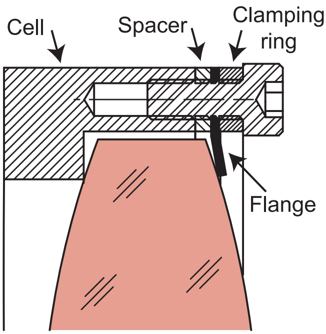

Stray light is a term that refers to any unwanted light that propagates through an optical system. Stray light can cause a variety of issues, including loss of image contrast and multiple images. For applications where it is important to minimize these effects, the edges of lenses are often blackened. Typically, a black epoxy ink is used, although COTS lenses are available that are edge blackened.

Another method of reducing stray light involves using **baffles** or **baffle threading**. Baffles are a series of vanes, flanges, or sharp edges that force light outside the field of view of the system to undergo multiple reflections, thereby blocking or reducing the amount of stray light that reaches the image plane. Simple coarse threading on the inside of a metal spacer or barrel can sometimes provide sufficient baffling for a system.

Lens Barrel Assemblies

The most common assembly method when mounting multiple lenses involves inserting them into a **metal barrel**. Assembling a system in a barrel provides protection from the environment and simplifies the system alignment. A number of factors can be considered when choosing a barrel material; favorable materials have low CTE and density (reduces weight), high stiffness, are corrosion resistant, easily machined, and can be blackened (to reduce stray light). Aluminum is the most common barrel material due to its low cost and ease of machining. Stainless steel is also popular because it has a low CTE and high stiffness. The lens system is often assembled with the barrel vertical by using a vacuum tool to pick up the lenses outside of their clear aperture and lower them into the barrel.

- The barrel is often given a 25–50-μm larger diameter than the lens outer diameter to provide room for loading the optics without jamming.
- Relief grooves or vent holes should be created in the barrel to relieve pressure when inserting elements into the barrel.
- The retaining rings and spacers should contact the lenses at the same diameter that the seats do; this avoids imparting a moment in the lens, causing distortion.
- The axial location of the lenses should not be determined by the retaining rings. Tightly fitted rings can cause stress in the lenses due to wedge error. To avoid this problem, either the fit of the retaining rings should be loose or some compliance should be provided (i.e., an O-ring). The lens position should be defined by machined seats in the barrel or by precision spacers.

After the system is assembled, it should be **sealed** to prevent dust, water, or other contaminants from entering the barrel. O-rings, adhesives, or internal pressurization in the barrel with dry gas are common sealing methods.

Lens Barrel Assembly Types

There are a number of ways to approach barrel mount designs, depending on system requirements; the most common barrel designs are shown below and on the next page in order of increasing accuracy and complexity.

In a **straight-barrel** design, all lenses are the same diameter and are separated by **spacers**. The assembly is typically held secure by a threaded **retaining ring** at the end.

- Simple, low-cost, easy assembly
- Precision limited mainly by the precision of the elements

Common-bore-diameter barrel: uses spacers to maintain element spacing.

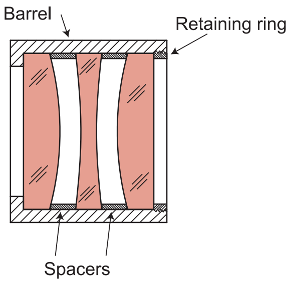

A **stepped-barrel design** can accommodate lenses of varying sizes and uses spacers and/or **machined seats** to hold the lenses at the proper separation. If the seats are machined into the barrel, tight tolerances are required on the wedge of each lens.

- More complex machining required than a straight barrel, easy assembly
- Precision limited by the machining: 50 μm is common, 10 μm is possible

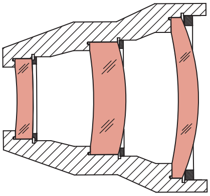

Stepped-diameter barrel: uses machined seats to place lenses.

Lens Barrel Assembly Types (cont.)

Spacing adjustments can be included for additional precision. One method adds shims to adjust for measured errors. Another method enters as-built data into a lens-design program and then machines the spacers to compensate for errors and optimize performance.

- Labor intensive
- Can achieve 25 μm easily, 5 μm is possible

Sometimes a **lateral adjustment** is included for one or more of the lenses in the barrel, providing the ability to decenter the lens during assembly to compensate for a specific aberration. The best element for this adjustment is usually determined by sensitivity analysis in a lens-design program.

- Labor intensive
- Can achieve 10 μm easily, 1 μm is possible

In **subcell mounting**, individual lenses are centered in their own subcell and fixed with adhesive. The subcells are then press (interference) fitted into a parent barrel, wherein centering is achieved by the tolerancing and form of the metal cells rather than the lenses.

Because it is easier to control the form of machined metal components than of polished optical elements, this process greatly improves the centering accuracy more than is traditionally possible. Subcell mounting has a higher cost for components and is more complex, but it is economical for assembly and for fulfilling difficult requirements; thus, it is commonly used in high-performance systems.

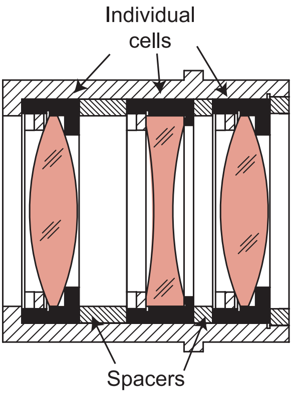

- Very labor intensive and expensive
- Can achieve 10 μm easily, < 1 μm is possible

Surface–Contact Interfaces

There are a few different ways the edges of a glass optic can interface with its mount.

A **sharp-corner contact** occurs when the glass sits on the corner of the mechanical mount. This contact provides the highest accuracy and is the easiest to fabricate and tolerance. However, a sharp corner can create high local stresses in the glass.

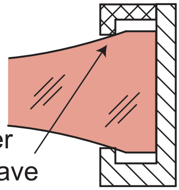

In practice, a true sharp corner is rarely produced. Typically, it will have a small radius. If the retainer has a specific controlled radius in the design, it is called a **toroidal contact**. This type of contact can be used for convex or concave surfaces and is seen in many high-quality assemblies due to the reduced compressive stress from the sharp-corner contact. The **maximum compressive axial stress** σ_a a lens will experience due to a preload force F on a retainer with radius R can be estimated by

$$\sigma_a = 0.4\sqrt{\frac{F}{2\pi y}\frac{E}{R}}$$

where y is the height at which the retainer contacts the lens, and R is the radius of curvature of the retainer edge, typically ~0.05 mm.

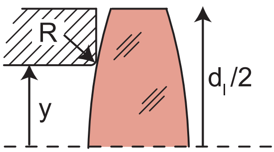

This estimation assumes that the Young's modulus values of the glass and metal are similar (ΔE <~ 25 GPa).

Surface–Contact Interfaces (cont.)

A **tangential contact** occurs when the mechanical mount contacts tangentially to the glass. This contact has relatively low stress and can be fabricated fairly easily. It cannot be used with concave surfaces; however, a flat can put on the edge of the glass to provide a seat for the retainer.

$$\sigma_a = 0.798\left[\frac{\frac{F}{2\pi y d_l}}{\left(\frac{1-\nu_l^2}{E_l}\right)+\left(\frac{1-\nu_r^2}{E_r}\right)}\right]^{\frac{1}{2}}$$

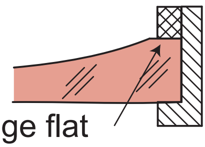

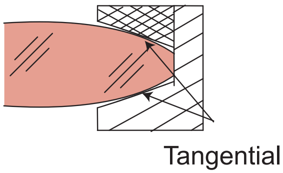

Conical mount contacts tangentially to glass.

A **spherical contact** occurs when the mechanical mount and glass have the same radius. This contact has the lowest stress but is very difficult to fabricate and tolerance and thus is the most expensive option.

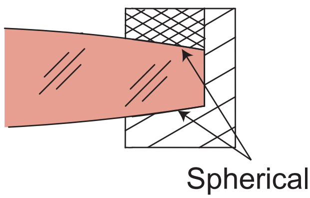

Mount and glass have same radius of curvature.

When a compressive contact stress occurs at an interface, a tensile stress also occurs as a result. Experience and data show that when a retaining ring is pressed against a lens, the tensile stress field is so small that performance is not affected.

Prism Types

Prisms are versatile optical components that can serve a variety of purposes in an imaging system. They are most commonly used to bend light at specific angles, fold an optical system to make it more compact, alter image orientation, or displace an image, among other functions. Prisms that have entrance faces that are tilted relative to the incoming beam should only be used in collimated light. Flat entrance surfaces can be used for collimated, converging, or diverging light.

A **roof** is often added to prisms to provide an additional 90- or 180-deg deviation in a given axis. The roof is insensitive to rotation in that axis and causes 2θ rotation in each of the other two axes.

A **rhomboid prism** is a direct-vision prism. It displaces incoming light without rotation or deviation. It is insensitive to rotation in all axes and is commonly used as a periscope or to create a binocular image. A binocular image requires two rhomboid prisms with a right angle (RA) prism cemented to one and a block of glass (B) used to create equal path lengths.

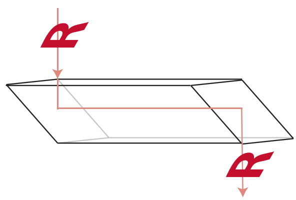

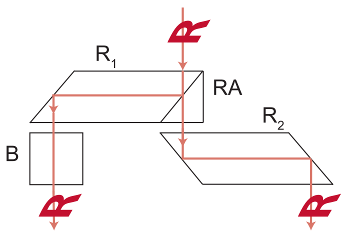

Prism Types (cont.)

A **right-angle prism**, **penta prism**, and **Amici roof prism** all provide a **90-deg beam deviation**. The penta prism has the special property of being insensitive to pitch, which means that in the plane of reflection, there is a constant deviation regardless of the incidence angle of the light. Thus, the penta prism is useful for systems such as optical range finders and for surface testing for large mirrors.

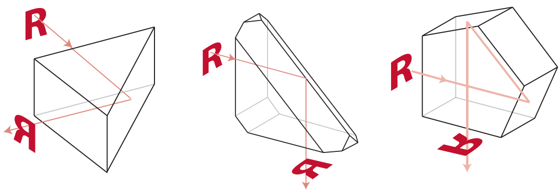

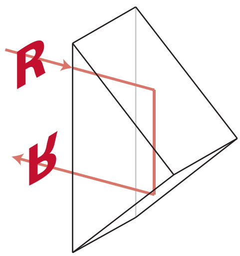

A **Porro prism** provides **180-deg deviation** and is also insensitive to pitch. A **cube corner prism** is a corner cut from a glass cube, forming a tetrahedron. Light entering the cube corner is reflected in a direction anti-parallel to the incoming ray, regardless of the prism orientation. This feature has a wide range of applications such as interferometry, transmitter/receiver systems, and arrays for commercial retroreflectors. A mirror version is also commonly used (a **hollow cube corner**) and has the advantage of reduced weight and a larger wavelength range than the refractive version.

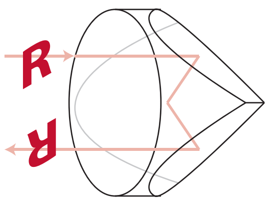

Image-Rotation Prisms

When a **Dove prism** is rotated by an amount θ around the optical axis, the image will be rotated by 2θ. A **double Dove prism** can be formed by attaching two Dove prisms at their hypotenuse faces. This arrangement can be used to scan the LOS of a system with collimated light over 180 deg. Multiple double Dove prisms can be cemented together to form an array.

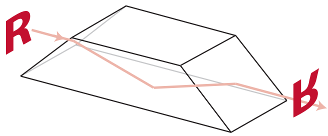

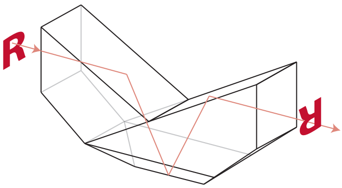

An **Abbe rotation prism** can be folded to form a **reversion** or **K prism**.

A **Pechan prism** is very compact and expensive. It can accommodate a wide field of view and can be used in converging, diverging, or collimated beams.

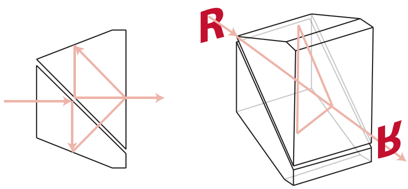

A **Schmidt prism** is a compact image rotator that has a 90-deg roof. It is commonly employed as an image-erecting system in telescopes.

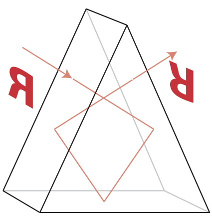

Image-Erection Prisms

The following prisms are commonly found in binoculars and telescopes to erect inverted images. The previous two prisms are often combined into a system called a **Pechan–Schmidt prism** or **Pechan–Schmidt roof**.

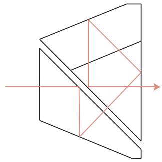

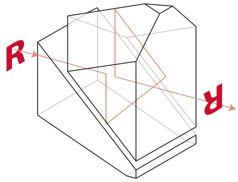

When two Porro prisms are oriented at 90 deg to each other, they create a **Porro prism pair** or **Porro erecting system**.

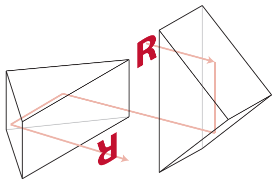

Using **prism matrix formalism**, a matrix can be written for each of the prisms shown above. Incoming light is defined as a unit vector in x, y, and z:

$$\begin{array}{c} \begin{array}{ccc} x & y & z \end{array} \\ \begin{bmatrix} 1 & 0 & 0 \\ 0 & 1 & 0 \\ 0 & 0 & 1 \end{bmatrix} \end{array}$$

When light exits the prism, it has a new coordinate system x', y', and z'. By defining the new system in terms of the original, a matrix can be formulated to describe the effect of the prism on the incoming light orientation. See also Mirror Matrices section.

Matrix construction of a penta prism

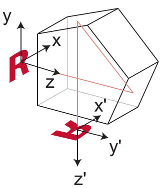

$$x' = x$$
$$y' = z$$
$$z' = y$$

$$\begin{array}{c} \begin{array}{ccc} x' & y' & z' \end{array} \\ \begin{bmatrix} 1 & 0 & 0 \\ 0 & 0 & -1 \\ 0 & 1 & 0 \end{bmatrix} \end{array}$$

Prism and Beamsplitter Mounting

In general, a **prism mount** should avoid contact with optically active areas, including those that provide total internal reflection. Mounting on surfaces that are at right angles to the optically active surfaces will help to minimize deflections. For any mounting approach, kinematic principles of mounting should be followed (i.e., six points should uniquely constrain the element).

If direct contact between a prism mount and an optically active surface is unavoidable, the flatness and coplanarity of the surfaces are critical. The permissible irregularity for the mounting surface can be estimated by

$$\partial_T = \frac{(W+F)h}{SE}$$

∂_T = irregularity tolerance for mount

W = weight of prism/window

F = clamping force on prism/window (= W if not clamped)

h= prism/window thickness

S = contact area between surface and mount

A very common mounting method for glass-to-metal interfaces is **bonding**. The bonding method is simple and quick, and often used for less rigorous applications (see figure). For large prisms, the prism is often bonded on two faces. The guidelines presented in the Adhesives section in regards to choice of adhesive, bond size, and thickness should be followed for bonding prisms. It is important that excess adhesive does not pool around the edge of the metal-to-glass interface, as this can cause added stress and distortion on the glass over temperature.

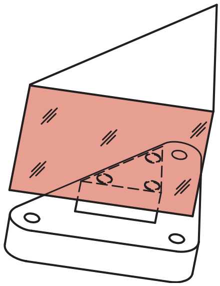

Prism and Beamsplitter Mounting (cont.)

For larger prisms or applications where minimizing mechanically or thermally induced distortions is critical, **flexures** may be bonded onto the prism and then attached to the metal. If the flexures are one axis, they should be compliant in the direction of the center of gravity of the prism. To reduce stress in the bonds, the flexures may be compliant in three directions.

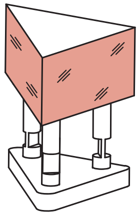

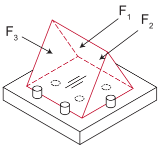

Prisms may also be mounted using **clamps** or by a **preload force** (i.e., **spring and locating pins**).

A flat pad on a spring provides a preload with an area contact, or a cylindrical pad can be used for a line contact. A **table and clamp** is one low-cost, off-the-shelf mount available for prisms and **beamsplitters**. The component sits on a kinematic mount table, held by gravity and a clamping arm. The mount then provides angular adjustment in all three axes.

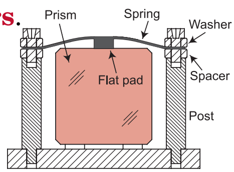

Filters typically have the easiest mounting requirements:

- Small distortions do not affect transmitted wavefront
- No need for sealing
- Position requirements not important (although some filter coatings are sensitive to the angle of incidence of the light)

Many off-the-shelf mounts discussed in the Lens Mounting section can also be used to mount filters. Additional filter mounts include a spring-loaded holder or potting the filter into a bezel.

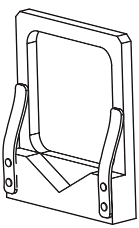

Thin-Wedge Systems

A **thin-wedge prism** creates a small angular deviation in a beam as well as chromatic dispersion. Because the apex angle is typically small, take sin $\alpha \approx \alpha$, and the deflection of the wedge is given by

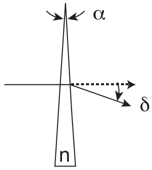

$$\delta = \alpha(n-1)$$

A **Risley wedge-prism system** is a pair of identical wedge prisms most commonly used for beam steering applications. By independently rotating the prisms in opposite directions, light entering normal to the prism face can be angularly deviated anywhere within a given cone angle.

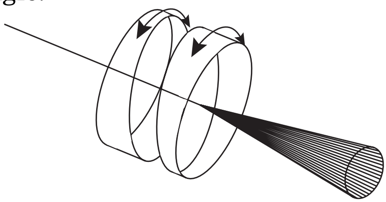

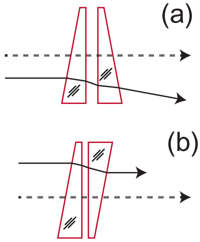

When the prism apexes are adjacent to each other (a), the maximum angular deviation is achieved. When the prism apexes are opposite each other (b), the system acts as a plane parallel plate and simply shifts the beam path.

An **anamorphic prism pair** is a pair of wedge prisms used to magnify light in one axis (in the plane of refraction) while leaving the beam in the orthogonal axis unchanged. These prisms are often used to circularize elliptical diode laser beams.

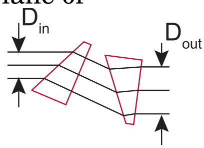

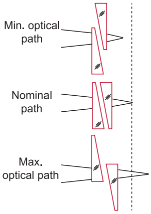

A **focus-adjusting wedge system** contains a pair of identical wedge prisms that can be laterally translated individually. The optical path through the glass can then be varied, allowing the system to image objects at various distances onto a fixed image plane.

Window Mounting

Windows are commonly used in systems where there is need for protection or isolation from the environment while still providing a transparent path through which light can travel. Windows are typically plane parallel plates that are transmissive at the required wavelength(s). Although the tilt of a window is not often important, the distortions induced by mechanical mounts, thermal changes, or pressure differences are critical. This is especially important when a window is near a pupil or stop, where it affects the transmitted wavefront the most. Windows placed near an image should be free of defects and dust because these can appear in the image.

Some additional issues to consider when designing and mounting windows are:

- strength
- wedge angle
- surface figure
- if the window needs to be sealed and how
- bowing due to pressure or temperature differential
- impact and erosion resistance
- loss of strength due to surface defects

The conventional mounting method for windows is to seat the window in a cell and secure it with a retainer. In systems that do not have large temperature changes, the retainer can be screwed onto the cell.

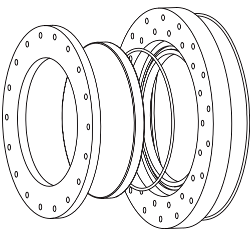

A common window mount includes a top plate, window, O-ring, bottom plate/cell in which the window sits, and second O-ring.

Window Mounting (cont.)

A flexure retainer that is screwed onto the cell can be used to provide some athermalization. One or more O-rings can be used as a pressure seal and to separate the glass-to-metal contact.

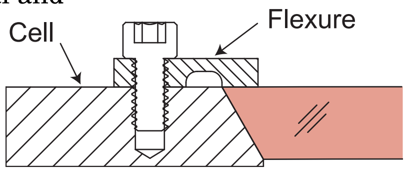

A window can also be **potted** into a cell using an adhesive. A retaining ring may or may not be included with a potted window. Shims can be used to hold the window at a fixed thickness from the cell edge and adhesive injected into small holes along the diameter of the cell. After curing, the shims can be removed and the resultant gaps filled with adhesive. Alternatively, but resulting in less reliability, adhesive can be applied to the window and cell edge before the window is placed in the cell. Excess adhesive should be cleaned off before curing.

Sapphire is a common window material due to its hardness and scratch resistance. Other common materials used for windows include fused silica, silicon, ZnS, ZnSe, MgF_2, and CaF_2. A window is often used where there are thermal or pressure differentials in a system. Thermal distortions in windows are covered in the Thermal Effects section. A simply mounted circular window with uniform loading will experience a change in OPD when there is pressure differential, given by

$$OPD \cong \left(8.89 \cdot 10^{-3}\right)\left[\frac{\left(n-1\Delta P^2 d^6\right)}{E^2 h^5}\right]$$

The minimum aspect ratio for a circular window with a pressure differential is given by:

$$\frac{h}{d} = C_{SF} C_{sp} \left(\frac{\Delta P}{\sigma_S}\right)^{\frac{1}{2}}$$

where C_{SF} is the safety factor, σ_S is the allowable stress on the window, and C_{sp} is the support condition. The support condition is 0.2165 for a clamped window and 0.265 for a simply supported one.

Window Mounting (cont.)

The thickness of a rectangular window can be estimated by the following relations, which include a safety factor of 4:

$$h \approx b\left[\left(\frac{P}{\sigma_{ys}}\right)\frac{3}{1+2\left(\frac{a}{b}\right)^3}\right]^{\frac{1}{2}} \qquad \text{Simply supported}$$

$$h \approx b\left[\left(\frac{P}{\sigma_{ys}}\right)\frac{2}{1+2\left(\frac{a}{b}\right)^4}\right]^{\frac{1}{2}} \qquad \text{Clamped}$$

where a = width of the window and b = length of the window.

The fundamental frequency for a simply supported circular window can be estimated by

$$f_{n-circ} = \left(\frac{\pi}{4}\right)\left(\frac{1}{r^2}\right)\left[\frac{gEh^2}{12\rho\left(1-\nu^2\right)}\right]^{\frac{1}{2}}$$

and for a simply supported rectangular window by

$$f_{n-rect} = \left(\frac{\pi}{2}\right)\left(\frac{1}{a^2}+\frac{1}{b^2}\right)\left[\frac{gEh^2}{12\rho\left(1-\nu^2\right)}\right]^{\frac{1}{2}}$$

Domes

One type of window is a **dome**, which is a deep shell that may be a section of a sphere or a hemisphere. Domes are typically used for systems that have a wide field of view that cannot be accommodated by a flat window. They are also advantageous for high-pressure differentials due to their added strength over a flat window. **Hyperhemispheres** are domes that reach beyond 180 deg.

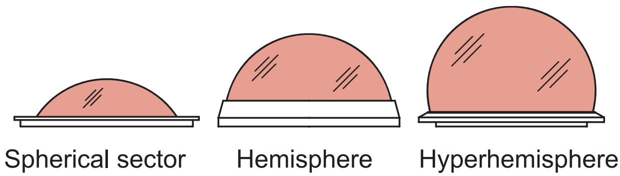

Typical mounting geometries include elastomeric mounting to a flange or directly to the system, clamping and sealing with an O-ring or elastomer, and brazing the optic to the housing.

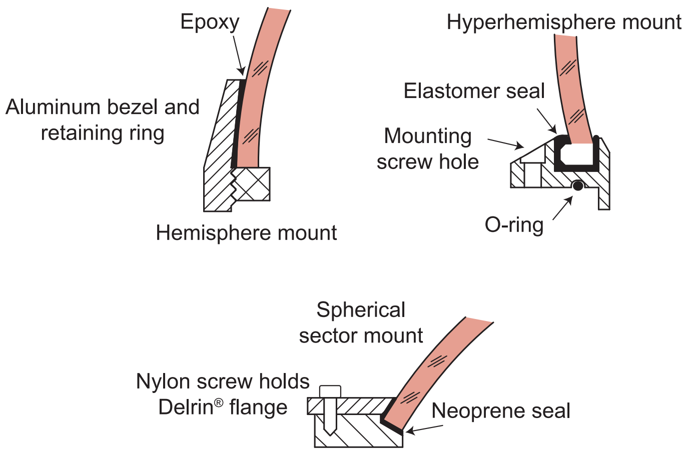

Dome Strength

It is typically more pertinent to evaluate the strength of a dome by calculating what stresses it will undergo than to determine what deformations will occur. **Dome stress** can be evaluated by using the **Lamé pressure vessel equations**:

$$\sigma_m = \sigma_h = -P\frac{R_0^3\left(R_i^3 + 2r^3\right)}{2r^3\left(R_0^3 - R_i^3\right)}$$

$$\sigma_r = -P\frac{R_0^3\left(r^3 - R_i^3\right)}{r^3\left(R_0^3 - R_i^3\right)}$$

Usually, if the dome is a hyperhemisphere, assume that the meridional membrane stress is twice the hoop membrane stress.

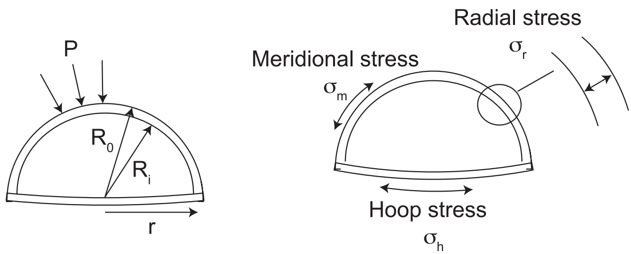

When the thickness of a dome is 10% or less of the radius, the dome can be classified as a **thin dome**, and simpler equations can be used:

$$\sigma_m = P\left(\frac{r}{h}\right)\frac{1}{1+\cos\varphi} \qquad \sigma_h = P\left(\frac{r}{h}\right)\left(\frac{1}{1+\cos\varphi} - \cos\varphi\right)$$

where h is the dome thickness ($\varphi = 0$ at the top of the dome and $\varphi = 90$ at the base). The strength of a glass dome can be approached in the same way as the strength of a lens (see page on Glass Strength). The equations for thin and thick domes can be applied to a self-weight-loaded dome as well. Domes can fail due to elastic buckling, so the critical pressure P_{cr}, which causes elastic instability, should also be calculated:

$$P_{cr} = \frac{0.8E}{\sqrt{1-\nu^2}}\left(\frac{h}{R_0}\right)^2$$

Small-Mirror Mounts: Off the Shelf

For mounting small mirrors, a number of **off-the-shelf mounts** are available. The attachment methods of these mounts are suitable for lab applications, but they are not robust enough for shipping or other dynamic environments (unlike the driving mechanisms/adjusters).

A **cell and set screw** is a simple, low-cost, low-precision edge mounting device with no kinematic adjustments. The screw should contact the mirror edge at its center so as not to impart a moment.

With a **kinematic mirror mount**, the mirror is mounted to a plate that is preloaded against two thumb screws mounted in opposite corners on back of the plate, allowing angular adjustment in x and y directions. A third screw is often attached to the mount to provide linear adjustment for focusing. This is a low-cost, simple-to-use mount that is available in many geometries. However, this type of mount has low repeatability and a small adjustment range, and adjustments are not completely independent; a slight translation also occurs with an angular adjustment.

Gimble mounts are similar to kinematic mounts except that the center of rotation is located at the mirror surface, eliminating small translations that typically occur with an angular adjustment. They also offer higher resolution, repeatability, and stability than kinematic and flexure mounts, but they are more expensive. Gimble mounts are available off the shelf in a variety of geometries.

Flexure mounts are similar to kinematic mounts except that the preloaded plate the mirror is mounted on is pressed against thin sheets of metal that bend with the screw adjustments. This design provides higher stability and repeatability than kinematic mounts. Flexure mounts are available off the shelf in a variety of geometries and performance levels, and can handle heavier loads than kinematic mounts. Small translations still occur with angular adjustments.

Small-Mirror Mounts: Adhesives and Clamping

The most common method for mounting small mirrors is bonding them on their back or into an edge bezel. For small, thick mirrors, the simplest method is to apply **adhesive** over the entire back of the mirror. If it is determined that the stress in the adhesive will be too large over temperature changes or if the distortions in the mirror are too large, the mirror can be **potted** into an edge bezel with an elastomer.

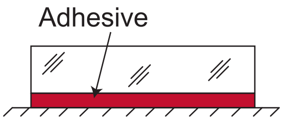

Other ways to reduce mount-induced distortions include:

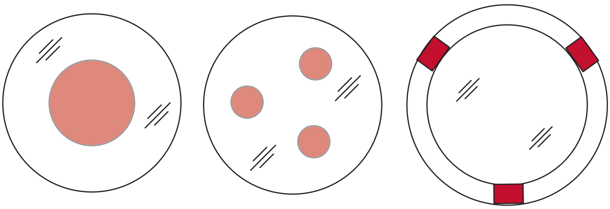

Applying adhesive only in the central region of the mirror.	Applying adhesive at three discrete locations.	Potting a mirror in an edge bezel at discrete locations.

Potting a mirror in an edge bezel at discrete locations provides easier assembly and better performance, but the result is not as stiff.

Supports and **clamp forces** provide another common and simple mounting method. The clamp forces should act along the same line as the supports to avoid imparting a moment on the mirror.

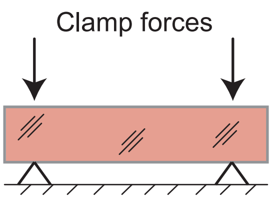

Small-Mirror Mounts: Tangent Flexure and Hub

Custom **tangent flexure mounts** can provide an athermal mount for small mirrors. In this design, three flexures, stiff in the tangential and axial directions, are attached to the edge of the mirror. As the temperature changes, the lens remains centered and free of stress—all of the expansion takes place in the flexures.

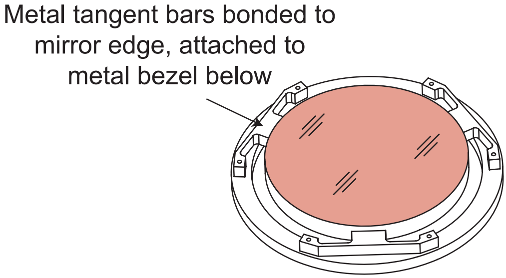

A higher-performance implementation of this concept is shown below: A metal ring has three long slots cut through it, creating an inner ring and outer ring attached only by three small flexure points. A lens can be adhered to the top of the inner ring and remain free of stress because it will be isolated from distortions in the outer ring.

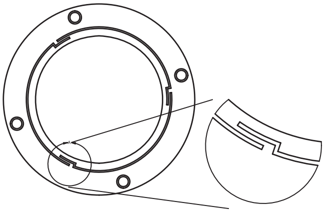

Many solid-substrate midsize mirrors can be **hub mounted**. In this type of design, a central stalk or hub is either machined directly into the mirror or bonded to the back of the mirror. The hub can then be clamped onto for mounting purposes.

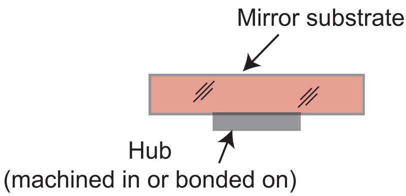

Mirror Substrates

When choosing a **mirror substrate**, some important factors to consider are:

- High stability: The mirror figure does not change due to internal stresses or external changes.
- High dimensional stability with time
- High specific stiffness (E/ρ); the material is less affected by fabrication, mounting, and use in varying environmental conditions.
- Ability to polish the material to an acceptable level of smoothness
- Cost and ease of fabrication

In general, the shorter the involved wavelength is, the higher the degree of smoothness that is required. Typically, a harder mirror can be polished better than a softer one, but most surfaces can be polished to an acceptable level if sufficient time is spent on them. Glasses used for mirrors all polish about the same; however, the same is not true for optical glass. For mirrors, glass is always a better choice than metal in terms of ease of polish.

Nonglass mirrors are common in IR systems and systems that are composed of only one material to achieve athermalization. They are also advantageous for high-energy beam applications because of their high thermal conductivities.

Mirror substrates are often plated with **electroless nickel** ($\alpha = 13 \times 10^{-6}/°\text{C}$) or alternate proprietary platings to prevent corrosion and wear as well as reduce scatter. Less than 1-nm-rms finish is possible on electroless nickel.

Mirror Substrates (cont.)

Nonglass mirror advantages:

- Ability to mount directly to the mirror (threaded holes can be drilled in the substrate)
- Higher thermal conductivity than glass

Nonglass mirror disadvantages:

- Dimensional instability with time
- Defects in the polish are much more noticeable than on glass substrates
- Stress and deformations occur over temperature due to thermal mismatch between the nickel plating and the substrate. Equally thick plating on both sides of the substrate can minimize deformations.

Material	**E/ρ (Nm/g)**	**Hardness**	**CTE $\times 10^{-6}$/°C**	**E (GPa)**	**ρ (g/cm^3)**	**λ(W/mK)**
Desired:	High	High	Low	High	Low	High
Glass substrates						
Borosilicate	26.9	480 (Knoop)	2.8	58.6	2.23	1.14
Fused silica 7940	33.1	500 (Knoop)	0.58	73	2.2	1.38
ULE® 7971	30.7	460 (Knoop)	0.02	67.6	2.21	1.31
Zerodur® (Class 0)	35.7	620 (Knoop)	0.02	90.3	2.53	1.6
Nonglass substrates						
Aluminum 6061	25.4	60 (Rockwell B)	23.6	68.2	2.7	167
Beryllium	157	80 (Rockwell B)	11.5	290	1.84	216
Copper C260	129	75 (Rockwell B)	20	110	8.53	120
Silicon	56.2	1150 (Knoop)	2.6	131	2.33	137
Silicon Carbide CVD	145	2540 (Knoop)	2.4	466	3.21	146

Mirror Substrate Examples

Aluminum 6061

- *General notes*: Low cost, difficult to achieve high stability
- *Polishing notes*: Can be polished bare to 5 nm rms; typically electroless nickel coated

Beryllium

- *General notes*: Very expensive due to complex fabrication process
- *Polishing notes*: When bare polished, does not give good finish and is 5–10× slower than glass; typically electroless nickel coated

Copper C260

- *General notes*: Easy to machine
- *Polishing notes*: Very soft; without extreme effort, expect low-quality finish.

Silicon

- *General notes*: Limited to small sizes
- *Polishing notes*: Can be polished to 1 nm rms with chemo-mechanical polishing using a diamond compound

Silicon Carbide CVD

- *General notes*: Excellent stiffness and thermal properties, but expensive and prone to fracture
- *Polishing notes*: Polish with diamond compound; finish depends on the material (there are different compositions).

Large-Mirror Mounting: Lateral Supports

The diameter-to-thickness ratio (**aspect ratio**) for a mirror is typically around 6 but can be acceptable from 4–20. Mirrors with an aspect ratio larger than 8–10 are defined as thin mirrors. As the aspect ratio of a mirror increases, the complexity of the support system and difficulty of fabrication also greatly increases.

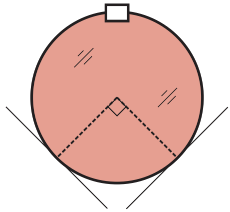

A **V-mount** is a simple support system used to hold medium- to large-size horizontal-axis mirrors. The rim of the mirror is supported by two posts at 90 deg, similar to how it would sit in a V-block. A safety clip is typically included at the top of the mount as a safety feature in case the mirror is bumped. The mirror is also typically supported by a three-point support on the back face, as discussed below.

Other **lateral supports** include edge bands, roller chains, and sling supports. For any of these configurations, the friction between the supports and the edge of the mirror should be as small as possible for best performance. **Edge bands** are fixed above the mirror and provide a sling for the mirror to sit in laterally.

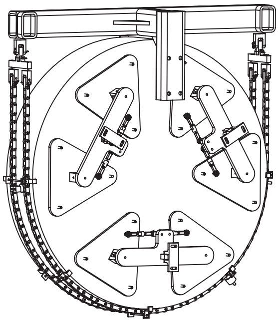

Roller chains are similar but provide reduced friction; they are commercially available in many different sizes and load capacities at relatively low cost.

Sling supports or **strap mounts** are commercial mounts that sit the mirror's rim in a U-shaped metal sling and are supported by a vertical plate. This configuration has increased friction and is only preloaded by gravity, which limits dynamic performance and shipping.

Large-Mirror Mounting: Point Supports

A simple mount for a vertical-axis mirror has equally spaced **point supports** on the back of the mirror, lying on a circle centered about the mirror's axis. Depending on the amount of self-weight deflection that can be tolerated, three- or six-point supports are often used. Equations for the optimal position of these supports can be found on the Self-Weight Deflection pages.

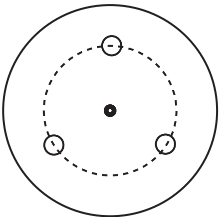

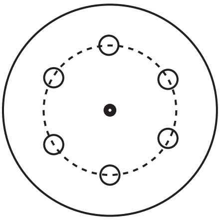

Whiffle tree mounts (or **Hindle mounts**) consist of a cascading system of kinematic supports used to support a mirror from multiple points; they provide an even load distribution, resulting in reduced surface deformation and stress in the mirror. Pivoting arms or triangular plates are individually balanced and equally spaced around the diameter (lateral support) or back (axial support) of the mirror. Whiffle tree mounts are a more complex, and therefore more expensive, solution that requires more space for the mounting structure.

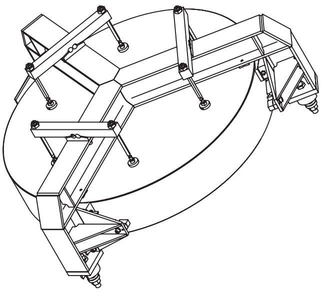

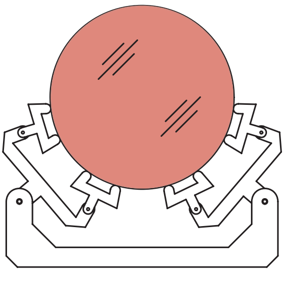

Large-Mirror Mounting: Active Supports

Counterweight supports are weighted levers that provide axial support at many discrete points and self-adjust for varying mirror orientations. They provide optimum performance for mirrors that will experience multiple gravity orientations but are complex and expensive. To reduce friction, flexures have replaced traditional ball bearings.

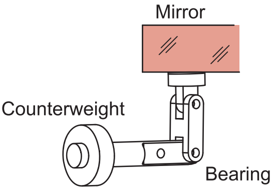

Actuators can be mounted on the back of a mirror to provide a dynamic, rather than static, mount. Systems that actively maintain the optimal form of a mirror are called **active optics**, whereas **adaptive optics** deform the surface of a mirror to cancel aberrations or compensate for other errors by using measurements and feedback; both types are used for atmospheric correction in telescopes, fabrication and assembly errors in deployable systems, and thermal and vibration effects.

> Any surface error that occurs on a mirror is multiplied by a factor of two in the reflected wavefront.

When a mirror is mounted in any orientation, gravity acts on it and causes deformations due to the mirror's weight; this is referred to as **self-weight deflection**, a primary concern when mounting a mirror. The rms self-weight deflection of a **mirror mounted laterally (axis horizontal)** can be estimated by

$$\delta_{Hrms} = \left(a_0 + a_1\gamma + a_2\gamma^2\right)\left(\frac{2\rho r^2}{E}\right) \quad \gamma = \left(\frac{r^2}{2hR}\right) = \left(\frac{\text{sag}}{\text{thickness}}\right)$$

where r is the half-mirror diameter, h is the mirror center thickness, and R is the mirror radius of curvature.

	Two-point support	Edge band
a_0	0.05466	0.073785
a_1	0.2786	0.106685
a_2	0.110	0.03075

Self-Weight Deflection: General

The rms self-weight deflection of a **mirror mounted axially (axis vertical)** can be calculated by

$$\delta_{Vrms} = C_{sp}\left(\frac{\rho g}{E}\right)\frac{r^4}{h^2}\left(1-\nu^2\right)$$

where C_{sp} is the geometric support constraint (see below), g is gravity (9.8 m/s^2), and ν is the Poisson ratio.

If a mirror is tilted, the self-weight deflection in the vertical and horizontal axes can be calculated individually by

$$\delta_{\theta-V} = \delta_{Vrms}\cdot\cos\theta \qquad \delta_{\theta-H} = \delta_{Hrms}\cdot\sin\theta$$

The overall rms self-weight deflection of a mirror mounted at an angle can be estimated by

$$\delta_{\theta rms} = \sqrt{(\delta_{\theta-V})^2 + (\delta_{\theta-H})^2}$$

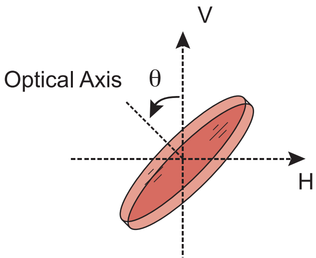

Support Constraint	C_{sp}	FORD*
Ring at 68% (of diameter)	0.028	11
6 points equally spaced at 68.1%	0.041	8
Edge clamped	0.187	1.5
3 points, equally spaced at 64.5%	0.316	–
3 points, equally spaced at 66.7%	0.323	~1
3 points, equally spaced at 70.7%	0.359	0.9
Edge simply supported	0.828	1/3
Continuous support along diameter	0.943	1/3
"Central support" (mushroom or stalk mount) (r = radius of stalk)	1.206	1/4
3 points equally spaced at edge	1.356	1/4

* Factor of reduced deflection compared to the 3-pt support

Self-Weight Deflection: Thin Plates

Mirrors with complex shapes (steep curvature, holes, contoured backs, etc.) have complex distortions. These are usually treated using finite element modeling.

For a flat, thin mirror (large aspect ratio) supported with any number of discrete points, the rms self-weight deflection can be found by

$$\delta_{rms} = \gamma_N \left(\frac{q}{D}\right)\left(\frac{\pi r^2}{N}\right)^2 \left[1 + 2\left(\frac{h}{u}\right)^2\right] \qquad D = \frac{Eh^3}{12(1-\nu^2)}$$

where γ_N is the support point efficiency, q is the force applied per unit area, D is the flexural rigidity, N is the number of support points, and u is the effective length between support points.

Since this equation is based on thin-plate theory, it has greater than 20–30% error for thick (small aspect ratio) mirrors. The variable γ_N is a fixed constant determined by finite element analysis (FEA) of an optimal design (see Ref. 4).

An estimate of γ_N for N number of support points:

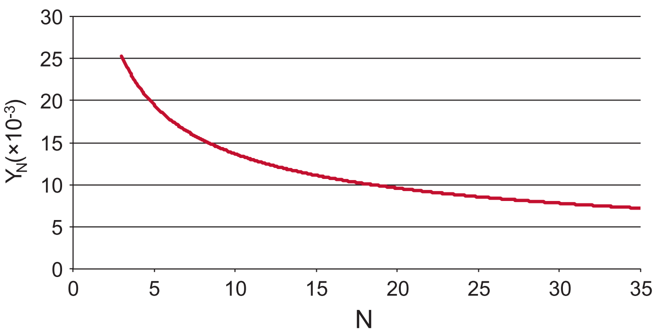

Self-Weight Deflection: Parametric Model

There is a **parametric model** that suits both large- and small-aspect-ratio mirrors: the equation below can determine the **rms deflection** δ_{rms} as well as the **peak-to-valley deflection** δ_{P-V} and the **rms** or **peak-to-valley slope error** ($\Delta_{P-V}d$ or $\Delta_{rms}d$, respectively), with or without **low-order curvature (power)**.

$$\delta_{rms}, \delta_{P-V}, (\Delta_{P-V}d), (\Delta_{rms}d) = \gamma\left(\frac{q}{D}\right)\left(\pi r^2\right)(1+f)$$

$$f = \frac{A}{\alpha}\cdot e^{-\upsilon} + \frac{B}{\sqrt{\alpha}}\cdot \nu + C$$

This equation applies only to flat mirrors (with no curvature or holes). It has less than 10% error for mirrors with a Poisson ratio ν of 0.1–0.35.

where α is the mirror aspect ratio (diameter-to-thickness ratio), D is the flexural rigidity, and γ, A, B, and C are parametrically determined constants. Parametric variables for a three-point, six-point, and continuous ring support:

Support	**Optimal target & position**	**Optical performance metric**	γ (×10^6)	***A***	***B***	***C*** (×10^2)
3-pt	δ_{rms} 66.3%	δ_{P-V}	246.7	0.50	4.10	–2.79
		δ_{rms}	58.58	1.27	2.93	–6.56
		$\Delta_{P-V}.d$	396.7	0.78	3.91	–6.39
		$\Delta_{rms}.d$	264.3	1.20	2.70	–5.38
6-pt	δ_{rms} 68.5%	δ_{P-V}	36.59	6.12	3.57	–24.4
		δ_{rms}	8.380	6.04	4.37	–36.7
		$\Delta_{P-V}.d$	116.5	4.74	2.30	–27.9
		$\Delta_{rms}.d$	67.17	3.68	1.14	–21.0
Ring	δ_{rms} 68.5%	δ_{P-V}	29.33	6.55	4.09	–29.2
		δ_{rms}	7.574	6.54	4.36	–39.0
		$\Delta_{P-V}.d$	91.94	5.12	2.53	–31.9
		$\Delta_{rms}.d$	59.98	3.31	0.74	–21.2

The second column lists the optimized parameter and the diameter percentage at which the supports should be placed. The third column lists the parameter calculated. The slope variable provides the amount of deflection for a unit diameter, but the result must be divided by the diameter to obtain the actual slope value (see Ref. 5).

Lightweighting Mirrors

For many applications, especially in flight and aerospace, weight is a driving requirement. Various techniques can be used to **lightweight** large mirrors by removing unused substrate material. The **stiffness-to-weight ratio** is an important factor to consider when lightweighting a mirror: the higher this ratio is, the better. **Flexural rigidity** describes the bending stiffness of a mirror and is also an important factor.

A **contoured-back mirror** has material removed from the back face that is not being used optically. Correctly done, a contour back provides reduced weight and an increased stiffness-to-weight ratio. Common contours are a taper or a spherical rear surface put into the back and single or double arches.

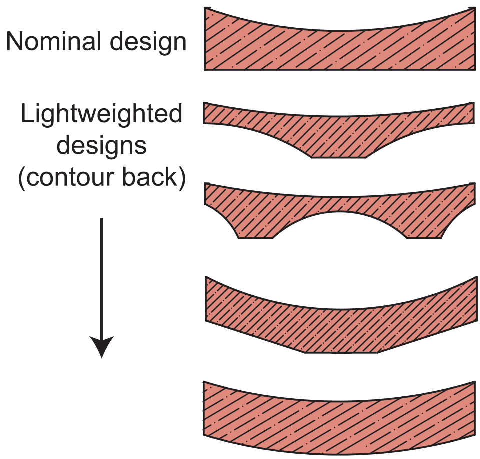

If the ratio of the self-weight deflection of a lightweight mirror to the self-weight deflection of a solid mirror of the same diameter is greater than one, the lightweight mirror has less stiffness and is generally not a good solution.

Lightweighting Mirrors (cont.)

In a **cellular-core mirror**, the back of the mirror may be open or closed, but the core is made of cells that are hexagonal, triangular, square, etc. One type of open-back-mirror has depressions machined into the back of the substrate to remove material and weight.

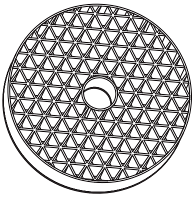

Another open-back configuration is the cast ribbed mirror, where a honeycomb structure is cast directly into the back of the glass. Alternatively, a closed-back (sandwich) mirror has access holes drilled into the back of the mirror, and material is removed

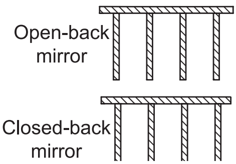

from the center of the substrate. A **fused core** can be made by welding many L-shape structures together; the front and back substrates are then fused onto the egg-crate core.

Mirror type	Weight vs height	Weight vs deflect	Height vs deflect	Weight vs efficiency
Single arch	3	5	5	5
Double arch	4	2	4	2
Open-back	1	4	2	3
Symmetric sandwich	2	1	1	1
Solid	5	3	3	4

Mirror type	Fabrication ease/speed	Fabrication cost	Mounting ease
Single arch	2	3	2
Double arch	3	2	3
Open-back	5	4	4
Symmetric sandwich	5	5	5
Solid	1	1	1

1 = best performance, 5 = worst performance (see Ref. 6).

Flexural Rigidity of Lightweighted Mirrors

The equivalent **flexural rigidity** of a lightweighted mirror can be calculated by

$$D = \frac{Eh_B^3}{12\left(1-\nu^2\right)}$$

Open-back mirror:

$$h_b^3 = \frac{[1-(\eta/2)]\left[t_F^4-\left(\eta h_C^4/2\right)\right]+(t_F+h_C)^4(\eta/2)}{t_F+(\eta h_C/2)}$$

Sandwich mirror:

$$h_b^3 = (2t_F+h_C)^3-(1-\eta/2)h_C^3; \qquad \eta = \frac{(2B+t_c)t_c}{(B+t_c)^2}$$

t_F = faceplate thickness

h_C = rib height (depth of core)

t_c = cell wall thickness

B = diameter of circle inscribed in a cell

$$(B_{square}=b, B_{triangle}=\sqrt{3}b, B_{hexagon}=b/\sqrt{3})$$

b = length of cell wall

h_b = equivalent bending thickness

η = rib solidity ratio

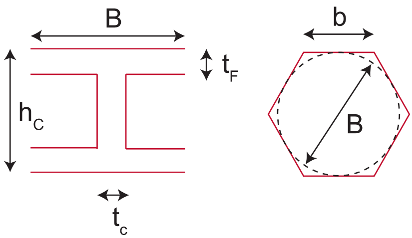

RMS, P–V, and Slope Specifications

When tolerancing surface quality for an optic, allowable errors are often expressed in root-mean-square and/or peak-to-valley error. The **peak-to-valley (P–V)** value gives the distance between the highest and lowest points on a given surface relative to a reference surface. This measurement can be easily skewed if dust or other contaminants are present on the surface. The **root-mean-square (rms)** value gives the standard deviation of the test surface height from a reference surface; it provides a better measurement of surface quality if there are a sufficient number of sampling points.

There is no set ratio between P–V and rms error, although values from 3–5 are commonly used. The specific relationship between the two errors depends on the fabrication process and how the surface is tested. The following table shows rms errors resulting from 1 μm of select P–V surface errors. These values are the normalized rms coefficients of the Zernike polynomial for the specific error.

As a rule of thumb, for a given amount of a low-order rms figure error, multiply by 4 to get the P–V error.

Surface error	RMS surface error (μm)	P–V : RMS ratio
Focus	0.29	3.45
Astigmatism	0.20	5.00
Coma	0.18	5.56
Spherical (4th order)	0.30	3.33
Trefoil	0.18	5.56
Astigmatism (4th order)	0.16	6.25
Coma (5th order)	0.14	7.14
Spherical (6th order)	0.19	5.26
Sinusoidal ripples	0.35	2.86

Finite Element Analysis

When a closed-form solution or equation is not available for a particular analysis, modeling the system in a finite-element-analysis program is an alternate approach to consider. The **finite element method (FEM)** or **finite element analysis (FEA)** is a numerical approximation method where a component or system is modeled in a computer program and analyzed for specific results. Common analyses include stress concentration, surface deformations, thermal effects, buckling, and identifying natural frequency and modes.

Before using FEA, some issues should be considered:

- Is FEA required for the problem (i.e., is there a simpler closed-form solution available)?
- Does the FEA program have the type of analysis required?

If FEA is an appropriate tool, other factors should be considered, including:

- How detailed does the model need to be? Analyzing stress concentration will require a detailed model for the part of interest, whereas determining the natural frequency only requires a basic model.
- Can a symmetric model be used to reduce processing time?
- What is the desired output? Does the program provide that output or is postprocessing required?

If a model is symmetric, analysis can be conducted on only a portion of the full model and then extrapolated due to the symmetry. This allows for smaller models and faster run times. This requires more user knowledge and cannot be applied to problems that are nonlinear or nonsymmetric.

> A "good" FEA model will lack the detail of a full CAD model.

Finite Element Analysis (cont.)

The basic steps involved in FEA are preprocessing, analysis, and postprocessing.

When defining the system geometry and coordinate system, keep in mind that most optical postprocessing programs require the ***z* axis** to be the **optical axis**.

In the **preprocessing** step, the system geometry is set by creating a solid model in a computer-aided-design (CAD) program. Constraints holding the part and forces imparted on that part are then added to the model, including mounting supports, gravity, and applied loads. The material properties of the elements are also defined for accurate results; the units should be verified. The continuous geometry of the model is then discretized into individual elements connected by **nodal points**, with each node defining a degree of freedom. The web of nodal points is referred to as a **mesh**.

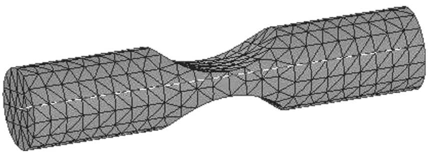

There are a variety of mesh shapes that can be used, and determining the proper mesh is important for accurate analysis. Meshes range from coarse (very few nodes) to fine (high density of nodes). Most FEA programs have automatic mesh generators and offer convergence algorithms (such as ***h*-adaptive** and ***p*-adapative**) that create finer meshes for more detailed portions of the model.

As a rule of thumb, there should be a minimum of four elements through the height or thickness of a part and eight elements in the radial direction.

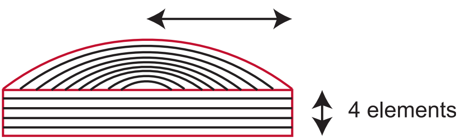

Finite Element Analysis (cont.)

A 10-node tetrahedral mesh provides more fidelity than a 4-node mesh, which will be stiffer and will underestimate deflections. The user should check the default settings for how many nodes are used for the automatic meshing.

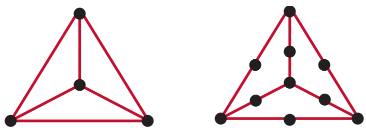

Tetrahedral mesh: 4- and 10-point nodes

The finer a mesh is, the more accurate the solution; however, accuracy comes at the cost of added computing time. Typically, a course mesh will yield accurate results for analyzing deformations, whereas a fine mesh is required for accurate stress analysis. A coarse mesh can also be used for initial analyses and then refined for later runs. For optical surfaces, a symmetric mesh should always be defined. The following figure shows possible symmetric models for a three-point mount:

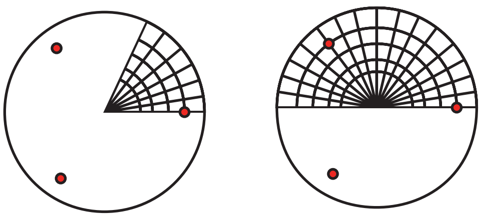

Before completing a detailed analysis, a simplified model should be analyzed and compared to a known solution to determine if the model is acting accurately. The validity of an FEA depends highly on generating a proper mesh and properly applying the loads and boundary constraints. It is important to verify the FEA model with hand calculations for expected results.

Finite Element Analysis (cont.)

Every FEA program has a **solver** that is used to complete the required **analysis**. Most programs offer a variety of solvers; each one has different advantages and disadvantages for a particular application. The help documentation should be consulted for details on how each solver operates and under what conditions each should be used.

A **convergence test** should also be completed to determine a reasonable mesh size. If symmetric loads and constraints are applied, the results should also be symmetric. This can check the accuracy of the model.

Most FEA programs provide the (optional) capability of **optimizing** a solid model. Analogous to a lens-design program, a model can be created with user-defined parameters as well as a user-defined merit function. The model can then be optimized to the merit function by altering the variables allowed by the user.

An FEA model often requires **postprocessing** of the generated data. This step involves exporting information from the FEA program in a format that is usable by an external code that outputs the final product. One example is exporting surface deflections to a spreadsheet and then importing the data into MATLAB® code that generates Zernike polynomials describing the surface error.

Vibration

A variety of environmental factors can affect the performance of an optical system; vibration, temperature, shock, humidity, pressure (altitude), corrosion, abrasion, and contamination, among others, are possible issues to take into consideration when designing a system. For a comprehensive list of the effects of these environments and of methods for laboratory testing, MIL-STD-810G or ISO 9022 should be consulted.

A single-degree-of-freedom system consists of a mass, spring, and damper held fixed at one end. If the mass is set into motion, it will oscillate at its fundamental, or natural, frequency in only one direction.

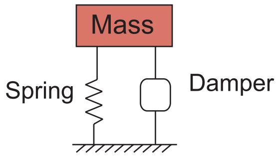

The **natural frequency** of a system is the frequency at which it resonates, given by

$$\omega_0 = \sqrt{\frac{k}{m}} \qquad f_0 = \frac{\omega_0}{2\pi}$$

The approximate motion of a system can be found by assuming that it only has one degree of freedom and finding the natural frequency.

Damping is the process in which mechanical energy is dissipated from a system and the amplitude of vibration at resonance is reduced. It is expressed by a damping coefficient C. **Critical damping** C_r is the damping coefficient that causes the system to return to its initial position in the shortest amount of time without over-oscillation. The **damping factor** is then defined as the ratio of the damping coefficient to the value of critical damping:

$$\zeta = \frac{C}{C_r}$$

Damping Factor

The higher the **damping factor** ζ, the more quickly vibrations at resonance are attenuated. The **maximum amplification at resonance** Q refers to the amount of vibration transmission that occurs at resonance. The damping factor and maximum amplification at resonance are related by

$$\zeta = \frac{1}{2Q}$$

A lower Q factor means a system will be better damped and more stable. For optomechanical systems, the damping factor can be estimated as < 0.025 (maximum amplification at resonance, $Q > 20$). For small amplitudes, such as ground vibrations, it is possible to have a damping factor as small as 0.005 ($Q = 100$). The damping factor is also related to the **logarithmic decrement**, which can be used to measure an underdamped system:

$$\zeta = \frac{\delta}{\sqrt{(2\pi)^2 + \delta^2}} \qquad \delta = \frac{1}{n} \ln \frac{A_i}{A_n}$$

where A_i and A_n are amplitudes, and n is the number of periods between the two measurements.

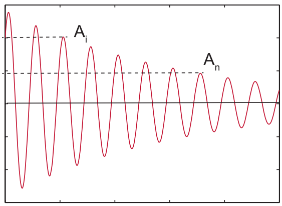

Power spectral density (PSD) measures the energy content of a system versus frequency: it shows how strongly a system will vibrate with a certain frequency. The units of PSD are energy per unit frequency (g^2/Hz), plotted on a log–log scale.

Isolation

The **isolation** of a system is accomplished by maintaining the proper relationship between the frequency of environmental vibrations and the natural frequency of the system. **Vibration isolators** can reduce the amount of vibration that is transferred from the environment to a system—when used, their resonant frequency should be at least an order of magnitude less than the system.

There are a wide variety of isolator materials and designs, and the specific isolator properties chosen will ultimately depend on the system requirements and vibration environment. Some of the common types of isolators include elastomeric isolators, springs, spring-friction dampers, springs with air dampings, springs with wire mesh, and pneumatic systems. Common environmental noise sources and their corresponding frequencies in hertz include the swaying of tall buildings (0.1–5), machinery vibration (10–100), building vibration (10–100), microseisms [threshold of disturbance of interferometers and electron microscopes] (0.1–1), and atomic vibrations (10^{12}).

Transmissibility T describes how much of any environmental vibrations are transmitted to the isolated system (i.e., lower transmissibility means more isolation).

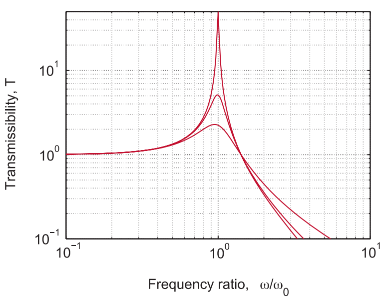

$$T = \sqrt{\frac{1+\left(2\frac{f}{f_0}\zeta\right)^2}{\left(1-\frac{f^2}{f_0^2}\right)^2+\left(2\frac{f}{f_0}\zeta\right)^2}}$$

When the driving frequency f is equal to the resonant frequency, the equation is at a maximum and reduces to the expression given earlier [$T_{max} = Q = 1/(2\zeta)$].

System Acceleration and Displacement

If a system is exposed to a spectrum of random vibrations, it will vibrate at its natural frequency. For a single-degree of-freedom system experiencing random vibrations, the rms **acceleration** can be estimated by the **Miles equation**:

$$a_{rms} = \sqrt{\frac{\pi}{2} \cdot f_0 \cdot Q \cdot PSD}$$

Although derived for a single-degree-of-freedom system, the Miles equation is useful in estimating the acceleration due to random vibrations at the natural frequency for a multiple-degree-of-freedom system. It should be noted, however, that the equation is based on the response of a system to a flat random input; it may significantly underpredict the acceleration for a shaped input, like those of transportation vehicles.

The value of a_{rms} provides a "1-sigma" value for the vibration response. In vibration engineering, it is typically assumed that the 3-σ peak response will cause the most structural damage, so the value of a_{rms} should be multiplied by three.

Assuming a single-degree-of-freedom system, the approximate motion of the system can be found by

$$\delta_{rms} = \frac{a_{rms}}{(2\pi f_0)^2}$$

When the PSD is given in units of g^2/Hz, a_{rms} will be in units of g. To convert to m/s^2, multiply a_{rms} by 9.8 m/s^2.

The sinusoid resonance that has the same damage potential as a random resonance has a peak acceleration that is $(4.5)^{0.5}$ times the rms value of the random resonance.

Thermal Effects

Most optical systems are designed and assembled at "room temperature," typically 20–23°C. When designing optomechanical systems, it is important to remember that materials expand or contract with temperature change. Therefore, if a system is to be used outside of a temperature-controlled environment, **thermal effects** should be considered.

Temperature extremes commonly endured by optics are:

1. Survival/Storage: −62 to 71°C (−80 to 160°F)
2. Operation: −54 to 52°C (−65 to 125° F)
3. Space: approaching absolute zero (~0 K, −273°C, 459° F)

Specifications that apply to the environmental testing of optical systems include MIL-STD-210, MIL-STD-810, ISO 10109, and ISO 9022.

The **coefficient of thermal expansion (CTE)** is a material property that describes the change in size of a material with temperature. It is represented by α and has units of 10^{-6} m/m/°C (ppm/°C). The CTE of a material is quoted at room temperature but may vary with temperature. The CTE value should be verified for extreme temperatures.

The change in length of a material due to a given uniform temperature change ΔT is given by

$$\Delta L = \alpha L \Delta T$$

The **thermal strain** experienced in a material is given by

$$\varepsilon = \frac{\Delta L}{L} = \alpha \Delta T$$

If a given linear dimension is constrained, the **thermal stress** induced in that dimension by a temperature change is given by

$$\sigma = E\alpha\Delta T$$

Thermal Effects (cont.)

The **thermal conductivity** of a material describes the ability of that material to conduct heat. Typically, a higher value of thermal conductivity is desirable because it will take less time for the material to reach thermal equilibrium, and it will be less affected by **thermal gradients**.

$$\lambda = \frac{QL}{\Delta T}$$

λ = thermal conductivity
Q = heat flux per unit area absorbed by the material

A gradient in the thermal strain can be caused by a temperature gradient (dT/dh) or a temperature change ΔT coupled with CTE gradient ($d\alpha/dh$). In general, the strain gradient is

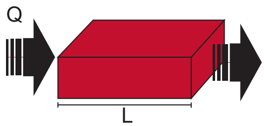

$$\frac{d}{dh}(\alpha T) = \alpha\frac{dT}{dh} + \Delta T\frac{d\alpha}{dh}$$

If a thermal gradient is driven by heat flux Q, then

$$\frac{d}{dh}(\alpha T) = \frac{\alpha}{\lambda}Q$$

A thermal gradient will cause the part to bend, changing the curvature by ΔC:

$$\Delta C = \Delta\left(\frac{1}{R}\right) = \alpha\frac{dT}{dh} = \frac{\alpha}{\lambda}Q$$

A curved part would suffer a change in radius:

$$\Delta R = -R^2\Delta C = -R^2\alpha\frac{dT}{dh} = -R^2\frac{\alpha}{\lambda}Q$$

The change in angle across the part is then

$$\Delta\theta = L\alpha\frac{dT}{dh}$$

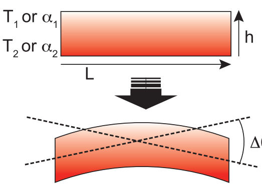

The change in sag across the part is

$$\Delta sag = \frac{L^2}{8}\Delta C = \frac{L^2\alpha}{8}\frac{dT}{dh}$$

Heat Flow

The **heat flow** through a material is given by

$$H = Q \cdot A$$

which allows for the calculation of the change in temperature after applying a given heat to a material.

Transient heat flux is a temperature distribution that changes over time. The **thermal diffusivity** describes how quickly a material responds to temperature change: the higher the diffusivity is, the quicker the response.

$$D = \frac{\lambda}{\rho C_p}$$

D = thermal diffusivity
C_p = specific heat capacity

The response of a system to a change in temperature is an exponential decay in the ratio of the internal to external temperatures. The time required for a system to change temperature by a factor of $1/e$ is defined as one **thermal time constant** τ:

$$\tau = \frac{t^2}{D}$$

where t is the material thickness.

After five thermal time constants (assuming temperature does not vary greatly with time), the system reaches <1% difference in internal to external temperatures—an acceptable threshold to assume the system is at equilibrium.

Temperature stabilization is important for many optical instruments, such as astronomical telescopes. Metal mirrors used with high-energy laser beams are often cooled with liquid. Temperature-controlled air can be passed through large, lightweighted structures for temperature stabilization.

Heat Flow (cont.)

Heat flow can be described by conduction, convection, or radiation. The equations for these processes are:

- **Steady-state heat flow** $Q = -\lambda \nabla T = -\lambda \dfrac{dT}{dx}$
- **Transient heat flow** $\dfrac{\partial T}{\partial i} = D \nabla^2 T = D \dfrac{\partial T^2}{\partial x^2}$
- **Convective heat transfer** $Q = h(T_w - T_0)$
- **Radiative heat transfer** $Q = \varepsilon\sigma\left(T_1^4 - T_0^4\right)$

where i is time, T_w is the surface temperature, T_0 is the fluid temperature, σ is the Stefan constant (5.57×10^{-8} W/m^{2}K^4), h is the heat-transfer coefficient [W/m^{2}K] (5–50 in air, 3000–5000 in water), and emissivity $\varepsilon = 1$ for a blackbody.

The **Biot number** is often used in heat-flow calculations:

$$B_i = \frac{ht}{\lambda}$$

Heat flow is limited by convection when $B_i < 1$, and limited by conduction when $B_i > 1$.

Temperature affects not only the geometry of a component or system but the optical properties as well. The **temperature coefficient of the refractive index** dn/dT defines the change in the index of refraction of a material due to a temperature change:

$$n' = n + \left(\frac{dn}{dT}\right)\Delta T$$

Typically, the temperature coefficient of the refractive index of air is called out in two different ways: measured in a vacuum [**absolute *dn/dT*** (dn_{abs}/dT)] and measured at standard temperature and pressure in dry air [**relative *dn/dT*** (dn_{rel}/dT)]. The two terms are related by

$$\left(\frac{dn_{abs}}{dT}\right) = n_{rel}\left(\frac{dn_{air}}{dT}\right) + n_{rel}\left(\frac{dn_{rel}}{dT}\right)$$

Air Index of Refraction

As temperature changes, the refractive index of the air also varies (dn_{air}/dT). The **air index of refraction** is commonly defined by the updated **Edlén equation** by Birch and Downs:

$$(n-1) = \left[\frac{P(n-1)_s}{96095.43}\right]\left\{\frac{\left[1+10^{-8}\left(0.601-9.72\cdot 10^{-3}T\right)P\right]}{1+3.661\cdot 10^{-3}T}\right\}$$

$$(n-1)_s = \left[8342.54+\frac{2406147}{\left(130-\sigma^2\right)}+\frac{15998}{\left(38.9-\sigma^2\right)}\right]\cdot 10^{-8}$$

where P = pressure (Pa), T = temperature (°C), and σ = vacuum wavenumber (μm^{-1}). The **Ciddor equation** is also commonly used and provides higher accuracy when working in extreme environments or over a broad wavelength range.

A useful tool to calculate the air index of refraction can be found in the Engineering Metrology Toolbox run by the **National Institute of Standards and Technology (NIST)** at http://emtoolbox.nist.gov.

A simple shop-floor calculation for the index of refraction of the air based on the pressure (in kPa), relative humidity (RH, in percent, i.e., 0–100), and temperature (in °C) is

$$n = 1+\frac{7.86\cdot 10^{-4}P}{273+t}-1.5\cdot 10^{-11}(\mathrm{RH})(T^2+160)$$

This is only valid for red He–Ne lasers at a wavelength of 633 nm. It has an uncertainty of approximately 1.5×10^{-7}.

The focal length of a system is then affected by each of these changes. The change in focal length of a lens with temperature can be quantified by

$$\Delta f = \beta f \Delta T \qquad \beta = \alpha - \frac{1}{n-1}\frac{dn_{rel}}{dT}$$

Athermalization

Athermalization is the process by which a system is made insensitive to temperature change. Due to the changes in geometry and optical properties that occur in a system when subjected to a temperature change, it is often necessary to athermalize either a whole or a part of a system. Often, the most important parameter is the defocus that occurs over temperature (especially for IR applications, because IR optics are sensitive to temperature changes due to their high dn/dT values).

Thermal properties of the optics, environment, and housing can be modeled by software, and the effects of temperature change minimized during the design process.

It is common to create an achromatic system by selecting a combination of lenses with the appropriate optical properties and design form to provide color correction over a range of wavelengths. Similarly, an athermal system can be designed by selecting a combination of lenses with thermal properties that provide minimal thermal defocus over a range of temperatures. For an **athermal doublet**,

$$\frac{\phi_1}{\phi} = \frac{\nu_1'}{\nu_1' - \nu_2'}; \quad \frac{\phi_2}{\phi} = -\frac{\nu_2'}{\nu_1' - \nu_2'}; \quad \nu' = \frac{1}{\beta}$$

A common passive mechanical method of athermalization uses two metals to compensate for focal plane shift. In general, in order to achieve athermalization, the two materials should satisfy the equation $\alpha_1 L_1 - \alpha_2 L_2 = \beta f$. Care should be taken to determine which direction the motion is occurring and adjust the sign of the variable accordingly (i.e., if the focus is shortening, it is moving to the left, and β should be negative).

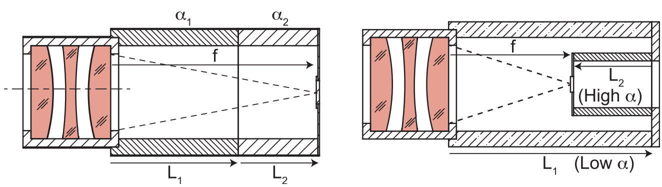

Passive Athermalization

Metering rods provide another passive mechanical solution utilizing low-CTE materials. In this technique, an optical system is mounted in a conventional manner but with individual element mounts having compliance in the axial direction. The elements are each attached to a metering rod made of low-expansion material. The housing then expands and contracts with temperature, but the optical elements remain in their nominal position.

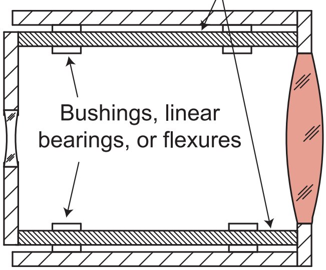

Low-CTE materials	CTE (10^{-6}/°C)
Borosilicate crown E6	2.8
Clearceram®-Z HS	0.02
Fused silica 7940	0.58
Graphite epoxy composites	varies (can tune to 0)
Invar®	0.8
Super Invar®	0.31
ULE® Corning 7972	0.02
Zerodur®	0.02

An **all-one-material design** also provides passive athermalization since all the optical elements and housing will expand contract together; only the overall size of the system will vary with temperature. For refractive systems, glass spacers and tubes can be used, although the system will be very fragile. For reflective systems, metals can be used for both the mirrors and the housing. All low-CTE materials can also be used to minimize thermal effects; however, this solution can be very expensive.

Active Athermalization

Active athermalization requires a motor, a power source, and a feedback loop to provide motion to a focusing element or to the image plane.

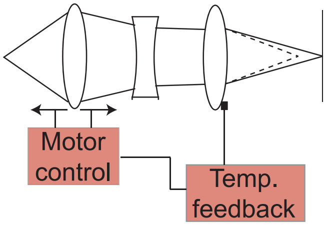

A lookup table can be created to provide input to the motor, which can drive the appropriate element(s) to refocus the image. Temperature sensors placed within the system provide the temperature. Depending on the specific system and environment, it may also be necessary to calibrate the difference between the external (actual) temperature and the internal temperature where the sensors are located.

When a mount or design is overconstrained, changes in temperature can cause stress in the materials. This stress can be estimated using an equivalent CTE and equivalent compliance. An example for the case where a single degree of freedom is overconstrained is developed below.

For the degree of freedom of interest, divide the overall distance L into sections, where

$$L = \sum L_i$$

Analogously, the overall change in length of the system comes from the change in each section:

$$\Delta L = \sum \alpha_i L_i \Delta T$$

This equation can be rewritten by defining an equivalent CTE, α_e:

$$\Delta L = \alpha_e L \Delta T \qquad \alpha_e = \frac{\sum \alpha_i L_i}{L}$$

Determining Thermally Induced Stress

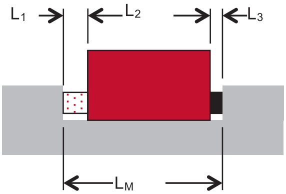

Take, for example, a glass beamsplitter in a mount (with length L_2), held by a compliant preload (length L_1) against a rigid constraint (length L_3).

Define path G as the path through the preload, glass, and rigid constraint, and path M as the path through the mount.

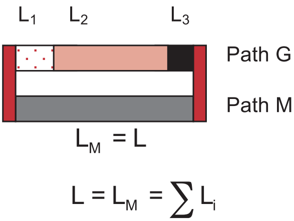

First, use the equivalent CTE to determine the expansion of each path, assuming they are unconstrained:

$$\Delta L_{GT} = \alpha_e L \Delta T = \sum \alpha_i L_i \Delta T \qquad \Delta L_{MT} = \alpha_M L \Delta T$$

Next, use an equivalent compliance (C_e) to determine the relationship between the force and the displacement of the paths back to their constrained position. Assuming that the part does not break, the change in length for the two paths must match.

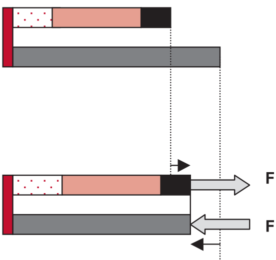

$$\Delta L_{GF} = C_e F = \sum C_i F$$
$$\Delta L_{MF} = -C_M F$$

$$\Delta L_G = \Delta L_M$$
$$\Delta L_{GT} + \Delta L_{GF} = \Delta L_{MT} + \Delta L_{MF}$$
$$\alpha_e L \Delta T + C_e F = \alpha_M L \Delta T - C_M F$$

Solve for the force F, due to overconstraint:

$$F = \frac{(\alpha_M - \alpha_e) L \Delta T}{C_e + C_M}$$

This force can be used to calculate thermally induced stresses, which are compared with the strength limit for the materials to determine the likelihood of failure.

Alignment

At the very basic level, **alignment** is a two-step process:

1. Assemble system based on mechanical properties.
2. Finely align system based on optical properties.

Optical alignment consists of two basic steps:

1. Align elements using all degrees of freedom to obtain correct first-order properties such as magnification and object and image height.
2. Reduce or eliminate aberrations with the remaining degrees of freedom while keeping first-order properties fixed.

A rotationally symmetric system is aligned when the centers of curvature of each element are on the **optical axis** and each element is at the correct axial position. This ensures that the optical axis of each element is coincident with the system optical axis.

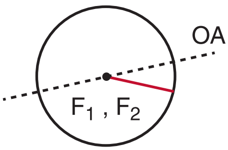

The optical axis of an element must have two points to be well defined. A **circle** or **sphere** has both foci at the center of curvature. Its optical axis can be defined in any direction as long as it passes through the foci.

A **parabola** has one focus at infinity and one at the focus of the reflecting surface. Its optical axis is defined by the line that passes through the focus and intersects the reflecting surface at normal incidence.

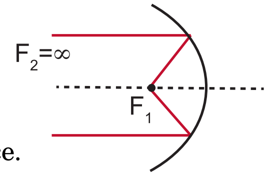

An **ellipse** has two real foci, whereas a **hyperbola** has one real and one virtual focus. The optical axis is defined by the two foci in each case.

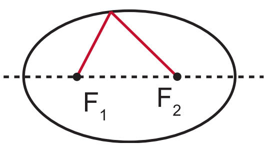

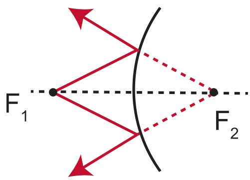

Optical and Mechanical Axis of a Lens

The **optical axis** of a **lens** is defined by the line connecting the centers of curvature of each surface. If a lens has an aspheric surface, there is no longer a uniquely defined optical axis.

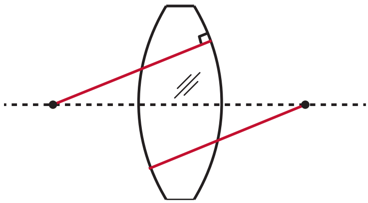

The **mechanical axis** passes through the physical center of the lens, perpendicular to the outside edges. If the mechanical and optical axes are not parallel to each other, there is **wedge** in the lens. Wedge is quantified by an angle or edge thickness difference.

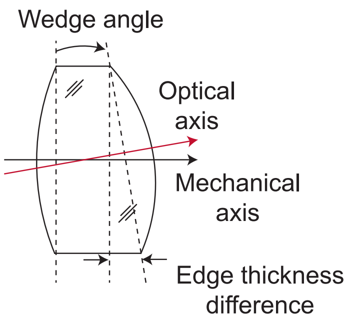

An **alignment telescope** is a specialized instrument that establishes an axis by focusing at different points along a line, anywhere from ~1 m to infinity; elements can then be aligned to the established axis. The accuracy of alignment depends on the quality of the telescope—a few arcseconds are typically possible.

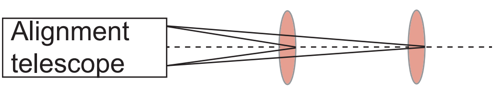

Alignment Tools

A **pip generator** is an accessory that can be attached to an alignment telescope. It supplies a point source (pinhole) or internally illuminated reticle that is reflected off of the different surfaces under test and reimaged at an eyepiece where the user can view the displaced image due to tilt of the surfaces. Because the system can focus on different surfaces as well as on the reflected images, the telescope must have a very large focus range. Laser alignment stations based on similar theory are also available to align elements and cemented doublets.

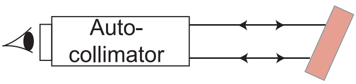

An **autocollimator** is a telescope focused at infinity that is used for angular measurements (i.e., wedge in a window) and is insensitive to displacement. A reticle is illuminated at the focal plane and focused to infinity by an objective lens. The light is then reflected off of the surface under testing and returned to the eyepiece where the user can view both the original and reflected reticle. The test surface is ideally perpendicular to the beam; any deviation results in a displacement of the reflected reticle. The amount of displacement between the two reticle images is given by $d = 2\alpha f$, where α is the tilt angle of the object under testing, and f is the focal length of the objective.

An **autostigmatic microscope** uses an internal fiber source and small CCD to send out a perfectly imaged point and detect the lateral location and focus of the return spot in three dimensions; it is used primarily to locate the center of curvatures and lens conjugates, and to align them to each other or to an axis. Such a microscope can also be used to measure the radius of curvature of a lens if the lens is mounted on an optical rail.

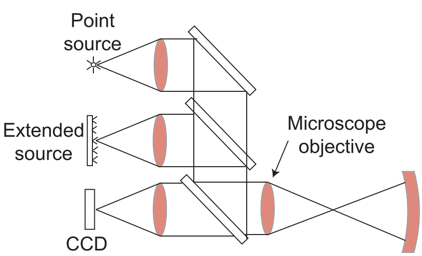

Geometric Dimensioning and Tolerancing

Geometric dimensioning and tolerancing (GD&T) is a way to provide tolerances on the geometry and fit of mechanical parts in order to describe the engineering intent of a part; it allows engineers to describe the size, form, orientation, and location of features in a way other than simple maximum and minimum dimensions (**limit dimensions**). The international standards for GD&T are ASME Y14.5-2009 and ISO1101(e)-2004.

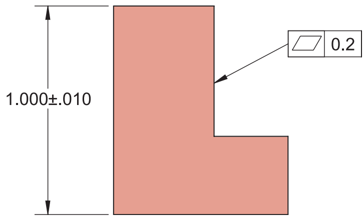

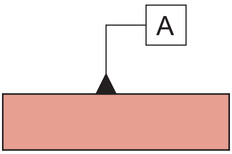

Tolerances and features in GD&T are called out using symbols. A tolerance on a feature is often called out in reference to a **datum**, which can be a line, point, axis, etc. established by a feature on the part. Datums should be chosen to adequately constrain the part and establish a **datum reference frame** consisting of three mutually perpendicular, intersecting datum planes. It is from the datum reference frame that the location or geometric relationship of another feature can be defined. Datums should be chosen based on the function of the part.

Basic dimensions are those that define a true position of a feature but are not toleranced. A **tolerance zone**, a zone within which a feature can vary, is then located with a basic dimension.

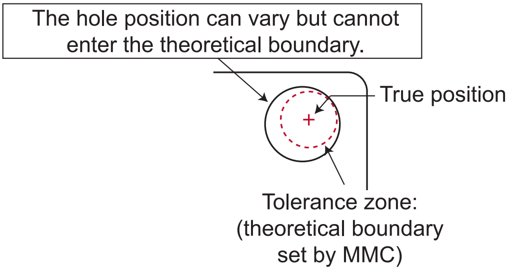

GD&T Terminology

Positional tolerances are used to define **features of size**. A feature of size is defined as an object that has opposing points (see left figure). Some examples of objects that are not features of size are a flat surface or line element (see right figure).

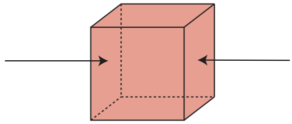

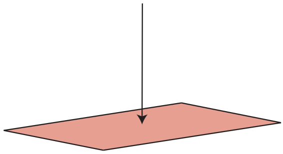

The **maximum material condition (MMC)** Ⓜ callout refers to a feature of size that has the maximum amount of material but remains within the size limits. Examples include the largest possible diameter of a pin or the smallest possible diameter of a hole.

Conversely, the **least material condition (LMC)** Ⓛ callout refers to a feature of size that has the minimum amount of material but remains within the size limits. Examples include the smallest possible diameter of a pin or the largest possible diameter of a hole. Material modifiers allow the size of the associated tolerance zone to be adjusted based on the measured size of the feature.

Pictorially demonstrated below is the **envelope principle**, or **Rule #1**. Given a (a) toleranced part, when that part is at MMC, it must have (b) perfect form. (c) Variation in form is permitted as the part varies from MMC. There is no requirement on the form of the part at LMC, but (d) the maximum variation that occurs at LMC must not exceed the boundaries set by MMC.

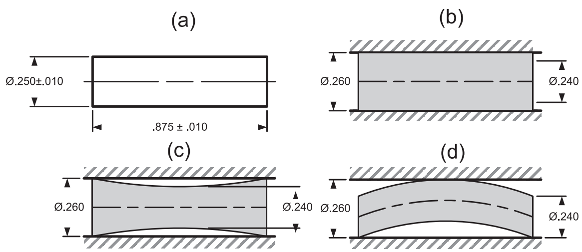

GD&T Symbology

On a drawing, individual tolerances and material conditions are called out in a **feature control frame**. First, the geometric symbol is called out, then the specific tolerance and any material conditions are stated, and finally, the primary datum from which the tolerance is referenced is listed. Sometimes secondary and tertiary datums are also included.

⌖	∅ 0.15 L	A	B	C L

The common geometric symbols used in **GD&T** are:

FORM	STRAIGHTNESS	—
	FLATNESS	⏥
	CIRCULARITY (ROUNDNESS)	○
	CYLINDRICITY	⌭
PROFILE	PROFILE OF A LINE	⌒
	PROFILE OF A SURFACE	⌓
ORIENTATION	ANGULARITY	∠
	PERPENDICULARITY	⊥
	PARALLELISM	//
LOCATION	POSITION	⌖
	CONCENTRICITY	◎
	SYMMETRY	⌯
RUNOUT	CIRCULAR RUNOUT	↗
	TOTAL RUNOUT	⌰

TERM	SYMBOL
AT MAXIMUM MATERIAL CONDITION	M
AT LEAST MATERIAL CONDITION	L
PROJECTED TOLERANCE ZONE	P
FREE STATE	F
TANGENT PLANE	T
DIAMETER	∅
SPHERICAL DIAMETER	S∅
RADIUS	R
SPHERICAL RADIUS	SR
CONTROLLED RADIUS	CR
REFERENCE	( )
ARC LENGTH	⌒
STATISTICAL TOLERANCE	ST
BETWEEN	◀▶

ISO 10110 Standard

The **ISO 10110 standard** provides details on the drafting of technical drawings for optical elements and systems, including rules on the presentation of component characteristics, optical properties, dimensions, and tolerances.

1: *General*

2: *Material imperfections—Stress birefringence* (0/)

On drawing as $0/A$, where A is the maximum permissible stress birefringence in nm/cm.

3: *Material imperfections—Bubbles and inclusions* (1/)

On drawing as $1/N \times A$, where N is the number of bubbles and inclusions, and A is a measure of their size (refer to the standard for details).

4: *Material imperfections—Inhomogeneity and striae* (2/)

On drawing as $2/A;B$, specifying the allowable class of inhomogeneity (A) and striae (B).

5: *Surface form tolerances* (3/)

On drawing as $3/A(B/C)$ or alternate forms, where A is the maximum spherical sag error from a test plate, B is the maximum irregularity ($P - V$), and C is the maximum rotationally symmetric P–V figure error.

6: *Centering tolerances* (4/)

On drawing as $4/\alpha$ or alternate forms, where α is the angle between the datum and the surface.

7: *Surface imperfection tolerances* (5/)

On drawing as $5/N \times A$, where N is the number of allowed imperfections, and A is a measure of size.

8: *Surface texture*

9: *Surface treatment and coating*

10: *Table representing data of optical elements and cemented assemblies*

11: *Non-toleranced data*

12: *Aspheric surfaces*

13: *Laser irradiation damage threshold* (6/)

On drawing as $6/H_{th}$ (or E_{th}); λ; τ_{eff} for pulsed laser irradiation and $6/F_{th}$; λ; τ_{eff} for long pulse and continuous wave (CW) operation, where (λ) is the laser wavelength, τ_{eff} is the effective pulse duration, H_{th} and E_{th} are the energy density threshold and power density threshold, respectively, and F_{th} is the linear power density threshold.

Tolerance Guides

Tolerance Guide for Lenses			
Parameter	**Baseline**	**Precision**	**High precision**
Lens diameter	±100 μm	±25 μm	±6 μm
Center thickness	±200 μm	±50 μm	±10 μm
Radius of curvature (%R)	0.50%	0.10%	0.05%
Radius of curvature (sag)	20 μm	2 μm	0.5 μm
Wedge	5 arcmin	1 arcmin	15 arcsec
Surface irregularity	λ	λ/4	λ/20
Surface finish	5 nm rms	2 nm rms	0.5 nm rms
Scratch/dig	80/50	60/40	20/10
Clear aperture	80%	90%	>90%

(Intended for standard-production spherical glass lenses)

Tolerance Guide for Glass Properties			
Parameter	**Baseline**	**Precision**	**High precision**
Refractive index – from nominal	$\pm 5 \cdot 10^{-4}$ (Grade 3)	$\pm 3 \cdot 10^{-4}$ (Grade 2)	$\pm 2 \cdot 10^{-4}$ (Grade 1)
Refractive index – measurement	$\pm 1 \cdot 10^{-4}$	$\pm 5 \cdot 10^{-6}$	$\pm 2 \cdot 10^{-6}$
Refractive index – homogeneity	$\pm 2 \cdot 10^{-5}$ (H1)	$\pm 5 \cdot 10^{-6}$ (H2)	$\pm 1 \cdot 10^{-6}$ (H4)
Dispersion – from nominal	±0.8% (Grade 4)	±0.5% (Grade 3)	±0.2% (Grade 1)
Stress birefringence	20 nm/cm	10 nm/cm	4 nm/cm
Bubbles/ inclusions >50 μm (area of bubbles per 100 cm^3)	0.5 mm^2	0.1 mm^2	0.029 mm^2 (Class B0)
Striae – based on shadow graph test	Fine	Small, in one direction	None detectable

Tolerance Guides (cont.)

Tolerance Guide for Injection-Molded Plastics			
Parameter	**Low cost**	**Commercial**	**Precision**
Focal length (%)	±3–5	±2–3	±0.5–1
Radius of curvature (%)	±3–5	±2–3	±0.8–1.5
Power (fringes)	10–6	5–2	1–0.5
Irregularity (fringes/10 mm)	2.4–4	0.8–2.4	0.8–1.2
Scratch/dig	80/50	60/40	40/20
Centration	$\pm 3'$	$\pm 2'$	$\pm 1'$
Center thickness (mm)	±0.1	±0.05	±0.01
Radial displacement (mm)	0.1	0.05	0.02
Lens-to-lens repeatability	2–1	0.5–1	0.3–0.5
Diameter–thickness ratio	2:1	3:1	5:1
Bubbles and inclusions	—	1×0.16	1×0.10
Surface imperfections	—	2×0.10	2×0.06
Surface roughness (nm rms)	10	5	2

Tolerance Guide for Machined Parts		
Machining level	**Metric**	**English**
Coarse dimensions (not important)	±1 mm	$\pm 0.040''$
Typical machining (low difficulty)	±0.25 mm	$\pm 0.010''$
Precision machining (readily available)	±0.025 mm	$\pm 0.001''$
High precision (needs special tooling)	<±0.002 mm	$< \pm 0.0001''$

Tolerance Guides (cont.)

Tolerance Guide for Edge Bevels	
Lens diameter (mm)	**Nominal bevel facewidth (mm)**
25	0.3
50	0.5
150	1
400	2

In mechanics, a bevel and chamfer generally have the same meaning. For optical components, the term bevel is most commonly used, and it is dimensioned by the facewidth. Typical optics bevels are at 45 deg, and the tolerance is 20–30% of the facewidth value.

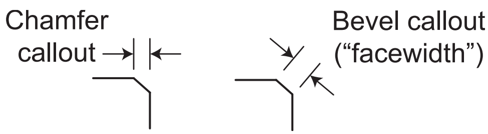

Clean-Room Classifications

For precision fabrication, a **clean room** that is free of dust and contaminants is often required. **Federal Standard 209** was the original document that defined clean-room classifications, but it has since been replaced by **ISO 14644**.

- According to Federal Standard 209, a clean-room classification defines the maximum number of particles ≥ 0.5 μm permitted per cubic foot of air (i.e., Class 100 has at most 100 particles/ft^3 that are ≥ 0.5 μm).
- According to ISO 14644-1, a clean room classification defines the order of magnitude of particles ≥ 0.1 μm permitted per cubic meter of air (i.e., Class 5 has at most 10^5 = 100,000 particles/m^3 that are ≥ 0.1 μm).

Clean-room classification	Typical uses
Class 1 and 10	Manufacturing electronic integrated circuits
Class 100	Manufacturing hard drives and medical implants
Class 1000	Pharmaceutical manufacturing
Class 10,000	Hospital operating rooms, manufacturing TV tubes
Class 100,000	Assembly of consumer optics, manufacturing ball bearings

	Equivalent classes of FS 209 and ISO 14644-1					
ISO class	3	4	5	6	7	8
FS 209 class	1	10	100	1,000	10,000	100,000

Clean-Room Classifications (cont.)

FS 209 class	Maximum concentration (particles/m^3) for a given particle size (μm)				
	≥0.1	≥0.2	≥0.3	≥ 0.5	≥5
1	35	7.5	3	**1**	—
10	350	75	30	**10**	—
100	—	750	300	**100**	—
1,000	—	—	—	**1,000**	7
10,000	—	—	—	**10,000**	70
100,000	—	—	—	**100,000**	700

ISO class	Maximum concentration (particles/m^3) for a given particle size (μm)					
	≥0.1	≥0.2	≥0.3	≥0.5	≥1	≥5
1	**10**	2	–	–	–	–
2	**100**	24	10	4	–	–
3	**1,000**	237	102	35	8	–
4	**10,000**	2,370	1,020	352	83	–
5	**100,000**	$2.37 \cdot 10^4$	$1.02 \cdot 10^4$	3,520	832	29
6	**1,000,000**	$2.37 \cdot 10^5$	$1.02 \cdot 10^5$	$3.52 \cdot 10^4$	8,320	293
7	—	—	—	$3.52 \cdot 10^5$	$8.32 \cdot 10^4$	2,930
8	—	—	—	$3.52 \cdot 10^6$	$8.32 \cdot 10^5$	$2.93 \cdot 10^4$
9	—	—	—	$3.52 \cdot 10^7$	$8.32 \cdot 10^6$	$2.93 \cdot 10^5$

Shipping Environments: Vibration

It is important to understand the environment in which a package is shipped to ensure that it is able to withstand transportation.

The following values are taken from power spectral density (PSD) versus frequency curves provided in ASTM Standard D7386-08:

Frequency (Hz)	PSD – pick-up/delivery vehicle (g^2/Hz)	PSD – over-the-road trailer (g^2/Hz)
1	0.001	0.0007
3	0.035	0.02
5	0.35	0.02
7	0.0003	0.001
13	0.0003	0.001
15	0.001	0.004
24	0.001	0.004
29	0.0001	0.001
50	0.0001	0.001
70	0.002	0.003
100	0.002	0.003
200	$5 \cdot 10^{-5}$	$4 \cdot 10^{-6}$
Overall, g rms	0.46	0.53

By knowing the PSD values over a spectrum of vibration frequencies, the approximate motion of the system can be found (see the sections on Vibration and Isolation).

Shipping Environments: Drop Heights

Multiple studies have been conducted to determine the shipping environments for various modes of delivery, carriers, and package weights and sizes. These studies have consistently found that, regardless of size and weight, 95% of the time packages were dropped from a height of 0.46–0.86 m. The 95th percentile was chosen to exclude outliers where drop heights were significantly larger than the average. The maximum drop heights were in the range of 0.9–2.0 m.

Package size/weight classification	Height at which 95% of drops occurred (m)
Small/light	0.76
Small/medium	0.61
Mid-size/light	0.46
Mid-size/medium	0.61
Mid-size/heavy	0.66
Large/medium	0.46
Large/heavy	0.46

Once an estimated drop height h has been determined, the acceleration experienced by the package (in units of g) can be calculated by:

$$a_g = \sqrt{\frac{h}{\delta_{SWEF}}}$$

The deflection due to a self-weight equivalent force variable δ_{SWEF} is the amount the packaging deflects if the system experiences a downward force equivalent to its own weight.

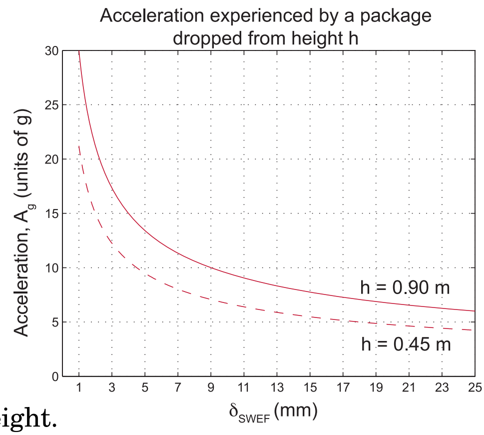

Unit Conversions

English	Metric	Metric	English
1 in	25.4 mm	1 mm	0.0394 in
1 ft	0.31 m	1 m	3.28 ft
1 mi	1.61 km	1 km	0.62 mi
1 oz	28.35 g	1 kg	35.27 oz
1 lb	0.45 kg	1 kg	2.2 lb
1 arcsec	4.85 μrad	1 μrad	0.21 arcsec
1 arcmin	291 μrad	1 mrad	3.44 arcmin
1 deg	17.5 mrad	1 rad	57.3 deg
1 psi	6895 Pa	1 MPa	145 psi
1 lb-force	4.45 N	1 N	0.22 lb-force
1 lb-in	0.113 N-m	1 N-m	8.85 lb-in
1 atm	760 mmHg	760 mmHg	1 atm
1 mph	0.45 m/s	1 m/s	2.24 mph

Temperature	
°C	$(°\mathrm{F} - 32) \cdot 5/9$
°F	$(°\mathrm{C} \cdot 9/5) + 32$
K	$°\mathrm{C} + 273.15$ K

The following table presents common terminology used in machining and their meanings:

Term	Value
a thousandth	$0.001''$
a thou	$0.001''$
a mil	$0.001''$ (1 "milli-inch")
40 thousandths	$0.040''$
40 thousandths	≈ 1 mm
two-tenths	$0.0002''$ (2/10 of 1 thousandth)
millionth	$0.0000001''$ (1 millionth of an inch)

Cost and Performance Tradeoffs for Linear Stages

The following charts provide relationships between the cost, travel range, angular deviation, and load capacity of various types of manual, one-axis, linear stages. The stages considered have less than a 2.5-in travel range and are sold by major optomechanical vendors.

DT = dovetail
BB = ball bearing
GA = gothic arch
CR = crossed-roller bearing
Flex = flexure

Property	DT	BB	GA	CR	Flex
Cost	Low	Mid	Mid	High	Mid/ High
Resolution	Low	Mid	Mid	High	Very High
Travel range	Large	Mid	Mid	Mid	Very Small
Load capacity	High*	Low	High	High	High
Angular deviation	High	Mid	Low	Low	–
Stiffness	High	Low	High	High	Mid
Resolution (μ**m**)**	~10–100	~0.5–1	~1–10	~1–10	No limit
Common uses	Coarse place-ment	Gen. precise place-ment	Gen. precise place-ment	Fiber optics place-ment	Fiber optics place-ment

* As a class in general, dovetail stages can handle very large loads. Stages in the example travel range (<2.5 in) are most concerned with low cost, resulting in the low load capacities shown in the charts.

** Resolution ranges provided here are approximate. Some manual stages offer resolution down to 0.1 μm with the proper driver.

Cost and Performance Tradeoffs for Linear Stages (cont.)

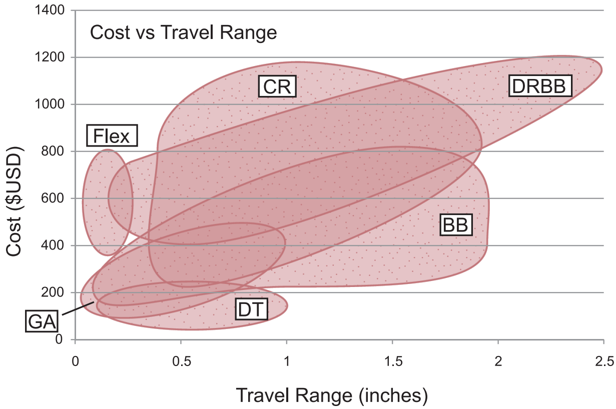

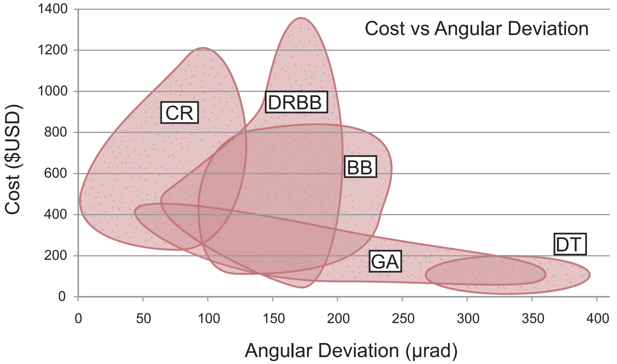

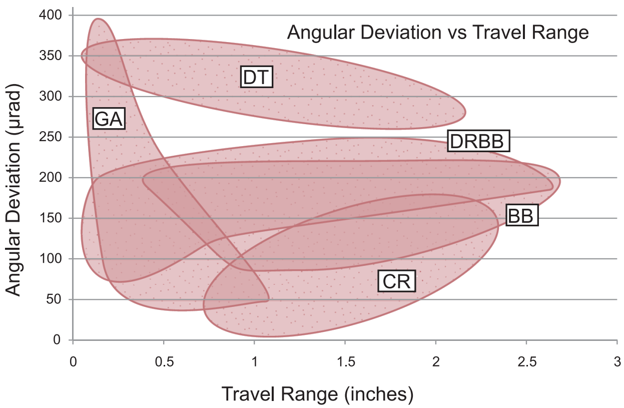

Cost and Performance Tradeoffs for Linear Stages (cont.)

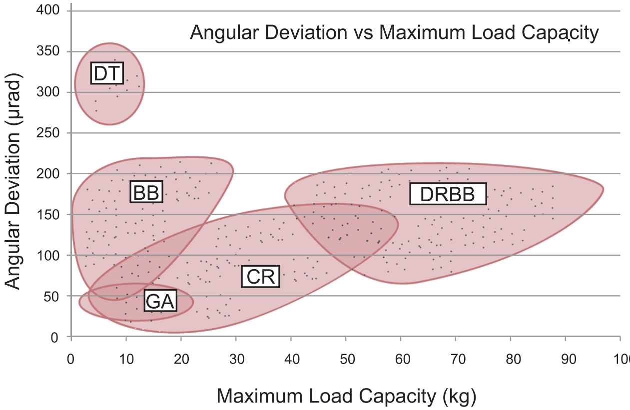

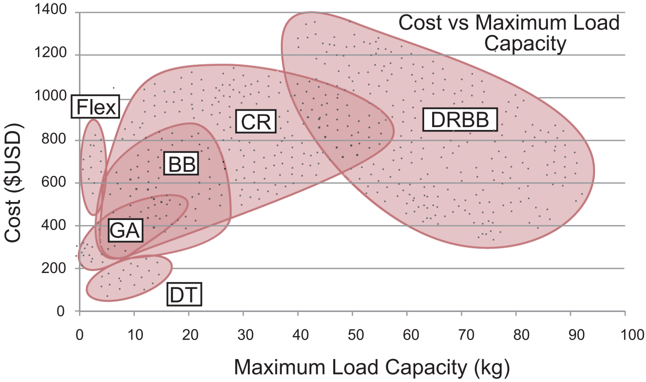

Torque Charts

Size	Bolt diameter D (in)	Stress area A (in^2)
4-40	0.1120	0.00604
4-48	0.1120	0.0061
6-32	0.1380	0.00909
6-40	0.1380	0.01015
8-32	0.1640	0.01400
8-36	0.1640	0.01474
10-24	0.1900	0.0175
10-32	0.1900	0.02000
1/4-20	0.2500	0.0318
1/4-28	0.2500	0.0364
5/16-18	0.3125	0.0524
5/16-24	0.3125	0.0580
3/8-16	0.3750	0.0775
3/8-24	0.3750	0.0878

SAE Grade-2 Bolts			
74,000-psi tensile strength; 55,000-psi-proof load			
Size	Clamp load P (lb)	Torque dry (in-lb)	Torque lubed (in-lb)
4-40	240	5	4
4-48	280	6	5
6-32	380	10	8
6-40	420	12	9
8-32	580	19	14
8-36	600	20	15
10-24	720	27	21
10-32	820	31	23
1/4-20	1320	66	49
1/4-28	1500	76	56
5/16-18	2160	11	8
5/16-24	2400	12	9
3/8-16	3200	20	15
3/8-24	3620	23	17

Torque Charts (cont.)

SAE Grade-5 Bolts			
120,000-psi tensile strength; 85,000-psi-proof load			
Size	**Clamp load *P* (lb)**	**Torque dry (in-lb)**	**Torque lubed (in-lb)**
4-40	380	8	6
4-48	420	9	7
6-32	580	16	12
6-40	640	18	13
8-32	900	30	22
8-36	940	31	23
10-24	1120	43	32
10-32	1285	49	36
1/4-20	2020	96	75
1/4-28	2320	120	86
5/16-18	3340	17	13
5/16-24	3700	19	14
3/8-16	4940	30	23
3/8-24	5600	35	25

SAE Grade-8 Bolts			
150,000-psi tensile strength; 120,000-psi-proof load			
Size	**Clamp load *P* (lb)**	**Torque dry (in-lb)**	**Torque lubed (in-lb)**
4-40	540	12	9
4-48	600	13	10
6-32	820	23	17
6-40	920	25	19
8-32	1260	41	31
8-36	1320	43	32
10-24	1580	60	45
10-32	1800	68	51
1/4-20	2860	144	108
1/4-28	3280	168	120
5/16-18	4720	25	18
5/16-24	5220	25	20
3/8-16	7000	45	35
3/8-24	7900	35	25

Adhesive Properties

Adhesive (Mfr.)	Type	Shear str. at 24 °C (MPa)	Suggested curing time
2216 B/A Gray (3M)	Epoxy (2-part)	22.1	30 min (93°C) 120 min (66°C)
A-12 (Armstrong) (mix 1:1)	Epoxy (2-part)	34.5	60 min (93°C) 5 min (149°C) 1 wk (24°C)
302-3M (Epo-tek)	Epoxy (2-part)	8.9	180 min (65°C) 1 day (24°C)
Hysol 0151 (Loctite)	Epoxy (2-part)	20.7	60 min (82°C) 120 min (60°C) 3 days (24°C)
2115 (Trabond)	Epoxy (2-part)	26.2	1–2 hr (65°C) 1 day (24°C)
Milbond (Summers)	Epoxy (2-part)	14.5	180 min (71°C)
Eccobond 285/ Catalyst 11 (Emerson & Cuming)	Epoxy (+catalyst)	14.5	30–60 min (120°C) 2–4 hr (100°C) 8–16 hr (80°C)
61 (Norland)	Urethane (1-part UV cure)	20.7	5–10 min (100 W Hg lamp)
349 (Loctite)	Urethane (1-part UV cure)	11	20–30 sec (100 W Hg lamp)
RTV142 (GE)	RTV	3.8	2 days (24°C)
RTV566 (GE)	RTV	3.2	1 day (24°C)
Q3-6093 (Dow Corning)	RTV	1.6	6 hr (24°C)

Adhesive Properties (cont.)

Adhesive (Mfr.)	CTE ($\times 10^{-6}/^\circ$ C)	%TML	%CVCM	Temp. range (°C)
2216 B/A Gray (3M)	102	0.77	0.04	−55 to 150
A-12 (Armstrong) (mix 1:1)	36	1.24	0.04	−55 to 170
302-3M (Epo-tek)	60	0.7	0.01	−55 to 125
Hysol 0151 (Loctite)	47	1.51	0.01	−55 to 100
2115 (Trabond)	55	NA	NA	−70 to 100
Milbond (Summers)	72	0.98	0.03	−60 to 100
Eccobond 285/ Catalyst 11 (Emerson & Cuming)	29	0.28	0.01	−55 to 155
61 (Norland)	240	2.36	0	−60 to 125
349 (Loctite)	80	NA	NA	−54 to 130
RTV142 (GE)	270	0.22	0.05	−60 to 204
RTV566 (GE)	280	0.14	0.02	−115 to 260
Q3-6093 (Dow Corning)	285	NA	NA	−60 to 100

Adhesive Properties (cont.)

Adhesive (Mfr.)	Advantages/ properties	Typical applications
2216 B/A Gray (3M)	High strength Low outgassing	General purpose Aerospace, cryo Metal-to glass
A-12 (Armstrong) (mix 1:1)	Flexibility/ strength can be controlled by mix	Aerospace, military optics bonding Glass-to-metal
302-3M (Epo-tek)	Clear, transmits 0.35–1.55 μm	Optical bonding Fiber-optic potting
Hysol 0151 (Loctite)	Clear	General purpose Glass-to-metal
2115 (Trabond)	Catalyst choices Low outgassing	Heat sinks
Milbond (Summers)	Low out-gassing/volatility Wide temp. range	Avoid high levels of volatile condensed materials
Eccobond 285/ Catalyst 11 (Emerson & Cuming)	Low outgassing Wide temp. range	Glass-to-metal Aerospace
61 (Norland)	Quick UV cure Transmissive from 0.4–5 μm	Optics and prism bonding (to glass, plastic, metal) Military/aerospace
349 (Loctite)	Quick UV cure	Glass-to-glass Glass-to-metal
RTV142 (GE)	Low outgassing Good adhesion with primer High operational temp.	Glass-to-metal
RTV566 (GE)	High adhesion Nonflowing Allow high shear	High shear General purpose Sealant
Q3-6093 (Dow Corning)	Clear	Bonding optics, laser fabrication

Glass Properties

Material	n_d	**Transmission range (μm)**	E **(GPa)**	α **(×10^{-6} /°C)**
N-BK7	1.5168	0.2–2.5	82	7.1
Borofloat 33 borosilicate	1.4714	0.35–2.7	64	3.25
Calcium fluoride	1.4338	0.35–7.0	75.8	21.28
Clearceram®-Z (CCZ) HS	1.546	0.5–1.5	92	0.02
Fused silica	1.4584	0.18–2.5	72	0.5
Germanium	4.004 (@ 10 μm)	2.0–14.0	102.7	6.1
Magnesium fluoride	1.3777 (n_o) 1.3895 (n_e)	0.12–7.0	138	13.7 (∥) 8.9 (⊥)
P-SK57	1.5843 (after molding)	0.35–2.0	93	7.2
Sapphire	1.7659 (n_o) 1.7579 (n_e)	0.17–5.5	400	5.6 (∥) 5.0 (⊥)
SF57	1.8467	0.4–2.3	54	8.3
N-SF57	1.8467	0.4–2.3	96	8.5
Silicon	3.148 (@ 10.6 μm)	1.2–15.0	131	2.6
ULE® (Corning 7972)	1.4828	0.3–2.3	67.6	0.03
Zerodur®	1.5424	0.5–2.5	90.3	0.05 (Class 1)
Zinc selenide (CVD)	2.403 (@ 10.6 μm)	0.6–16	67.2	7.1
Zinc selenide (Cleartran)	2.2008 (@ 10 μm)	0.4–14.0	74.5	6.5

Glass Properties (cont.)

Material	**ρ (g/cm^3)**	***dn/dT* (absolute) ($\times 10^{-6}$/°C)**	**ν**	**λ (W/mK)**	***K* (10^{-12}/Pa)**
N-BK7	2.51	1.1	0.206	1.11	2.77
Borofloat 33 borosilicate	2.2	–	0.2	1.2	4
Calcium fluoride	3.18	–11.6	0.26	9.71	–1.53 @ 546 nm ($q_1 - q_2$)
Clearceram®-Z (CCZ) HS	2.55	–	0.25	1.54	–
Fused silica	2.2	11	0.17	1.35	3.5
Germanium	5.33	396	0.28	58.61	–
Magnesium fluoride	3.18	1.1 (n_o)	0.271	11.6	–
P-SK57	3.01	1.5	0.249	1.01	2.17
Sapphire	3.97	13.1	0.27	46	–
SF57	5.51	6	0.248	0.62	0.02
N-SF57	3.53	–2.1	0.26	0.99	2.78
Silicon	2.33	130	0.279	137	–
ULE® (Corning 7972)	2.21	10.68	0.17	1.31	4.15
Zerodur®	2.53	15.7	0.243	1.6	3
Zinc selenide (CVD)	5.27	61 @ 10.6	0.28	18	–1.6
Zinc selenide (Cleartran)	4.09	40 @ 10.6 54.3 @ 0.632	0.28	27.2	–

Glass Properties (cont.)

Material	Pros	Cons	Common applications
N-BK7	Easy to make high quality Availablity Inexpensive	Transmission only in visible/ near IR	Versatile for everyday optical applications
Borofloat boro-silicate	CTE matches silicon Low melt temp Low cost at high volume	Poor optical transparency	Windows Thermal stability
Calcium fluoride	Wide trans-mission range High laser-damage threshold	Soft Hydrophilic High CTE	Color correction UV (windows, filters, prisms)
Clearceram®-Z (CCZ) HS	Very low CTE Available as large blanks		Telescope mirror substrates Space
Fused silica	Wide transmission range Low CTE	Higher dn/dT than BK7	Standard optics, high-power laser applications
Germanium	Low dispersion	High density (heavy), high dn/dT	IR applications
Magnesium fluoride	Wide transmission range Birefringent	Poor thermal properties Hydrophillic	Anti-reflection coating UV optics Excimer laser applications
P-SK57	Low trans-formation temp (good for molding)		Precision molding - optics/ aspheres for consumer products

Glass Properties (cont.)

Material	Pros	Cons	Common applications
Sapphire	Very hard; scratch resistant; wide transmission range	Difficult to machine, expensive	Windows/ domes for UV, IR, and visible
SF57	Low stress-optic coefficient	Softer material	Color correction
Silicon	Wide IR transmission range; lower CTE	High dn/dT	Filter substrates, IR windows
ULE® (Corning 7972)	Very low CTE	Poor optical properties; expensive	Telescope mirror substrates; space
Zerodur®	Very low CTE; available as large blanks	Poor optical properties; expensive	Telescope mirror substrates; space
Zinc selenide	Transmission in IR and visible	Soft; expensive	IR windows and lenses; CO_2 laser optics for 10.6 μm
Zinc sulfide	Transmission in IR and visible	Expensive	IR windows and lenses; combined visible/IR systems

Metal Properties

Material	E (GPa)	α ($\times 10^{-6}$/°C)	ρ (g/cm^3)	ν	λ (W/mK)	Hardness
Aluminum (6061-T6)	68	23.6	2.7	0.33	167	Rockwell B – 60
Beryllium	290	11.5	1.84	0.08	216	Rockwell B – 80
Copper C260	110	20	8.53	0.38	120	Rockwell F – 54
Graphite epoxy (CFRP)	180	0.02	1.7		11.5	–
Invar® 36	148	1.3	8	0.29	10.2	Rockwell B – 90
Molybdenum	320	5	10.2	0.31	138	Brinell 1500 MPa
Silicon carbide CVD	466	2.4	3.2	0.21	146	Rockwell F – 95
Stainless steel CRES 17-4PH	190	10.8	7.81	0.27	17.8	Rockwell C – 35
Stainless steel CRES 316	193	16	8	0.3	16.3	Rockwell B – 93
Titanium	108	8.6	4.5	0.31	16.3	Rockwell B – 80

Metal Properties (cont.)

Material	Pros	Cons
Aluminum (6061-T6)	Inexpensive Easy to machine Lightweight	Higher CTE Soft material
Beryllium	High stiffness Lightweight Low CTE	Toxic/hazardous to machine Very expensive
Copper C260	High thermal conductivity (quick time to thermal equilibrium)	Soft material Dense
Graphite epoxy (CFRP)	Young's modulus and CTE are tunable Strong material High stiffness Low CTE Low density	Unstable in humidity Expensive
Invar®	Very low CTE	Difficult to machine Dense Unstable over time
Molybdenum	Very stiff	Difficult to machine
Silicon carbide	Very hard High rigidity Low CTE High thermal conductivity	Expensive material Expensive processing
Stainless steel	Similar CTE to glass Excellent corrosion resistance	Heavier material (3× weight of aluminum) Low thermal conductivity
Titanium	High yield strength Very corrosion resistant Similar CTE to glass Stable during machining	Difficult to machine High cost Low thermal conductivity

Equation Summary

Focus shift and lateral shift of light passing through a plane parallel plate:

$$\Delta z = t\frac{(n-1)}{n} \qquad \Delta x_i = \frac{t\Delta\theta_p(n-1)}{n}$$

Stress (normal and shear):

$$\sigma = \frac{F}{A} \qquad \tau = \frac{V}{A}$$

Strain (normal and shear):

$$\varepsilon = \frac{\Delta L}{L} = \frac{\sigma}{E} \qquad \gamma = \frac{\tau}{G}$$

Young's modulus and bulk modulus:

$$G = \frac{E}{2(1+\nu)} \qquad K = \frac{E}{3(1-2\nu)}$$

Wavefront retardance due to stress:

$$\Delta W_p = \frac{K_s \sigma t}{\lambda}$$

Stiffness (normal and shear):

$$k = \frac{EA}{t} \qquad k_{shear} = \frac{GA}{t}$$

Preload torque for a retaining ring on a lens:

$$P = \frac{Q}{[D_T(0.577\mu_M + 0.5\mu_G)]} \approx \frac{5Q}{D_T}$$

Equation Summary

Bondline thickness necessary for an athermalized bonded mount:

$$h = \frac{d_l(\alpha_m - \alpha_l)}{2(\alpha_a - \beta_m)}$$ (Bayar equation)

$$h = \frac{d_l}{2}\frac{(\alpha_m - \alpha_l)}{\alpha_a - \alpha_m + \frac{2\nu}{1-\nu}\left(\alpha_a - \frac{\alpha_l - \alpha_m}{2}\right)}$$ (van Bezooijen or Muench equation)

Tensile and compressive stress relationship:

$$\sigma_T = \frac{(1-2\nu_G)\sigma_C}{3}$$

Deviation from a thin wedge:

$$\delta = \alpha(n-1)$$

The minimum aspect ratio for a circular window with a pressure differential:

$$\frac{h}{d} = C_{SF}C_{sp}\left(\frac{\Delta P}{\sigma_S}\right)^{\frac{1}{2}}$$

$C_{sp} = 0.2165$ (Clamped)
$C_{sp} = 0.265$ (Simply supported)

The thickness of a rectangular window (includes a safety factor of 4):

$$h \approx b\left[\left(\frac{P}{\sigma_{ys}}\right)\frac{3}{1+2\left(\frac{a}{b}\right)^3}\right]^{\frac{1}{2}}$$ Simply supported

$$h \approx b\left[\left(\frac{P}{\sigma_{ys}}\right)\frac{2}{1+2\left(\frac{a}{b}\right)^4}\right]^{\frac{1}{2}}$$ Clamped

Equation Summary

Fundamental frequency for a simply supported window:

$$f_{n-circ} = \left(\frac{\pi}{4}\right)\left(\frac{1}{r^2}\right)\left[\frac{gEh^2}{12\rho\left(1-\nu^2\right)}\right]^{\frac{1}{2}} \qquad \text{Circular}$$

$$f_{n-rect} = \left(\frac{\pi}{2}\right)\left(\frac{1}{a^2}+\frac{1}{b^2}\right)\left[\frac{gEh^2}{12\rho\left(1-\nu^2\right)}\right]^{\frac{1}{2}} \qquad \text{Rectangular}$$

Lamé pressure vessel equations:

$$\sigma_m = \sigma_h = -P\frac{R_0^3\left(R_i^3+2r^3\right)}{2r^3\left(R_0^3-R_i^3\right)}$$

$$\sigma_r = -P\frac{R_0^3\left(r^3-R_i^3\right)}{r^3\left(R_0^3-R_i^3\right)}$$

RMS self weight deflection for a flat, thin mirror (large aspect ratio) supported with any number of discrete points:

$$\delta_{rms} = \gamma_N\left(\frac{q}{D}\right)\left(\frac{\pi r^2}{N}\right)^2\left[1+2\left(\frac{h}{u}\right)^2\right]$$

Flexural rigidity:

$$D = \frac{Eh^3}{12\left(1-\nu^2\right)}$$

Natural frequency:

$$\omega_0 = \sqrt{\frac{k}{m}} \qquad f_0 = \frac{\omega_0}{2\pi}$$

Equation Summary

Transmissibility:

$$T = \sqrt{\frac{1+\left(2\frac{f}{f_0}\zeta\right)^2}{\left(1-\frac{f^2}{f_0^2}\right)^2+\left(2\frac{f}{f_0}\zeta\right)^2}}$$

Miles equation:

$$a_{rms} = \sqrt{\frac{\pi}{2}\cdot f_0 \cdot Q \cdot PSD}$$

Change in length due to uniform temperature change:

$$\Delta L = \alpha L \Delta T$$

Thermal stress and strain:

$$\sigma = E\alpha\Delta T$$

$$\varepsilon = \frac{\Delta L}{L} = \alpha\Delta T$$

Thermal conductivity:

$$\lambda = \frac{QL}{\Delta T}$$

Thermal diffusivity:

$$D = \frac{\lambda}{\rho C_p}$$

Equation Summary

Change in index with temperature:

$$n' = n + \left(\frac{dn}{dT}\right)\Delta T$$

Air index of refraction:

$$(n-1) = \left[\frac{P(n-1)_s}{96095.43}\right]\left\{\frac{\left[1+10^{-8}\left(0.601-9.72\cdot 10^{-3}T\right)P\right]}{1+3.361\cdot 10^{-3}T}\right\}$$

$$(n-1)_s = \left[8342.54 + \frac{2406147}{\left(130-\sigma^2\right)} + \frac{15998}{\left(38.9-\sigma^2\right)}\right]\cdot 10^{-8}$$

Change in focal length of a singlet with temperature:

$$\Delta f = \beta f \Delta T$$

$$\beta = \alpha - \frac{1}{n-1}\frac{dn_{rel}}{dT}$$

For an athermal doublet:

$$\frac{\phi_1}{\phi} = \frac{\nu_1'}{\nu_1' - \nu_2'}$$

$$\frac{\phi_2}{\phi} = -\left(\frac{\nu_2'}{\nu_1' - \nu_2'}\right)$$

$$\nu' = \frac{1}{\beta}$$

Bibliography

Ahmad, A., *Handbook of Optomechanical Engineering*, CRC Press, Boca Raton, FL (1997).

Baiocchi, D., "Design and Control of Lightweight, Active Space Mirrors," Ph.D. Thesis, Univ. of Arizona (2004).

Barnes, W. P., "Optical Windows," in *Optomechanical Design*, P. R. Yoder, Ed., pp. 232–253, SPIE Press, Bellingham, WA (1992).

Baumeister, T., A. M. Sadegh, and E. A. Avallone, *Marks' Standard Handbook for Mechanical Engineers*, McGraw-Hill, New York (2007).

Bäumer, S., *Handbook of Plastic Optics*, pp. 7–34, Weinheim: Wiley-VCH, Berlin (2005).

Bayar, M., "Lens barrel optomechanical design principles," *Opt. Eng*. **20**(2), 181–186 (1981).

Birch, K. P. and Downs, M. J., "An updated Edlen equation for the refractive index of air," *Metrologia* **30**, 155–162 (1993).

Blanding, D. L., *Principles of Exact Constraint Mechanical Design*, Eastman Kodak, Rochester, NY (1992).

Burge, J. H., "An easy way to relate optical element motion to system pointing stability," *Proc. SPIE* **6288**, 628801 (2006) [doi:10.1117/12.677917].

Chen, W. T. and C. W. Nelson, "Thermal stress in bonded joints," *IBM J. Res. Develop.* **23**(2) 179–188 (1979).

Ciddor, P. E., "Refractive index of air: new equations for the visible and near infrared," *Appl. Optics* **35**, 1566–1573 (1996).

Culpepper, M. L., "Design of quasi-kinematic couplings," *Precision Engineering* **28**, 338–357 (2004).

Doremus, R. H., "Fracture statistics: A comparison of the normal, Weibull, and Type I extreme value distributions," *J. App. Phy.* **54**(1), 193–198 (1983).

Bibliography

Doyle, K. B. and M. A. Kahan, "Design strength of optical glass," *Proc. SPIE* **5176**, 14–25 (2003) [doi:10.1117/12.506610].

Ealey, M., R. Paquin, and T. Parsonage, eds., *Advanced Materials for Optics and Precision Structures*, SPIE Press, Bellingham, WA (1997).

Fischer, R. E., "Optimization of lens designer to manufacturer communications," *Proc. SPIE* **1354**, 506–522 (1991) [doi:10.1117/12.47955].

Gibbons, R. C., "Athermal infrared optics," Equipment Group, Texas Instruments, Inc., 1–12 (Feb. 1976).

Hale, L. C., "Principles and Techniques for Designing Precision Machines," Ph.D. Thesis, MIT, LLNL (1999).

Hibbard, D. L., "Electroless nickel for optical applications," Chapter 9 in *Advanced Materials for Optics and Precision Structures*, Ealey, M., R. Paquin, and T. Parsonage, eds., SPIE Press, Bellingham, WA (1997).

Jamieson, T. H., "Athermalization of optical instruments from the optomechanical viewpoint" (Critical Review Vol CR43, (1992).

Jones, G. E., "High-performance lens mounting," *SPIE Proc.* **73**, 9–17 (1975).

Mehta, P. K., "Flexural rigidity characteristics of lightweighted mirrors," *Proc. SPIE* **748**, 158–171 (1987).

"Military standard environmental test methods for aerospace and ground equipment," MIL-STD-810, United States Air Force, http://www.dtc.army.mil/publications/810June1962.pdf (1962).

Monti, C. L., "Athermal bonded mounts: incorporating aspect ratio into a closed-form solution," *Proc. SPIE* **6665**, 666503 (2007) [doi:10.1117/12.730275].

Bibliography

Nelson, J. E., J. Lubliner, and T. S. Mast, "Telescope mirror supports: plate deflections on point supports," *Proc. SPIE* **332**, 212–228 (1982).

"Optical components for fire control instruments; general specification governing the manufacture, assembly, and inspection of," MIL-PREF-13830B, United States Army, http://snebulos.mit.edu/projects/reference/MIL.../MIL-PRF-13830B.pdf (1963).

Povey, V., "Athermalisation techniques in infrared systems," *Proc. SPIE* **655**, 142–153 (1986).

"Preparation of drawings for optical elements and systems," ISO 10110, International Organization for Standardization, http://www.iso.org/iso/iso_catalogue/ catalogue_tc/catalogue_detail.htm?csnumber=35991 (2006).

Schwertz, K., "Cost and performance trade-offs for commercially available linear stages," *Proc. SPIE* **7793**, 77930Q (2010) [doi:10.1117/12.868245].

Schwertz, K. and J. H. Burge, "Relating axial motion of optical elements to focal shift," *Proc. SPIE* **7793**, 779306 (2010) [doi:10.1117/12.868244].

Sheridan, P. M., F. O. James, and T. S. Miller, "Design of Components," in *Engineering with Rubber*: *How to Design Rubber Components*, Second Edition, A. N. Gent, Ed., Hanser Gardner Publications, Cincinnati, OH (2001).

Singh, S. P., G. J. Burgess, J. Singh, and M. Kremer, "Measurement and analysis of the next-day air shipping environment for mid-sized and lightweight packages for DHL, FedEx, and United Parcel Service," *Packing Technology and Science* **19**(4), 227–235 (2006).

Singh, S. P., J. Singh, K. C. Chiang, and K. Saha, "Measurement and analysis of small packages in next-day air shipments," *Packing Technology and Science* **23**(1), 1–9 (2010).

Slocum, A. H., *Precision Machine Design*, Society of Manufacturing, Dearborn, MI (1992).

Bibliography

Smith, S. T., *Flexures: Elements of Elastic Mechanisms*, Gordon & Breach, Amsterdam (2000).

Smith, W. J., *Modern Optical Engineering*, Third Edition, McGraw-Hill, New York (2000).

Stachiw, J. D., "Design parameters for germanium windows under uniform pressure loading," *Proc. SPIE* **131**, 57–72 (1978).

Stone, R., "FEA Presentation: Common pitfalls/problems, tips, and examples," Lecture at the Univ. of Arizona, Tucson, AZ (6 Nov 2009).

Valente, T. M., "Scaling laws for lightweight optics," *Proc. SPIE* **1340**, 47–66 (1990) [doi:10.1117/12.23035].

Valente, T. M. and D. Vukobratovich, "A comparison of the merits of open-back, symmetric sandwich, and contoured back mirrors as light-weighted optics," *Proc. SPIE* **1167**, 20–36 (1989).

Vukobratovich, D. and R. Richard, "Flexure mounts for high-resolution optical elements," *Proc. SPIE* **959**, 18–36 (1988).

Weber, M. J., *Handbook of Optical Materials*, CRC Press, Boca Raton, FL (2003).

Yoder, P. R., *Mounting Optics in Optical Instruments*, Second Edition, SPIE Press, Bellingham, WA (2008) [doi:10.1117/3.785236].

Yoder, P. R., *Design and Mounting of Prisms and Mirrors in Optical Instruments*, SPIE Press, Bellingham, WA (1998).

Yoder, P. R., *Opto-mechanical Systems Design*, CRC Press, Boca Raton, FL (2006).

Young, W. C., *Roark's Formulas for Stress and Strain*, McGraw-Hill, New York (2000).

References

1. NIST/SEMATECH, *e-Handbook of Statistical Methods*, http://www.itl.nist.gov/div898/handbook/index.htm.

2. Schott - Technical Note. *TIE-33: Design strength of optical glass and Zerodur* (2004).

3. http://outgassing.nasa.gov

4. Nelson, J. E., Lubliner, J., and Mast, T. S., "Telescope mirror supports: plate deflection on point supports," *Proc. SPIE* **332** (1982).

5. Park, W. H., "Parametric modeling of self-weighted distortion for plane optical mirrors," (2010).

6. Valente, T. M., Vukobratovich, D., "Comparison of the merits of open-back, symmetric sandwich, and contoured back mirrors as lightweight optics," *Proc. SPIE* **1167** (1989).

7. Kimmel, R. K. and Parks, R. E., *ISO 10110 Optics and Optical Instruments: Preparation of Drawings for Optical Elements and Systems*: *A User's Guide*. Washington, DC: Optical Society of America (1995).

Index

Index

Index

Index

Index

Index

Katie Schwertz received her BS in Optics from the University of Rochester Institute of Optics in 2008 and an MS in Optical Sciences from the University of Arizona in 2010. Her graduate work focused on optomechanics, during which she completed the report *Useful Estimations and Rules of Thumb for Optomechanics* under the guidance of Jim Burge. She currently works as an optomechanical designer for Edmund Optics at their Tucson Design Center.

Jim Burge is a Professor of Optical Sciences and Astronomy at the University of Arizona, leading research and curriculum development in the areas of optomechanical engineering, optical-systems engineering, and optical manufacturing. Dr. Burge has a BS degree from Ohio State University in Engineering Physics with Mechanical Engineering, and MS and PhD degrees in Optical Sciences from the University of Arizona.